

國立東華大學生命科學系生物技術碩士班

碩士論文

指導教授： 彭國証 博士

木黴菌二次代謝產物之殺真菌功能及
imidazolium salts 合成化合物之殺真菌功能

*Fungicides screening from the Trichoderma secondary metabolites and
antifungal potency of the organic ethoxy ether functionalized
imidazolium salts*



研究生：施惠儂 撰

中華民國一百年一月

國立東華大學
學位論文授權書

※說明※

本授權書請撰寫並簽名後，裝訂於紙本論文書名頁之次頁。

本授權書所授權之論文為立書人在國立東華大學 生命科學系生物技術碩士班

九十九 學年度第 一 學期取得 理學碩 士學位之論文。

論文名稱：木黴菌二次代謝產物之殺真菌功能及 imidazolium salts 合成化合物之殺真菌功能

Fungicides screening from the *Trichoderma* secondary metabolites and antifungal
potency of the organic ethoxy ether functionalized imidazolium salts

指導教授姓名：彭國証

學生姓名：施惠儂

學號：69713003


授權事項：

一、立書人具有著作財產權之上列論文全文資料，基於資源共享理念、回饋社會與學術研究之目的，非專屬、無償授權國立東華大學及國家圖書館，得不限地域、時間與次數，以微縮、光碟或數位化等各種方式重製散布、發行或上載網路，提供讀者非營利性質之線上檢索、閱覽、下載或列印。

二、上述數位化公開方式如下：(若未勾選下表，立書人同意視同授權校內、外立即公開。)

校 內	校 外	說 明
<input type="checkbox"/> 立即公開 <input type="checkbox"/> 於 1 年後公開 <input checked="" type="checkbox"/> 於 3 年後公開	<input type="checkbox"/> 立即公開 <input type="checkbox"/> 於 1 年後公開 <input checked="" type="checkbox"/> 於 3 年後公開	未立即公開原因：發表國外學術性期刊 <input type="checkbox"/> 申請專利(案號：) <input type="checkbox"/> 因隱私權需要(請指導教授附函說明特殊原因)

三、授權內容均無須訂立讓與及授權契約書，授權之發行權為非專屬性發行權利。依本授權所為之收錄、重製、發行及學術研發利用均為無償。

具有本論文 著作財產權 人共同簽名 (親筆正楷)	 施惠儂	日期 中華民國 99 年 1 月 29 日
---------------------------------------	--	-----------------------

學位考試委員會審定書

國立東華大學 生命科學系生物技術碩士班
研究生 施惠儂 君所提之論文

木黴菌二次代謝產物之殺真菌功能及imidazolium salts合成化合物之殺真菌功能

(題目) Fungicides screening from the Trichoderma secondary metabolites and antifungal potency of the organic ethoxy ether functionalized imidazolium salts

經本委員會審查並舉行口試，認為

符合碩士學位標準。

學位考試委員會召集人

委員

委員

委員

指導教授

系主任
(所長)

簽章

簽章

簽章

簽章

簽章

簽章

中華民國 100 年 1 月 20 日

Acknowledgement

在繁忙的生活中，轉眼間，在東華求學已滿兩年半，也終於完成了碩士論文。在我求學的路上，受到許多人的照顧和指引，讓我在實驗、課業與生活上都過得很充實並成長。首先是感謝我的父母，總是不斷的鼓勵並支持我所決定的事，並提供我在東華生活上的需求，雖然每天都會通電話，但是隨著實驗越來越忙，忍受一年只能見到兩次面。感謝我的指導教授彭國証老師，您的督促與指導讓我在學術與實驗數據整理的路上受益良多，並在我實驗遇到瓶頸時，適時與不厭其煩的指引我，讓我可以順利完成研究。感謝羅朝村老師，您從我大學開始就不斷的教導我並提供許多菌株讓我實驗，您和師母也總是關心我的實驗進度與生活，並不斷的鼓勵我，使得我可以順利進行研究。感謝林志彪老師，您在實驗上的指導以及合成化合物的提供，讓我可以順利進行另一方面的研究並完成我的論文，希望學生未來也能有機會繼續跟您合作。感謝劉淑瑛老師，您的幫助與參與使我的實驗更加的完美。感謝亦涵學姐、怡汝學姐、宜仁老師和國欽學長，對我研究路上的指導和生活上的關心。感謝阿吉學長，在我研究生涯中，不斷鼓勵我，並在交換意見和看法中，也讓我學習和成長。感謝琪樺學姐和家安學長，讓我增加許多學術的知識並學習到一些人生的看法，讓我在求學生涯中充滿了歡笑，謝謝你們。感謝中鋒學長，不辭辛苦且耐心的指導我關於論文的撰寫，讓我學習到許多以前我不會注意的細節。感謝化學系林志彪老師實驗室的蚊子和筱婷，謝謝你們提供的實驗材料，讓我的研究可以順利進行，跟你們合作的過程中，讓我學習許多也相當愉快。感謝一路一起奮鬥過來的俊伯，有你的陪伴和分享各自的看法，讓我在研究的路上不會孤單。感謝來自印度的 SHIBU，時常的讓我練習英文並指導我英文，讓我受益良多。感謝柏淵和志瑋，雖然你們是學弟，但是我們相處下來更像朋友，謝謝你們在我生活上的幫助並帶來歡笑。再次感謝各位陪我度過這兩年半的時光，陪我一起努力、難過、歡笑，我愛你們。

2011/01/20 施惠儂

Abstract

Secondary metabolites play a pivotal role in the antagonistic activities of some biocontrol species of *Trichoderma* resulting in the suppression of plant pathogens. *T. koningii* RIS 3-8, among other 22 strains, was the best *Trichoderma* spp. tested against phytopathogens, *Fusarium solani*, *F. oxysporum*, *Rhizoctonia solani* and *Botrytis cinerea* in vitro. Removing proteins by heat-treatment and protease-treatment showed proteins had no role in the antagonistic tests that lead to the secondary metabolites be the primary candidates. To discern the determinants of the *T. koningii* RIS 3-8 secondary metabolites, antifungal oriented assays were performed. The metabolites from the 9th day chloroform extract processed best antifungal activity against pathogens. Five bioactive compounds of *T. koningii* RIS 3-8 were isolated chromatographically: 1-hydroxy-3-methylanthracene-9,10-dione, methyl 4-hydroxybenzoate, methyl 4-hydroxycinnamate, 4-hydroxybenzaldehyde, 4-hydroxyacetophenone that all but 1-hydroxy-3-methylanthracene-9,10-dione were firstly isolated from *T. koningii*.

Meanwhile, [C_n-im-3OEG][Cl], amphiphilic ionic liquids and ionic liquid crystals were tested their fungicidal potency. [C₁₄-im-3OEG][Cl] possesses the best antifungal activity against *R. solani* with an IC₅₀ of 130 µM. Rupture of the bioenvelop appears to be operative in the process of antifungal activity.

Keywords: Biocontrol; *Trichoderma*; Secondary metabolites; Green chemicals; Ionic liquids (ILs); Imidazolium salts; *Rhizoctonia*

中文摘要

木黴菌是生物防治真菌之一，木黴菌的二次代謝產物在拮抗作用中扮演了一個重要能夠去抑制植物病原真菌的角色。本實驗是利用抗真菌活性來進行篩選分析，並利用稻草培養後的*T. koningii* RIS 3-8二次代謝產物，來有效的抑制植物病原菌。由本實驗結果可知，在體外的拮抗測試中，從23株木黴菌中顯示出*T. koningii* RIS 3-8可以最有效地抑制*Fusarium solani*, *F. oxysporum*, *Rhizoctonia solani* and *Botrytis cinerea*。利用加熱處理以及蛋白酶來移除蛋白質後，發現*T. koningii* RIS 3-8能有效抑制*F. solani*，主要是由於二次代謝產物，而蛋白質在抗真菌測試中完全沒有活性。本實驗結果顯示*T. koningii* RIS 3-8在固態培養第九天之代謝物，以及利用分配萃取後之氯仿層部分有最好的抗真菌活性。更進一步地利用活性導向和色譜分析法來分離和純化*T. koningii* RIS 3-8的二次代謝產物，分別為1-hydroxy-3-methylanthracene-9,10-dione，methyl 4-hydroxybenzoate，methyl 4-hydroxycinnamate，4-hydroxybenzaldehyde和4-hydroxyacetophenone共五個化合物，其中methyl 4-hydroxybenzoate，methyl 4-hydroxycinnamate，4-hydroxybenzaldehyde和4-hydroxyacetophenone是第一次從*Trichoderma*中被分離出來的。

此外，我們的研究從ethoxy ether functionalized imidazolium salts合成的化合物中的imidazolium上陽離子不同的10、12、14、16和18碳鏈長度的衍生物，去篩選能對抗植物病原菌立枯絲核菌的活性物質並且探討其機制。本實驗結果顯示imidazolium salts在14碳鏈長度的im-009 1-(2-(2-(2-hydroxyethoxy)ethoxy)ethyl)-3-tetradecyl-1H-imidazol-3-ium chloride最具有抑制立枯絲核菌的生長能力。探討立枯絲核菌在處理im-009後，利用倒立式螢光顯微鏡去觀察立枯絲核菌的細胞壁和細胞核在形態學上的作用機制。

關鍵字：生物防治；木黴菌；二次代謝物；綠色化學；離子液體；咪唑鹽類；立枯絲核菌

Table of contents

	Page
Acknowledgement	I
Abstract	II
中文摘要	III
Table of contents	V
Figure legends	X
Table contents	XIV
Part I Fungicides screening from the <i>Trichoderma</i> secondary	
metabolites	1
1. Introduction	3
2. Experimental materials and methods	7
2.1 Fungal strains	7
2.2 <i>Trichoderma</i> cultivation	8
2.3 Metabolites preparation	9
2.4 Plate confrontation test	10
2.5 Exclude proteins from the <i>Trichoderma</i> culture	10

2.6 Bioactivity of the metabolite of <i>Trichoderma</i>	11
2.7 Purification the antifungal molecules from <i>Trichoderma</i>	12
2.8 Structure determination by NMR	19
 3. Results	 21
3.1 Antagonistic potency of <i>Trichoderma</i> strains	21
3.2 <i>T. koningii</i> RIS 3-8 cultivation on PDA	23
3.3 Secondary metabolites contribute major potency of <i>T. koningii</i> RIS 3-8 against phytopathogens	 25
3.4 <i>T. koningii</i> RIS 3-8 cultivation on straw residue medium.....	27
3.5 Isolation and characterization of bioactive secondary metabolites	 28
3.5.1 The variation of metabolite between dry weight and cultivation on days	 28
3.5.2 The antifungal activities of Extraction	30
3.5.3 The antifungal activity of partitioned EG	35
3.6 Structure determination of isolated compound	35
3.7 The antifungal assay of compounds	38
3.8 Effect of the compounds on the growth of <i>Trichoderma</i>	40

4. Discussion	43
5. Conclusion	45
6. References	47

Part II Antifungal potency of the organic ethoxy ether functionalized imidazolium salts	49
1. Introduction	51
2. Experimental Materials and Methods	55
2.1 Preparation of ethoxy ether functionalized imidazolium salts	55
2.2 <i>Rhizoctonia</i> cultivation	56
2.3 Antifungal assays	56
2.4 IC₅₀ determination	56
2.5 Morphological observation by fluorescent stereomicroscope	57
3. Results	59
3.1 Antifungal activity	59
3.2 Morphological observation	60

4. Discussion	65
5. Conclusion	67
6. References	69
7. Appendix	71
7.1 Fungicides screening from the <i>Trichoderma</i> secondary metabolites	71
7.1.1 Characteristics of Common Organic Solvents	71
7.1.2 The secondary metabolites of the most important fungal <i>Trichoderma</i>, include classes and structures	73
7.1.3 Purification the antifungal molecules by TLC and HPLC	97
7.1.4 ¹H-NMR spectra of Compound A	104
7.1.5 ¹H-NMR spectra of Compound B	105
7.1.6 ¹H-NMR spectra of Compound C	106
7.1.7 ¹H-NMR spectra of Compound D	107
7.1.8 ¹H-NMR spectra of Compound E	108
7.1.9 ¹H-NMR spectra of Compound F	109

7.2 Antifungal potency of the organic ethoxy ether functionalized	
imidazolium salts	110
7.2.1 The <i>R. soloni</i> morphology cell wall observation	110
7.2.2 The <i>R. soloni</i> morphology nucleus observation	112
7.2.3 Calculate the hyphal length and the hyphae amount	113

Figure legends

Part I

- Fig. 1** The strategy of isolation compounds A, B, C, D, E, and F. 18
- Fig. 2** Morphology development of cultivated *T. koningii* RIS 3-8 on the PDA plates at 28 °C. 24
- Fig. 3** The antifungal activity assays of culture media without treatment (■), heat (■), and protease K (■). 26
- Fig. 4** Cultivation of *Trichoderma* on pulverized rice straw residue medium soaked with liquid mineral medium. *Trichoderma* mycelia side view (a) and (b); mycelia side view and green conidia (c); bottom view mycelia and green conidia (d). 27
- Fig. 5** The dry weight of chloroform/methanol extracted fractions from *T. koningii* RIS 3-8 in pulverized rice straw medium supplement with Extraction C (◆), Extraction G (■) and Extraction F (▲). 29
- Fig. 6** The antifungal activities of metabolite extraction of 3rd, 6th, 9th, 12th, 15th, 18th and 21st days from EC (a), EG (b), and EF (c). Fungicide (×), sample concentrations 15 µg plug⁻¹ (◆), 150 µg plug⁻¹ (▲), 1500 µg plug⁻¹ (■). Values are means of three replications ± SE. 32

Fig. 7 The antifungal activities of metabolite of 3rd, 6th, 9th, 12th, 15th, 18th and 21st days from EC₁₅₀₀ (◆), EG₁₅₀₀ (■), and EF₁₅₀₀ (▲). Values are means of three replications ± SE.	33
Fig. 8 The antifungal activities of metabolite of 9th days from EC₁₅₀₀, EG₁₅₀₀, and EF₁₅₀₀. Values are means of three replications ± SE (P < 0.05).	34
Fig. 9 Scheme of each purified compound.	
1-hydroxy-3-methylanthracene-9,10-dione (a), methyl 4-hydroxybenzoate (b), methyl 4-hydroxycinnamate (c), 4-hydroxybenzaldehyde (d), 4-hydroxyacetophenone (e). ...	37
Fig. 10 Mycelia growth and sporulation promotion of <i>Trichoderma</i> by the 4-hydroxybenzaldehyde (HBA) and 4-hydroxyacetophenone (Piceol) in 500µg mL⁻¹	42
Fig. 11 The fractions A1-1-1, and observed by 254 nm (a). The wavelengths of UV light were 254 nm (green background).	97
Fig. 12 The pure compound A14-7-2 was separated from A14-7. The fractions A14-7, and observed by 254 nm (a); The HPLC chromatogram (b).	98
Fig. 13 The pure compound A14-7-3 was separated from A14-7. The fractions A14-7, and observed by 254 nm (a); The HPLC	

chromatogram (b). 99

Fig. 14 The distribution of components from fractions A15-1 to A15-6. Lane 1: A15-1, lane 2: A15-2, lane 3: A15-3, lane 4: A15-4, lane 5: A15-5, lane 6: A15-6, and observed by 254 nm (a) and burning TLC (b). The wavelengths of UV light were 254 nm (green background) and burning TLC (gray background). 100

Fig. 15 The pure compound A15-4-1 was separated from A15-4. The HPLC chromatogram (a); The wavelengths of UV light were 254 nm (b). 101

Fig. 16 The distribution of components from fractions A16-1 to A16-6. Lane 1: A16-1, lane 2: A16-2, lane 3: A16-3, lane 4: A16-4, lane 5: A16-5, lane 6: A16-6, and observed by 254 nm (a), 365 nm (b) and burning TLC (c). The wavelengths of UV light were 254 nm (green background), 365 nm (blue background) and burning TLC (gray background). 102

Fig. 17 The pure compound A16-5-1 was separated from A16-5. The HPLC chromatogram (a); The wavelengths of UV light were 254 nm (b); burning TLC (c). 103

Figure legends Continue

Part II

Fig. 1 The inhibition capacity of various alkyl length of the
[C_n-im-3OEG][Cl] compounds to *R. soloni*. 59

Fig. 2 The *R. soloni* morphology observation in the present of 130
μM , [C₁₄-im-3OEG][Cl] under the 600 x Fluorescent
stereomicroscope. Scale bars = 0.5 mm. The more septa and
hyphae swelled along with longer period of treatment. Many
tiny blue dots and blue smear area were debris of lysed hyphae.
Arrow indicated the position of the septum . (A), (C), (E)
Control groups: (B), (D), (F) [C₁₄-im-3OEG][Cl] treatment
groups. (A), (B) 24hpi; (C), (D) 72hpi; and (E), (F) 144hpi.
Treatment the present of 2000 μM, 144hpi (G). 62

Fig. 3 The *R. soloni* nuclei morphology observation in the present of
130 μM [C₁₄-im-3OEG][Cl] 72hpi under the 600 x
Fluorescent stereomicroscope. Scale bars = 0.5 mm. More
bright spots, represented nuclei, showed in the
[C₁₄-im-3OEG][Cl] treated hyphae 72 hpi (D) then control
group (B). Also, the septa shorter and hyphae swelled can be
observed. 63

Table contents

Part I

Table. 1 Antagonistic potency of <i>Trichoderma</i> strains	22
Table. 2 Information of isolated compounds	36
Table. 3 Inhibition bioactivity of purified compounds from <i>Trichoderma</i> against <i>F. solani</i> , <i>F. oxysporum</i> , <i>R. solani</i> and <i>B. cinerea</i> . Values are inhibition percentage in means of three replicates in percentage \pm SD.	39
Table. 4 Among the various pathogens growth length of the <i>Trichoderma</i> of compounds 1 to 5.	41

Part I

木黴菌二次代謝產物之殺真菌功能

Fungicides screening from the *Trichoderma* secondary metabolites

1. Introduction

Fungi are among the most important organisms in the world with the figure of 1.5 million estimated fungal species (Mueller & Schmit, 2007). The Fungi are classified as the *Eumycota* kingdom. The major fungal characters are their cell wall composed mainly of chitin while cellulose of plant and they are saprophore (Bartnicki-Garcia, 1968). Based on their sexual or asexual reproductive characteristics, fungi have been classified to Chytridiomycota, Neocallimastigomycota, Blastoclasiomycota and Basidiomycota.

Biological control agents (BCAs) provide an alternative route to regulated plant pathogens population in the field other than chemical fungicides (Jose *et al.*, 2008; Lorito *et al.*, 2008; Harman *et al.*, 2004; Sweetingham, 1995; Compant *et al.*, 2005). *Trichoderma* spp. are proven to be excellent BCAs in greenhouse and in field as biopesticides and biofertilizers (Harman *et al.*, 2004). The fungal *Trichoderma* species are present in a diverse array of habitats, including soil, marine sediments, marine sponges, and mangroves. *Trichoderma* belongs to Eukaryota (Superkingdom), Fungi kingdom, Ascomycota, Pezizomycotina, Sordariomycetes, Hypocreomycetidae, Hypocreales, Hypocreaceae, *Trichoderma*. The most common BCAs of the *Trichoderma* spp. are *T.*

harzianum, *T. virens* and *T. viride*, which have been studied extensively (Verma *et al.*, 2007; Hermosa *et al.*, 2000). *Trichoderma* are well-known producers of volatile and nonvolatile secondary metabolites with antibiotic activity such as T22 azaphilone and harzianopyridone (Sivasithamparam and Ghisalberti 1998; Reino *et al.* 2008; Vinale *et al.* 2008a; Vinale *et al.*, 2009). At high concentrations they act as chemical defense against competition with other microorganisms in species-rich environments, such as the rhizosphere. However, at low concentrations, they work as quorum-sensing molecules for intra- or interspecies signaling (Fajardo *et al.*, 2008). The mechanism of these compounds might be being antibiotics, elicitor of systemic or acquired resistant to enhance host plant defense themselves against phytopathogens. Among these antibiotics, the production of gliovirin, gliotoxin, viridin, pyrones, peptaibols and others have been described (Vey *et al.*, 2001). Moreover, research has identified compounds produced by fungi that have inhibitory biological effects against viruses (Meselhy *et al.*, 1998; Halawany *et al.*, 2008), bacteria, fungi, and cancer cells (Hetland *et al.*, 2008).

In this study, *T. koningii* RIS 3-8 exhibits the best antifungal potency, among 23 isolates of *Trichoderma* spp., against tested phytopathogens. Antifungal assays were performed using *Trichoderma* spp. secondary

metabolites produced against pathogens. *T. koningii* RIS 3-8 bioactive secondary metabolites against phytopathogens were isolated and named 4-hydroxybenzaldehyde (1), 4-hydroxyacetophenone (2), 1-hydroxy-3-methylanthracene-9,10-dione (3), methyl 4-hydroxybenzoate (4), methyl 4-hydroxycinnamate (5).

2. Experimental materials and methods

All the solvents except Hexanes (ACS grade, Mallinckrodt Chemicals, Paris, Kentucky, USA) and Benzene (SHOWA, Japan) were purchased from ECHO Chemical, Miaoli, Taiwan. 254 nm and 365 nm UV lamp (VL-6.LC 254/365 nm, Vilber Lourmat, France) was used for visualization. Silica gels of G60, 70~230 meshes, pH 7 (SILICYCLE, Québec, Canada) were used.

2.1 Fungal strains

All 23 tested *Trichoderma* spp. and eight fungal pathogens were obtained from the Microbiology laboratory of National Formosa University. The 23 *Trichoderma* spp. used in this research were *T. atroviride* ETS1-1-2, *T. atroviride* ETS1-1-4, *T. atroviride* ETS1-1-10, *T. harzianum* ETS3-1-1, *T. harzianum* ETS3-2-1, *T. harzianum* ETS3-3-2, *T. harzianum* ETS4-2-1, *T. virens* KS-CO R8-8, *T. virens* LN-PA R3-2, *T. virens* LN-PA R4-2, *T. virens* LN-PA S16-2, *T. virens* LN-PA S16-9, *T. harzianum* NT-TA R1-9, *T. harzianum* NT-TA S3-9, *T. harzianum* SL-BN R1-4, *T. harzianum* SL-BN R1-9, *T. harzianum* SL-BN S5-2, *T. virens* YAM 1-1, *T. virens* YAM 1-5, *T. virens* YAM 3-1, *T. virens* YAM 3-5, *T. koningii* TA-GL R1-6 and *T.*

koningii RIS 3-8. Other phytopathogenic fungi tested in this research were *Colletotrichum gloeosporioides*, *F. solani* f. sp. Fs-69, *F. solani* f. sp. Fs-75, *F. oxysporum* f. sp. Fo-43, *F. oxysporum* f. sp. Fo-59, *Rhizoctonia solani*, *Sclerotinia sclerotiorum* and *Sclerotium rolfsi*. The fungal strains were maintained on potato dextrose agar (PDA, Becton, Dickinson and Company, New Jersey, USA) slants at room temperature.

2.2 *Trichoderma* cultivation

Ten mL PDA plate (90 x 15mm petri dish, Alpha lus scientific corp., Taoyuan, Taiwan) was prepared by dissolving PDA (39 g L⁻¹) in demonized water by Milli-Q (18 µΩ, Millipore, MA, USA) and sterilized by TM-329 (TOMIN, Taipei, Taiwan) at 121 °C, 1.2 kg cm⁻² for 15 min. *Trichoderma* spp. was inoculated on PDA and cultivated at 28 °C for 5 days in the incubator, stored at 4 °C until use. Conidia were collected by flushing the cultivated medium with 6 mL of sterile water to acquire 10⁶ conidia mL⁻¹ conidia suspension.

2.3 Metabolites preparation

To obtain the *Trichoderma* secondary metabolites, straw residue were dried at 50 °C in an oven for 5 days and pulverized by a homogenizer. Later, 60 g straw residue pulverized were soaked and mixed with 120 mL liquid mineral medium, which contains: $\text{CaCl}_2 \cdot 2\text{H}_2\text{O}$ (0.12 g L⁻¹, Showa, Tokyo, Japan), Na_2HPO_4 (2 g L⁻¹, TEDIA, Ohio, USA), $\text{MgSO}_4 \cdot 7\text{H}_2\text{O}$ (1.5 g L⁻¹, J. T. Baker, Phillipsburg, USA), FeCl_3 (2 mg L⁻¹, Sigma, St Louis, Missouri, USA), $(\text{NH}_4)_2\text{SO}_4$ (0.5 g L⁻¹, Showa), KH_2PO_4 (7 g L⁻¹, J. T. Baker), $\text{ZnSO}_4 \cdot 7\text{H}_2\text{O}$ (1 mg L⁻¹, Ferak, Berlin, Germany) in a 2800 mL Erlenmeyer flask. The medium was autoclaved at 121 °C, 1.2 kg cm⁻² for 15 min before used. 6 mL of suspension of conidia was inoculated into the mixture and cultivated at 28 °C in the dark for 9 days in the incubator. Cultivated *Trichoderma* medium was extracted with solvent after drying at 50 °C in the oven. The straw residue cultures were filtered through filter paper (Advantec No. 1, Toyo Roshi Kaisha, Tokyo, Japan) by a vacuum filtration apparatus. The solvent of the filtrate was removed by a rotary evaporator at 35 °C. The solvent was applied back to the medium to intensify the extraction then solvent was removed. The procedure would be preceded 5 times until filtrates were colorless. Each extract was placed in the oven at 50 °C and dry weight of equal volume chloroform/methanol

extracted metabolites was determined.

2.4 Plate confrontation test

Mycelia of tested fungus were obtained from actively growing margin of PDA. Two 5-mm diameter plugs each contained one of the twenty-three *Trichoderma* strains and one of the eight fungal pathogens, respectively, were placed opposite side of the PDA plate and growth diameter were recorded daily until two species mycelia contacted.

2.5 Exclude proteins from the *Trichoderma* culture

Trichoderma conidia 10^6 conidia mL⁻¹ were inoculated in 250 mL of minimal medium, which contains: 0.5 mg of CaCl₂ · 2H₂O, 1.25 mg of FeCl₃, 0.125 g of MgSO₄ · 7H₂O, 0.25g of peptone, 0.34 g of KH₂PO₄, 0.125 g of Na₂CO₃ · H₂O, 0.35 mg of ZnSO₄ · 7H₂O, plus 1 % glucose (Media I) or in 1 % of heat deactivated *F. solani* mycelia (Media II). Each culture medium was lyophilized and resuspended in 3 mL Milli-Q (18 µΩ) water. An aliquot of 1 mL solution was treated by protease K (100 µL protease K (50 µg/mL) and 900 µL culture medium), 37 °C, 24 hr; another

1 mL aliquot was heated in 100 °C, cool down to room temperature, repeat this procedure for another two times; the remaining material would be the control group. Then, each preparation was mixed with 49 mL of one-fifths concentration of PDA and three 90 x 15 mm petri dishes were prepared. A plug of *F. solani* was placed in the center of above mentioned preparations and the growth of mycelia in cm was recorded daily for 6 days at 37 °C. Each treatment consisted of three replicates.

2.6 Bioactivity of the metabolite of *Trichoderma*

After mixing 60 g of pulverized rice straw residue with 120 mL of liquid mineral medium supplemented with 1 % glucose or 1 % deactivated *F. solani* mycelia, 6 mL of *Trichoderma* conidia solution (10^6 conidia mL⁻¹) was added. The mixture was incubated at 28 °C in the dark for 3, 6, 9, 12, 15, 18, and 21 days. Cultivated media were extracted with solvent and drying at 50 °C in the oven. Chloroform / methanol, 1:1 (v/v) were used to extract the metabolites from three different cultivated media that were with untreated (Extraction C, EC), or supplemented either with 1 % glucose (Extraction G, EG) or with 1 % deactivated *F. solani* mycelia (Extraction F, EF), respectively. Antifungal assays were performed using *Trichoderma*

secondary metabolites produced against *F. solani*. The pathogen *F. solani* growth was determined by measuring the diameter (cm) of the mycelium plugs after 40 hpi. Each treatment consisted of three replicates.

2.7 Purification the antifungal molecules from *Trichoderma*

Chloroform / methanol, 1:1 (v/v) was used to extract the secondary metabolites from *Trichoderma* cultivated for 9 days. The extract was partitioned using CHCl₃ / H₂O, 1:1 (v/v), and the dry weight of CHCl₃ layer and H₂O layer were recorded. Nineteen fractions (A1 to A19) were obtained from the CHCl₃ extract after fractionation by silica gel column (56 × 500 mm) eluting with Benzene/EtOAc, 50:1, 25:1, 15:1, 10:1, 5:1 3:1, 2:1, 1:1 (v/v) (step gradient with EtOAc). The isolation strategy of each purified compound was shown in Fig.1.

Purification method for the compound A:

Chloroform / methanol, 1:1 (v/v) was used to extract the metabolites from *Trichoderma* cultivated medium. The extract was partitioned using CHCl₃ / H₂O, 1:1 (v/v), and the dry weights of CHCl₃ layer and H₂O layer were recorded. Nineteen fractions (A1 to A19) were obtained from the

CHCl₃ extract after fractionation by silica gel column (G60, 70~230 meshes, 56 × 500 mm) eluting with Benzene/EtOAc, 50:1, 30:1, 15:1, 10:1, 5:1, 3:1, 1:1 (v/v) (step gradient of EtOAc), with 1 mL min⁻¹ flow rate. Two fractions (A1-1 and A1-2) of the fraction A1 was obtained by silica gel column (G60, 70~230 meshes, 56 × 500 mm) eluting with Hexanes/EtOAc, 10:1 (v/v). Compound A was obtained by eluting fraction A1-1 in silica gel column silica gel column (G60, 70~230 meshes, 56 × 500 mm) with Hexanes/EtOAc, 20:1 (v/v).

Purification method for the compound B:

Chloroform / methanol, 1:1 (v/v) was used to extract the metabolites from *Trichoderma* cultivated medium. The extract was partitioned using CHCl₃/ H₂O, 1:1 (v/v). Nineteen fractions (A1 to A19) were obtained from the CHCl₃ extract after fractionation by silica gel column (silica gel column (G60, 70~230 meshes, 56 × 500 mm) eluting with Benzene/EtOAc, 50:1, 30:1, 15:1, 10:1, 5:1, 3:1, 1:1 (v/v) (step gradient of EtOAc), flow rate 1 mL min⁻¹. Fraction A11 was chromatographed in silica gel column (G60, 70~230 meshes, 56 × 500 mm) with by Benzene / Acetone, 30:1 (v/v) and 15 fractions (fractions A11-1 to 15) were collected. Compound B was obtained by eluting fraction A11-6 with MeOH/H₂O, 55:45 (v/v), and flow

rate of 0.3 mL min⁻¹ in the reversed phase column (Discover[®] C18 HPLC column, 250 mm × 4.6 mm, 5 μm, Supelco, Bellefonte, Pennsylvania, USA).

Purification method for the compound C:

Chloroform / methanol, 1:1(v/v) was used to extract the metabolites from *Trichoderma* cultivated medium. The extract was partitioned using CHCl₃ / H₂O, 1:1 (v/v). Nineteen fractions (A1 to A19) were obtained from the CHCl₃ extract after fractionation by silica gel column (56 × 500 mm) eluting with Benzene / EtOAc, 50:1, 30:1, 15:1, 10:1, 5:1, 3:1, 1:1 (v/v) (step gradient with EtOAc). Fraction A14 was separated to 10 fractions (fraction A14-1 to 10) by silica gel column (silica gel column (G60, 70~230 meshes, 56 × 500 mm) using CHCl₃ / Acetone, 100:1 (v/v), as mobile phase. Compound C in fractions A14-7 contained was obtained by loading the fraction A14-7 to the reversed phase Discover[®] C18 HPLC column (250 mm × 4.6 mm, 5 μm) using MeOH / H₂O, 90:10 (v/v) as mobile phase with flow rate of 0.4 mL min⁻¹.

Purification method for the compound D:

Chloroform / methanol, 1:1(v/v) was used to extract the metabolites from *Trichoderma* cultivated medium. The extract was partitioned using CHCl_3 / H_2O , 1:1 (v/v), and the dry weights of CHCl_3 layer and H_2O layer were recorded. Nineteen fractions (A1 to A19) were obtained from the CHCl_3 extract after fractionation by silica gel column (G60, 70~230 meshes, 56×500 mm) eluting with Benzene/EtOAc, 50:1, 30:1, 15:1, 10:1, 5:1, 3:1, 1:1 (v/v) (step gradient with EtOAc). Fraction A14-7 was obtained by further fractionation of fraction A14 by silica gel column (silica gel column (G60, 70~230 meshes, 56×500 mm) by CHCl_3 / Acetone, 100:1 (v/v) and 10 fractions were collected (A14-1 to 10). Among them, compound D in fraction A14-7 contended was obtain by loaded the fraction A14-7 to the reversed phase Discover[®] C18 HPLC column (250 mm \times 4.6 mm, 5 μm) using MeOH / H_2O , 90:10 (v/v) as mobile phase with flow rate of 0.4 mL min⁻¹.

Purification method for the compound E:

Chloroform / methanol, 1:1(v/v) was used to extract the metabolites from *Trichoderma* cultivated medium. The extract was partitioned using CHCl_3 / H_2O , 1:1 (v/v), and the dry weights of CHCl_3 layer and H_2O layer

were recorded. Nineteen fractions (A1 to A19) were obtained from the CHCl_3 extract after fractionation by silica gel column (G60, 70~230 meshes, 56×500 mm) eluting with Benzene / EtOAc, 50:1, 30:1, 15:1, 10:1, 5:1, 3:1, 1:1 (v/v) (step gradient with EtOAc). Fraction A15-4 was obtained from fraction A15 that was further separated to 6 fractions (A15-1 to 6) by A15-loaded silica gel column (G60, 70~230 meshes, 56×500 mm) eluting with Benzene / Acetone, 15 : 1 (v/v). Compound E was purified from the fraction A15-4 by the reversed phase Discover[®] C18 HPLC column ($250 \text{ mm} \times 4.6 \text{ mm}$, $5 \mu\text{m}$) using MeOH / H_2O , 20:80 (v/v) as mobile phase with flow rate of 0.5 mL min^{-1} .

Purification methods for the compound F:

Chloroform / methanol, 1:1 (v/v) was used to extract the metabolites from *Trichoderma* cultivated medium. The extract was partitioned using CHCl_3 / H_2O , 1:1 (v/v), and the dry weights of CHCl_3 layer and H_2O layer were recorded. Nineteen fractions (A1 to A19) were obtained from the CHCl_3 extract after fractionation by silica gel column (G60, 70~230 meshes, 56×500 mm) eluting with Benzene/EtOAc, 50:1, 30:1, 15:1, 10:1, 5:1, 3:1, 1:1 (v/v) (step gradient of EtOAc), with 1 mL min^{-1} flow rate. Fraction A16 was further fractionated to 6 fractions by loading fraction

A16 to silica gel column (G60, 70~230 meshes, 56×500 mm) eluting with Benzene / Acetone, 30:1 (v/v). Compound F was obtained from fractions A16-5 by applying fraction A16-5 to the reversed phase Discover[®] C18 HPLC column ($250 \text{ mm} \times 4.6 \text{ mm}$, $5 \mu\text{m}$) using MeOH / H₂O, 20:80 (v/v) as mobile phase with flow rate of 0.5 mL min^{-1} .

Trichoderma secondary metabolites (9 days) C/M, 1:1 (v/v)

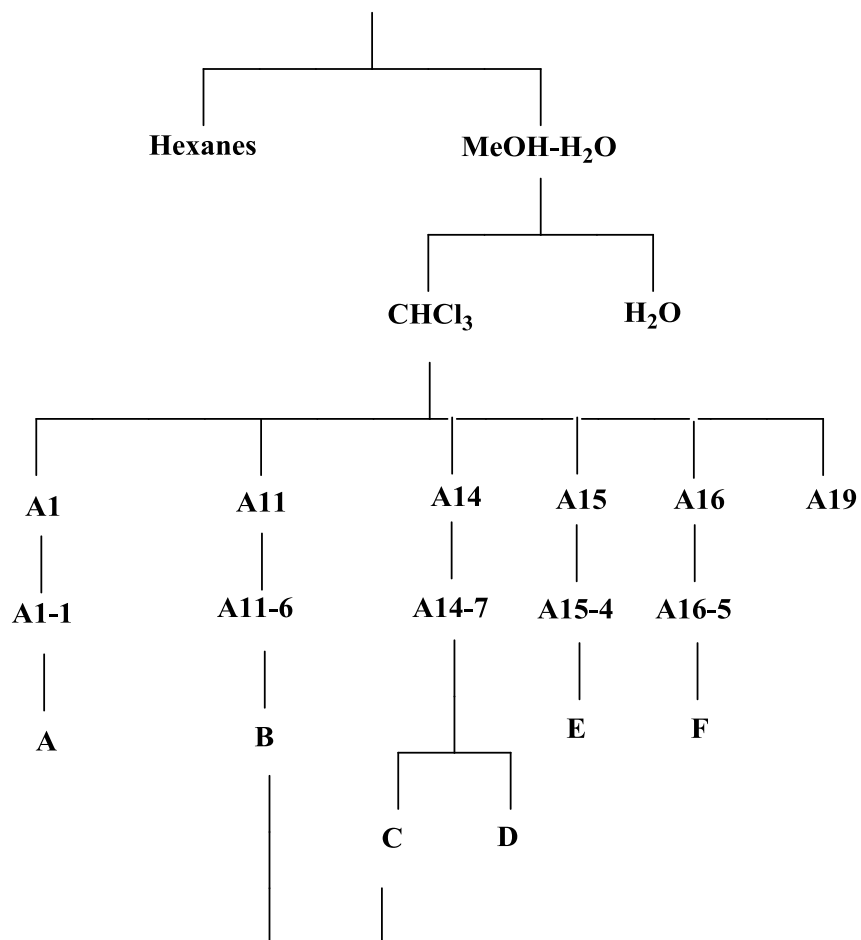


Fig. 1 The strategy of isolation compounds A, B, C, D, E, and F

2.8 Structure determination by NMR

The structure of each purified compound was determined by the nuclear magnetic resonance (NMR) (Appendix 7.1.4 to 7.1.9). Compound A is 1-hydroxy-3-methylanthracene-9,10-dione, ^1H NMR (400 MHz, CDCl_3 , ppm): δ 2.45 (s, 3H, H_{11}), 7.17 (d, 1H, H_1), 7.31 (2d, 1H, H_7), 7.62 (d, 1H, H_5), 7.69 (d, 1H, H_4), 8.27 (d, 1H, H_8), 12.55 (s, OH) (Fig. 15a) (Liu *et al.*, 2009). Compound B and Compound C have same structure, it is named methyl 4-hydroxybenzoate, ^1H NMR (400 MHz, CDCl_3 , ppm): δ 3.91 (s, 3H, $-\text{COOCH}_3$), 6.86 (2d, 2H, Ar-CH), 7.95 (s, 1H, -OH) (Fig. 15b) (Vijayan *et al.*, 2003). Compound D is named methyl 4-hydroxycinnamate, ^1H NMR (400 MHz, CDCl_3 , ppm): δ 3.75 (s, 3H, CO_2CH_3), 6.30 (d, 1H, H_2), 6.85 (2d, 2H, H_3 and H_5), 7.53 (2d, 2H, H_2 and H_6); 7.63 (d, 1H, H_7) (Fig. 15c) (Daayf *et al.*, 1997). Compound E is named 4-hydroxybenzaldehyde, ^1H NMR (400 MHz, CDCl_3 , ppm): δ 6.96 (2d, 2H, Ar-CH), 7.82 (2d, 2H, Ar-CH), 9.87 (s, 1H, -CHO) (Fig. 15d) (Chena *et al.*, 2010). Compound F is named 4-hydroxyacetophenone, ^1H NMR (400 MHz, CDCl_3 , ppm): δ 2.56 (s, 3H, $-\text{COCH}_3$), 6.89 (2d, 2H, Ar-CH), 7.91 (s, 1H, -OH) (Fig. 15e) (Anzenbacher *et al.*, 1999).

3. Results

3.1 Antagonistic potency of *Trichoderma* strains

Various *Trichoderma* species own different potency against diverse fungal phtopathogens. To have the best *Trichoderma* candidate that might produce the most potent metabolites, a matrix of duel experiments and extent of antagonistic potency of *Trichoderma* strains against fungal phytopathogens was determined (Table. 1). From the scale of A to D that higher score indicates better antifungal pathogens activity, *T. koningii* RIS 3-8 poses the best antagonistic potency among all the tested *Trichoderma*. In the other words, phytopathogens such as *F. solani* (Fs), *F. oxysporum* (Fo), *C. gloeosporioides* (Ch), *R. solani* (RS), *S. sclerotiorum* (Ds) and *S. rolfsi* (Sc) were highly susceptible to *T. koningii* RIS 3-8 antagonization.

Table. 1 Antagonistic potency of *Trichoderma* strains

PDA	Fs-69	Fs-75	Fo-43	Fo-59	Ch	RS	DS	SC
ETS 1-1-2	B	C	B	B	C	C	C	C
ETS 1-1-4	B	A	B	B	C	C	C	C
ETS 1-1-10	B	B	C	B	C	C	C	C
ETS 3-1-1	B	C	B	B	C	C	C	C
ETS 3-2-1	B	D	C	C	D	D	C	D
ETS 3-3-2	B	B	B	B	C	C	C	C
ETS 4-2-1	B	C	B	B	C	C	C	A
KS-CO R8-8	B	B	C	B	C	C	C	C
LN-PA R3-2	D	C	D	B	C	A	C	A
LN-PA R4-2	B	B	B	B	C	C	C	C
LN-PA S16-2	B	C	B	B	C	C	C	C
LN-PA S16-9	B	C	B	B	C	C	C	C
NT-TA R1-9	B	C	D	C	D	D	D	C
NT-TA S3-9	B	B	B	B	C	A	C	A
SL-BN R1-4	C	B	C	B	B	C	C	C
SL-BN R1-9	B	B	C	B	B	C	C	C
SL-BN S5-2	B	B	D	C	D	D	D	C
TA-GL R1-6	B	B	B	B	B	B	C	A
YAM 1-1	B	B	C	C	B	A	C	A
YAM 1-5	B	B	C	B	C	C	C	C
YAM 3-1	B	A	B	B	C	C	C	C
YAM 3-5	A	A	C	B	C	C	C	C
RIS 3-8	B	D	D	C	D	D	D	C

A: The growth of Pathogen overwhelm *Trichoderma*; B: Both of each can't cover each other; C: The growth of *Trichoderma* partially over pathogen; D: *Trichoderma* fully overwhelm pathogen.

3.2 *T. koningii* RIS 3-8 cultivation on PDA

To confirm the identity of the *T. koningii* RIS 3-8, green conidia were inoculated on the center of the new PDA plates and cultivated at 28 °C for 5 days. The morphology in hyphae, hyphae growth, sporulation and color of the conidia are typical *T. koningii* RIS 3-8 (Fig. 2). The hyphae growth began to germinate on the 0 hour post inoculation (hpi) (Fig. 2 (a)). The conidia began to germinate and white mycelia grew rapidly and covered half of the PDA plates on the 24 hpi (Fig. 2 (b)). The white hyphae covered whole plate on the 48 hpi (Fig. 2 (c)), then covered completely and a few green conidia were formed on the 72 hpi (Fig. 2 (d)). The amount of green conidia increased gradually and some green metabolites were secreted on the 96 hpi (Fig. 2 (e)), and fully development of green conidia spread all over the PDA plates on the 120 hpi (Fig. 2 (f)).

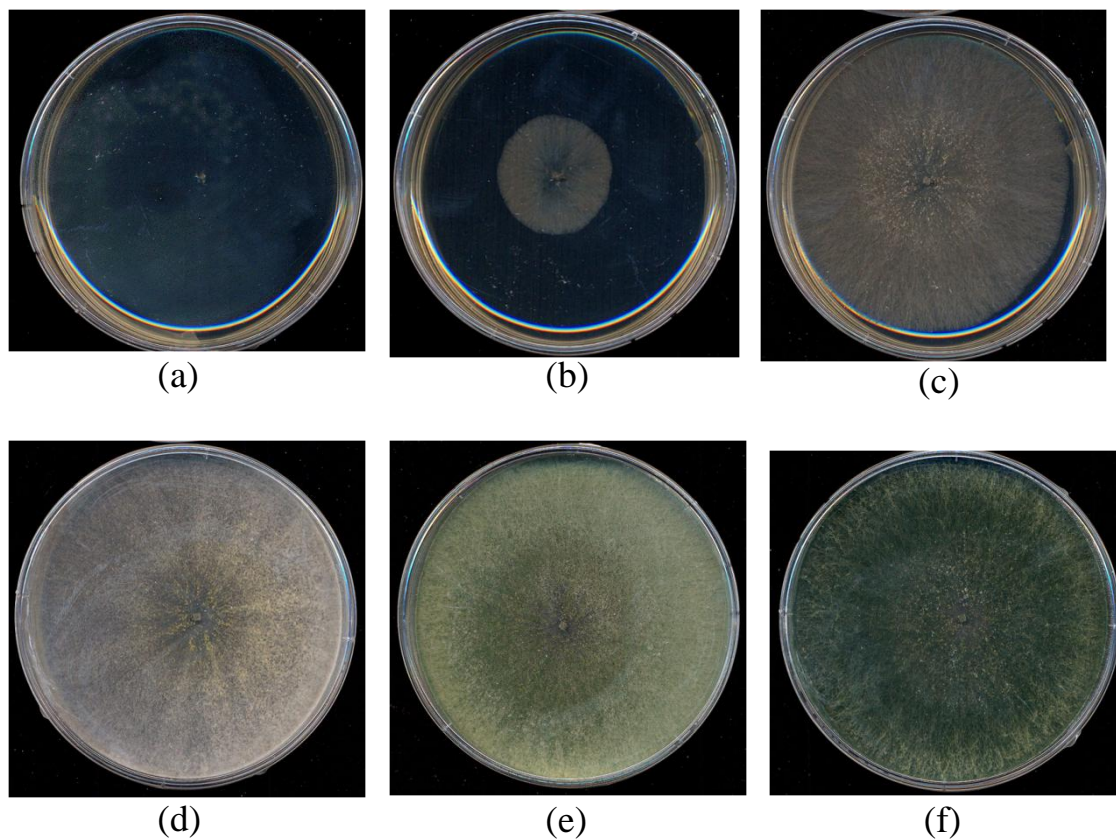


Fig. 2 Morphology development of cultivated *T. koningii* RIS 3-8 on the PDA plates at 28 °C. *Trichoderma* hyphae growth began to germinate on the 0 hpi (a), 24 hpi, a few white and covered half mycelia grew (b), 48 hpi, the white hyphae growth rapidly and covered of the PDA plates (c), 72 hpi, covered completely and a few green conidia were formed (d), 96 hpi, sporulation of green conidia (e) and 120 hpi, hyphae and green conidia spread all over the PDA plates (f).

3.3 Secondary metabolites contribute major potency of *T. koningii* RIS

3-8 against phytopathogens

The secretome of the *T. koningii* RIS 3-8 are composed of two major parts: organic compounds and proteins that both might contribute to its fungicidal potency. To distinguish each contribution, the heat-treated and protease-treated secretomic components of the *T. koningii* RIS 3-8 in minimal medium contained glucose (Media I) or heat-inactivated *F. solani* *f. sp.* Fs-75 (Media II) were tested their fungicidal potency (Fig. 3). It showed both treatments totally loss fungicidal activity indicate proteins had no role in the antagonistic tests that the secondary metabolites be primary components secreted by *T. koningii* RIS 3-8 to against *F. solani* on PDA (Fig. 3).

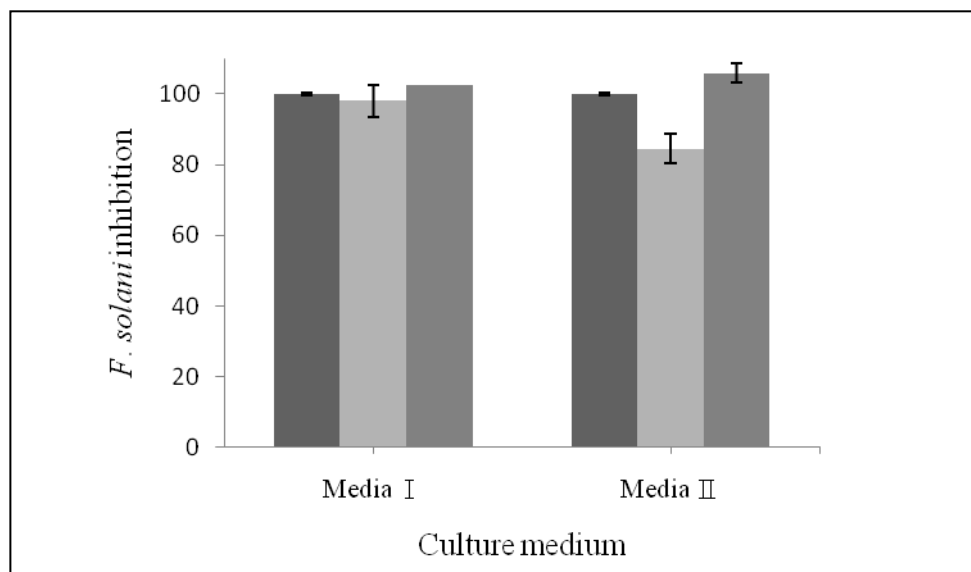


Fig. 3 The antifungal activity assays of culture media without treatment (■), heat (■), and protease K (■).

3.4 *T. koningii* RIS 3-8 cultivation on straw residue medium

For the cost effective mass production of the *T. koningii* RIS 3-8 secondary metabolites, the conidia of *T. koningii* was inoculated on pulverized rice straw residue medium soaked with liquid mineral medium. After 15 days, the media were covered with the hyphae of the *T. koningii* RIS 3-8 (Fig. 4 (a) to Fig. 4 (d)). Further tested the hyphae on to the PDA plate showed the same morphology characters (Fig. 2) of the *T. koningii* RIS 3-8.

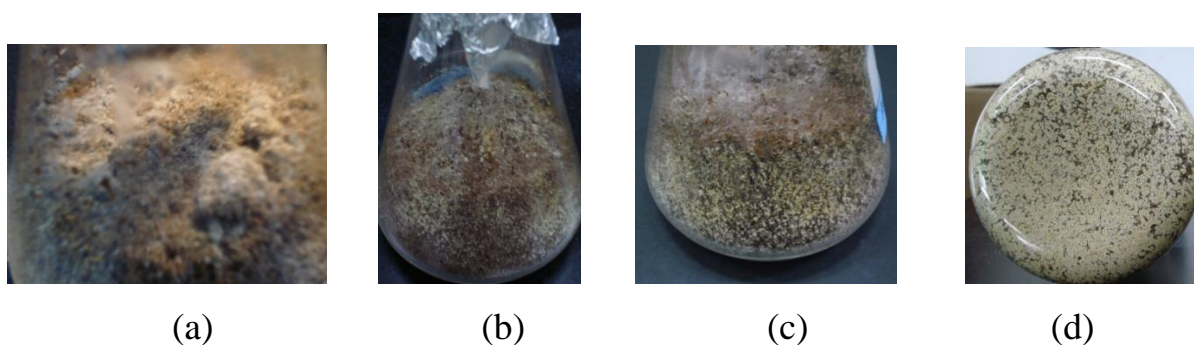


Fig. 4 Cultivation of *Trichoderma* on pulverized rice straw residue medium soaked with liquid mineral medium. *Trichoderma* mycelia side view (a) and (b); mycelia side view and green conidia (c); bottom view mycelia and green conidia (d).

3.5 Isolation and characterization of bioactive secondary metabolites

3.5.1 The variation of metabolite between dry weight and cultivation on days

In order to learn the largest metabolites production in the *T. koningii* RIS 3-8 pulverized rice straw, the cultures were cultivated Extraction C for 3, 6, 9, 12, 15, 18 and 21 days, dry weight were 4.43, 4.63, 5.10, 4.82, 4.82, 5.01 and 5.01 g, respectively, Extraction G for 3, 6, 9, 12, 15, 18 and 21 days, dry weight were 4.75, 4.47, 4.88, 5.25, 4.67, 4.84 and 4.94 g, respectively, and Extraction F for 3, 6, 9, 12, 15, 18 and 21 days, dry weight were 4.28, 4.77, 4.83, 5.39, 4.65, 5.03 and 5.12 g, respectively, (Fig. 5).

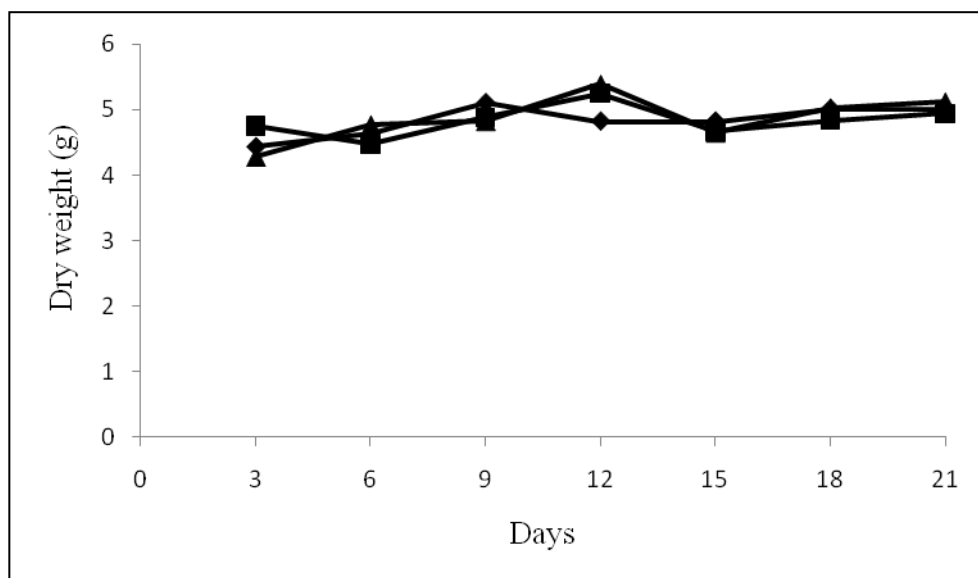
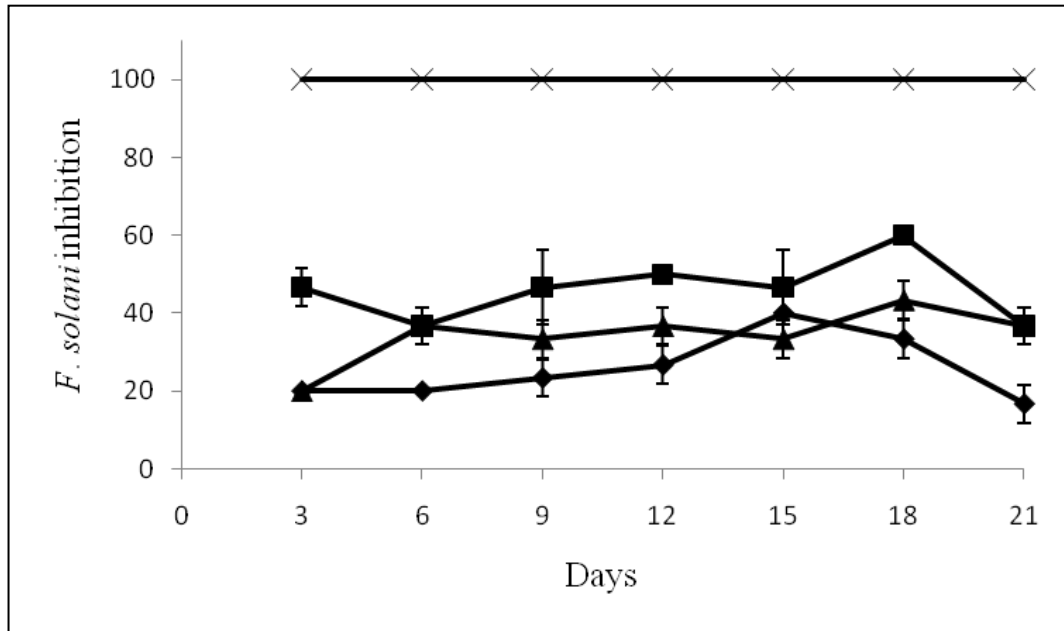


Fig. 5 The dry weight of chloroform / methanol extracted fractions from *T. koningii* RIS 3-8 in pulverized rice straw medium supplement with Extraction C (◆), Extraction G (■) and Extraction F (▲).

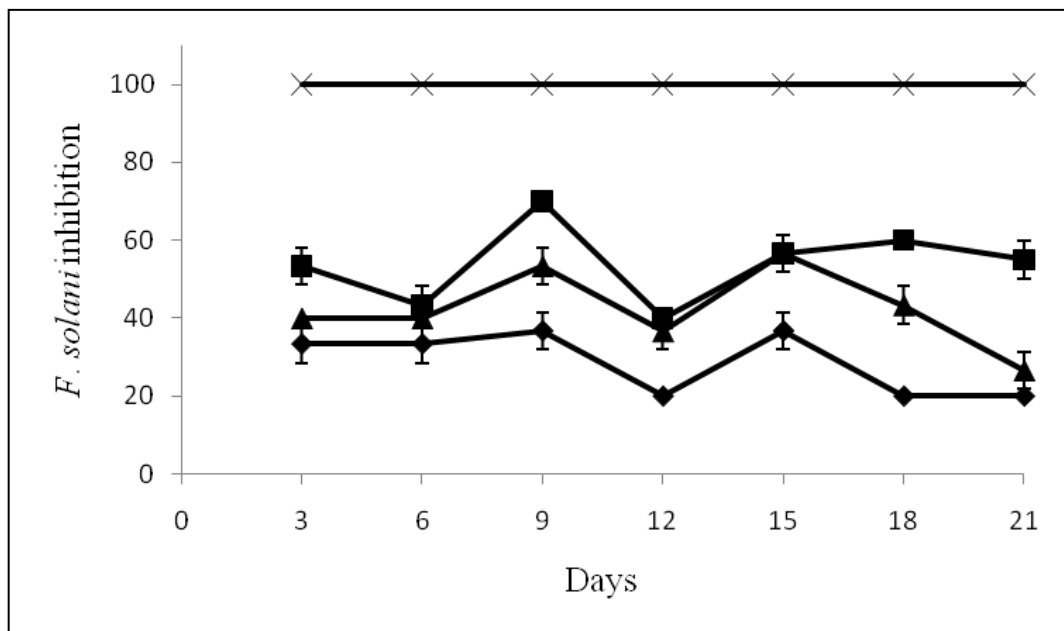
3.5.2 The antifungal activities of Extraction

To obtain the best potency against the *F. solani*, the antifungal activity of different concentrations of metabolites from different cultural conditions at various days ($EXN_{[C]}$, $EX = EC$, EG , and EF ; N = cultivated day; $[C] = \mu\text{g plug}^{-1}$) were determined (Fig. 6 and 7). Among tested three concentrations, $15 \mu\text{g plug}^{-1}$, $150 \mu\text{g plug}^{-1}$ and $1500 \mu\text{g plug}^{-1}$, showed positive concentration dependency. The *F. solani* inhibition potency of EC_{18} showed 33 % ($15 \mu\text{g plug}^{-1}$), 43 % ($150 \mu\text{g plug}^{-1}$), and 60 % ($1500 \mu\text{g plug}^{-1}$). $EC_{18_{1500}}$ had best potency against *F. solani* among tested days that were 47 %, 37 %, 47 %, 50 %, 47 %, 60 % and 37 % of 3rd, 6th, 9th, 12th, 15th, 18th and 21st day (Fig. 7). EG_9 showed 37 % ($15 \mu\text{g plug}^{-1}$), 53 % ($150 \mu\text{g plug}^{-1}$), and 70 % ($1500 \mu\text{g plug}^{-1}$) inhibition against *F. solani*. $EG_{9_{1500}}$ had best potency against *F. solani* among tested days that were 53 %, 43 %, 70 %, 40 %, 57 %, 60 % and 55 % of 3rd, 6th, 9th, 12th, 15th, 18th and 21st day (Fig. 7). EF_9 showed 33 % ($15 \mu\text{g plug}^{-1}$), 40 % ($150 \mu\text{g plug}^{-1}$) and 57 % ($1500 \mu\text{g plug}^{-1}$). $EF_{9_{1500}}$ showed best potency against *F. solani* among tested days that were 40 %, 53 %, 57 %, 47 %, 50 %, 57 % and 40 % of 3rd, 6th, 9th, 12th, 15th, 18th and 21st day (Fig. 8).

(a)



(b)



(c)

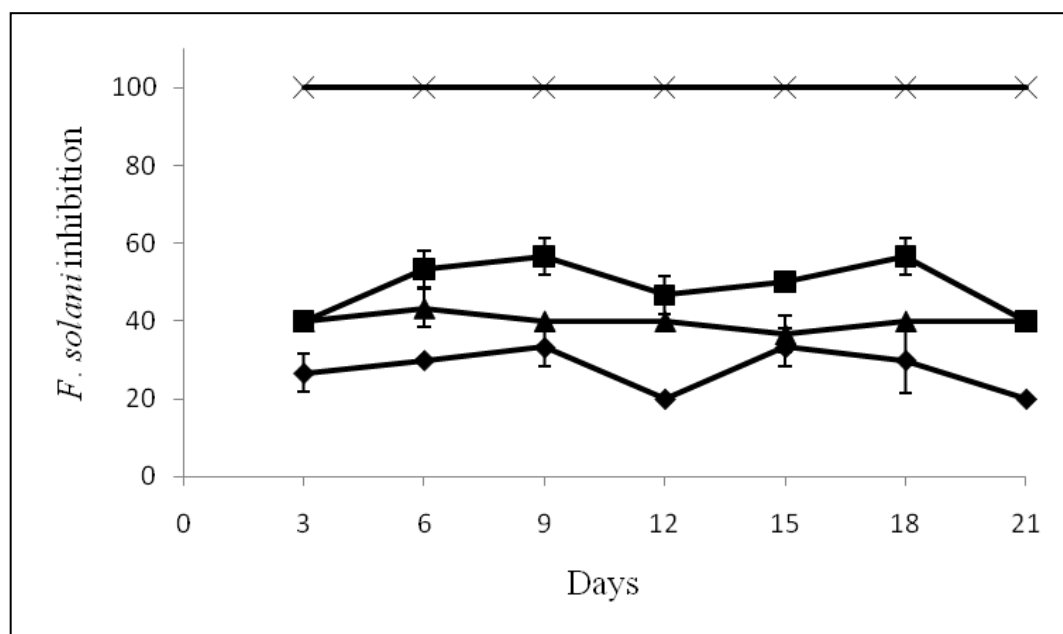


Fig. 6 The antifungal activities of metabolite extraction of 3rd, 6th, 9th, 12th, 15th, 18th and 21st days from EC (a), EG (b), and EF (c). Fungicide (x), sample concentrations 15 µg plug⁻¹ (◆), 150 µg plug⁻¹ (▲), 1500 µg plug⁻¹ (■). Values are means of three replications ± SE.

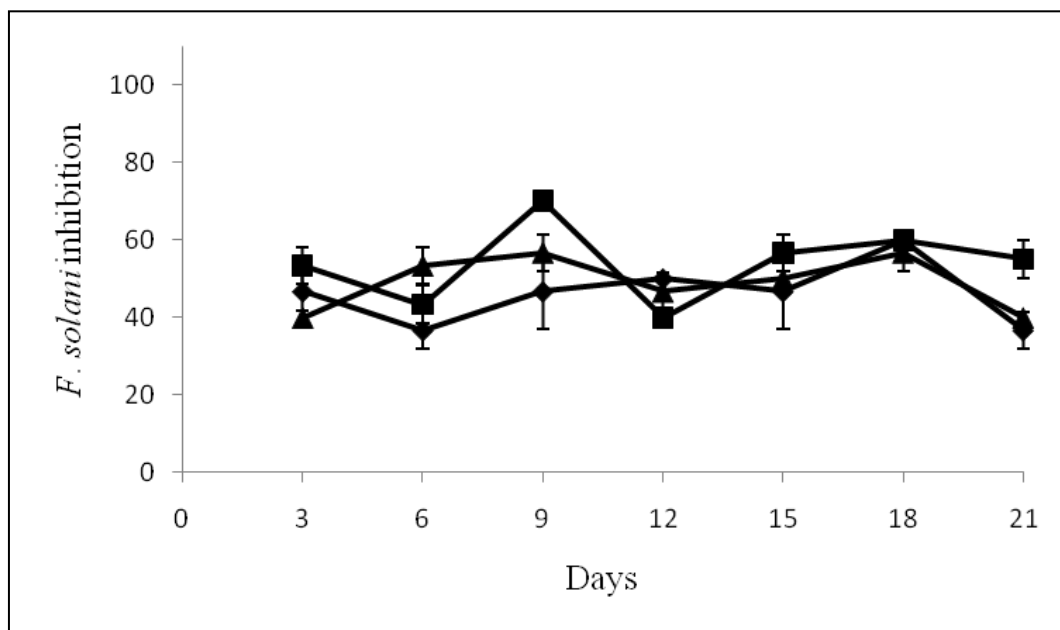


Fig. 7 The antifungal activities of metabolite of 3rd, 6th, 9th, 12th, 15th, 18th and 21st days from EC₁₅₀₀ (◆), EG₁₅₀₀ (■), and EF₁₅₀₀ (▲). Values are means of three replications \pm SE.

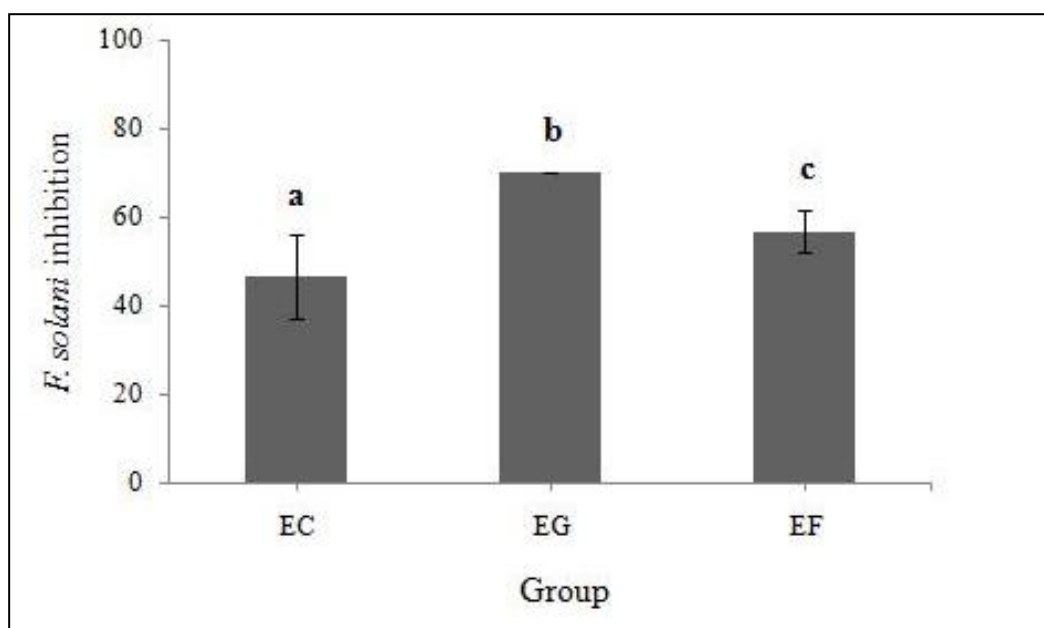


Fig. 8 The antifungal activities of metabolite of 9th days from EC₁₅₀₀, EG₁₅₀₀, and EF₁₅₀₀. Values are means of three replications \pm SE ($P < 0.05$).

3.5.3 The antifungal activity of partitioned EG

The EG9 metabolite was further partitioned with hexane and methanol which further partitioned with $\text{CHCl}_3\text{-H}_2\text{O}$ (1:1, v:v). The potency against *F. solani* of each partition, 1500 $\mu\text{g plug}^{-1}$, was 41.7 ± 0.0 % of hexane fraction, 24.3 ± 4.8 % of MeOH, and 79.9 ± 4.8 % of CHCl_3 . The CHCl_3 fraction was further fractionated through several chromatography columns to obtain 6 homogeneous compounds, A, B, C, D, E, and F. Later, structure determination showed compound B and C were identical material so that their information would be merged together. The yield of each compound was 0.049 % of A (5 mg), 0.023 % of B + C (2 mg), 0.025 % of D (2.2 mg), 0.022 % of E (1.9 mg), and 0.015 % of F (1.3 mg) (Table 2).

3.6 Structure determination of isolated compound

The structure of each compound was determined by the NMR. Compound A is 1-hydroxy-3-methylanthracene-9,10-dione; compound B + C is methyl 4-hydroxybenzoate; compound D is methyl 4-hydroxycinnamate; compound E is 4-hydroxybenzaldehyde (HBA); and compound F is 4-hydroxyacetophenone (Piceol) (Fig. 9).

Table. 2 Information of isolated compounds

Compound	IUPAC name	Molecular Formula	Molecular Weight	Dry weight (mg)	Production ratio (%)
A	1-hydroxy-3-methylanthracene-9,10-dione	C ₁₅ H ₁₀ O ₃	238.2381	5	0.049
B and C	methyl 4-hydroxybenzoate	C ₈ H ₈ O ₃	152.15	2	0.023
D	methyl 4-hydroxycinnamate	C ₁₀ H ₁₀ O ₃	178.18	2.2	0.025
E	4-hydroxybenzaldehyde (HBA)	C ₇ H ₆ O ₂	122.12	1.9	0.022
F	4-hydroxyacetophenone (Piceol)	C ₈ H ₈ O ₂	136.15	1.3	0.015

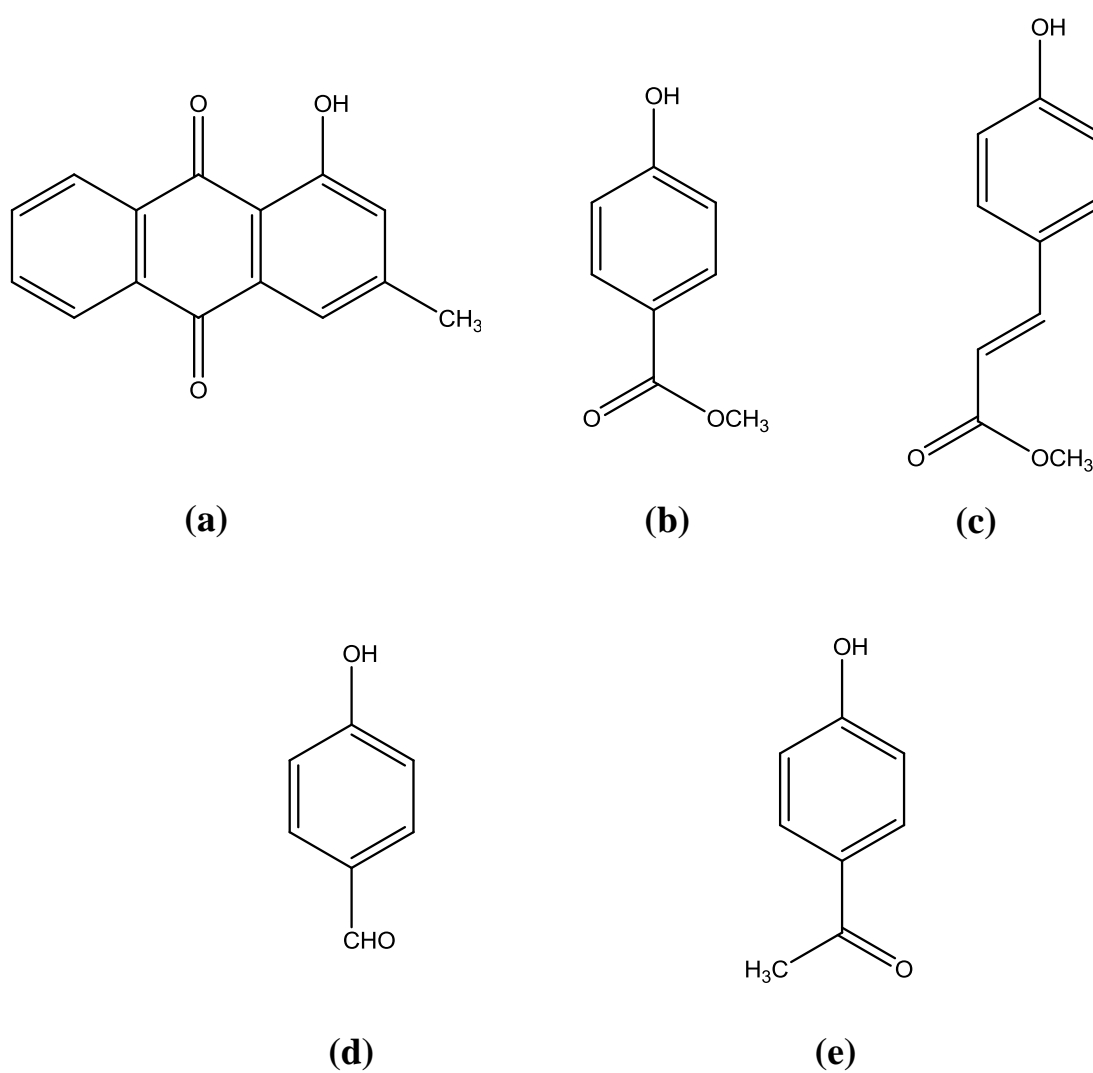


Fig. 9 Scheme of each purified compound.

1-hydroxy-3-methylanthracene-9,10-dione (a), methyl 4-hydroxybenzoate (b), methyl 4-hydroxycinnamate (c), 4-hydroxybenzaldehyde (d), 4-hydroxyacetophenone (e).

3.7 The antifungal assay of compounds

Antifungal activity of various concentrations of 4-hydroxybenzaldehyde derivatives and one anthraquinone possessed inhibition against *F. solani*, *F. oxysporum*, *R. solani* and *B. cinerea* (Table. 3). Each compound showed 100 % inhibition against *F. solani* and *F. oxysporum* 24 hpi then quickly loss inhibition capability after 48 hpi in 50 and 250 $\mu\text{g mL}^{-1}$ but not 500 $\mu\text{g mL}^{-1}$ which retained at least 56.4 % of 1-hydroxy-3-methylanthracene-9,10-dione to *F. oxysporum* in 48 hpi. All but 4-hydroxybenzaldehyde isolated compound from *Trichoderma* in 250 $\mu\text{g mL}^{-1}$ but not 500 $\mu\text{g mL}^{-1}$ showed 100 % inhibition in 48 hpi but inhibition potency down to less than 10 % after 72 hpi with exception of 500 $\mu\text{g mL}^{-1}$ methyl 4-hydroxycinnamate of 100 % still. 4-hydroxybenzaldehyde has little inhibition capacity against *B. cinerea* that no more than 25 % inhibition even in the highest tested concentration 500 $\mu\text{g mL}^{-1}$. Little inhibition capability, 66.7 % 24 hpi of 500 $\mu\text{g mL}^{-1}$, of 1-hydroxy-3-methylanthracene-9,10-dione to *R. solani* and decending to 15.2 % 48 hpi. 4-hydroxyacetophenone showed the best inhibition capacity against *R. solani*, retained 100 % activity of all tested concentrations 48 hpi. Although, 100 % inhibition 24 hpi to *R. solani*, methyl 4-hydroxybenzoate activity dissipitate totally 48 hpi.

Table. 3 Inhibition bioactivity of purified compounds from *Trichoderma* against *F. solani*, *F. oxysporum*, *R. solani* and *B. cinerea*. Values are inhibition percentage in means of three replicates in percentage \pm SD.

Compound ($\mu\text{g mL}^{-1}$)	<i>F. solani</i>		<i>F. oxysporum</i>		<i>R. solani</i>		<i>B. cinerea</i>	
	24 hpi	48 hpi	24 hpi	48 hpi	24 hpi	48 hpi	48 hpi	72 hpi
1-hydroxy-3-methylanthracene-9,10-dione								
50	100.0 \pm 0.0	19.6 \pm 0.0	100.0 \pm 0.0	10.9 \pm 3.2	4.2 \pm 0.0	0.0 \pm 0.0	0.0 \pm 0.0	0.0 \pm 2.7
250	100.0 \pm 0.0	45.7 \pm 0.0	100.0 \pm 0.0	22.2 \pm 0.0	33.3 \pm 0.0	11.8 \pm 0.0	0.0 \pm 0.0	3.1 \pm 2.7
500	100.0 \pm 0.0	65.2 \pm 0.0	100.0 \pm 0.0	56.4 \pm 0.0	66.7 \pm 0.0	15.2 \pm 1.7	100.0 \pm 0.0	21.3 \pm 0.0
methyl 4-hydroxybenzoate								
50	100.0 \pm 0.0	10.4 \pm 3.6	100.0 \pm 0.0	17.0 \pm 0.0	100.0 \pm 0.0	0.0 \pm 0.0	100.0 \pm 0.0	-4.8 \pm 2.8
250	100.0 \pm 0.0	25.0 \pm 0.0	100.0 \pm 0.0	28.3 \pm 0.0	100.0 \pm 0.0	0.0 \pm 2.9	100.0 \pm 0.0	-4.8 \pm 2.8
500	100.0 \pm 0.0	100.0 \pm 0.0	100.0 \pm 0.0	100.0 \pm 0.0	100.0 \pm 0.0	100.0 \pm 0.0	100.0 \pm 0.0	54.8 \pm 2.8
methyl 4-hydroxycinnamate								
50	100.0 \pm 0.0	7.7 \pm 0.0	100.0 \pm 0.0	14.0 \pm 3.5	100.0 \pm 0.0	0.0 \pm 0.0	100.0 \pm 0.0	-3.2 \pm 2.8
250	100.0 \pm 0.0	28.8 \pm 3.3	100.0 \pm 0.0	39.6 \pm 3.6	100.0 \pm 0.0	70.1 \pm 0.8	100.0 \pm 0.0	9.4 \pm 2.7
500	100.0 \pm 0.0	100.0 \pm 0.0	100.0 \pm 0.0	100.0 \pm 0.0	100.0 \pm 0.0	100.0 \pm 0.0	100.0 \pm 0.0	100.0 \pm 0.0
4-hydroxybenzaldehyde								
50	100.0 \pm 0.0	53.2 \pm 3.7	100.0 \pm 0.0	34.0 \pm 0.0	41.7 \pm 0.0	35.5 \pm 1.1	-8.3 \pm 2.9	-6.5 \pm 1.9
250	100.0 \pm 0.0	65.2 \pm 3.8	100.0 \pm 0.0	58.8 \pm 0.0	100.0 \pm 0.0	54.1 \pm 1.2	15.4 \pm 3.3	4.3 \pm 1.9
500	100.0 \pm 0.0	87.0 \pm 0.0	100.0 \pm 0.0	72.0 \pm 3.5	100.0 \pm 0.0	62.2 \pm 0.0	25.0 \pm 5.5	14.3 \pm 0.0
4-hydroxyacetophenone								
50	100.0 \pm 0.0	52.1 \pm 3.8	100.0 \pm 0.0	40.0 \pm 0.0	100.0 \pm 0.0	100.0 \pm 0.0	0.0 \pm 4.7	-2.3 \pm 0.0
250	100.0 \pm 0.0	77.7 \pm 3.8	100.0 \pm 0.0	64.0 \pm 0.0	100.0 \pm 0.0	100.0 \pm 0.0	100.0 \pm 0.0	100.0 \pm 0.0
500	100.0 \pm 0.0	87.0 \pm 0.0	100.0 \pm 0.0	75.5 \pm 0.0	100.0 \pm 0.0	100.0 \pm 0.0	100.0 \pm 0.0	100.0 \pm 0.0
Control	0.0 \pm 0.0	0.0 \pm 0.0	0.0 \pm 0.0	0.0 \pm 0.0	0.0 \pm 0.0	0.0 \pm 0.0	0.0 \pm 0.0	0.0 \pm 0.0
Fungicides	100.0 \pm 0.0	100.0 \pm 0.0	100.0 \pm 0.0	100.0 \pm 0.0	100.0 \pm 0.0	100.0 \pm 0.0	100.0 \pm 0.0	100.0 \pm 0.0

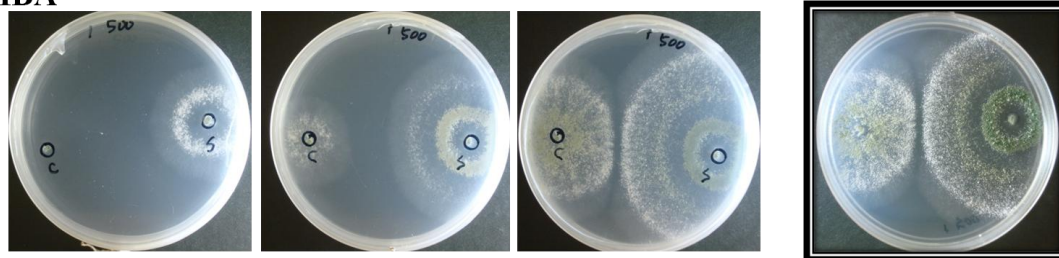
3.8 Effect of the compounds on the growth of *Trichoderma*

Other than fungicidal activity, it is intriguing to learn if any of isolation compounds might have elicitor property that can promote the compound produce host mycelia growth (Table. 4). Each compound can promote the mycelia growth from 2 folds of methyl 4-hydroxycinnamate to 8 folds 24 hpi and less profound 48 hpi of 2 folds of both 4-hydroxybenzaldehyde and 4-hydroxyacetophenone in 250 and 500 $\mu\text{g mL}^{-1}$. However, there was no significant promotion in *Trichoderma* mycelia growth both of 1-hydroxy-3-methylanthracene-9,10-dione and methyl 4-hydroxybenzoate 24 hpi and 48 hpi in every tested concentration. The morphological images of the elicitor property of both 4-hydroxybenzaldehyde and 4-hydroxyacetophenone showed much faster mycelia growth and higher sporulation (Fig. 10).

Table. 4 Among the various pathogens growth length of the *Trichoderma* of compounds 1 to 5.

Compound ($\mu\text{g mL}^{-1}$)	<i>Trichoderma</i> mycelia (cm)	
	24 hpi	48 hpi
1-hydroxy-3-methylanthracene-9,10-dione		
50	0.20 ± 0.03	1.37 ± 0.00
250	0.40 ± 0.03	1.37 ± 0.00
500	0.55 ± 0.00	1.65 ± 0.00
methyl 4-hydroxybenzoate		
50	0.20 ± 0.03	1.37 ± 0.00
250	0.30 ± 0.03	1.37 ± 0.00
500	0.55 ± 0.00	1.60 ± 0.00
methyl 4-hydroxycinnamate		
50	0.10 ± 0.00	1.37 ± 0.00
250	0.55 ± 0.00	1.37 ± 0.00
500	0.50 ± 0.00	1.60 ± 0.00
4-hydroxybenzaldehyde		
50	0.82 ± 0.03	1.83 ± 0.03
250	2.02 ± 0.03	3.23 ± 0.06
500	1.98 ± 0.03	3.58 ± 0.03
4-hydroxyacetophenone		
50	0.42 ± 0.03	2.88 ± 0.03
250	1.83 ± 0.03	2.97 ± 0.06
500	2.00 ± 0.00	3.27 ± 0.06
Control	0.25 ± 0.05	1.37 ± 0.00

HBA



Piceol

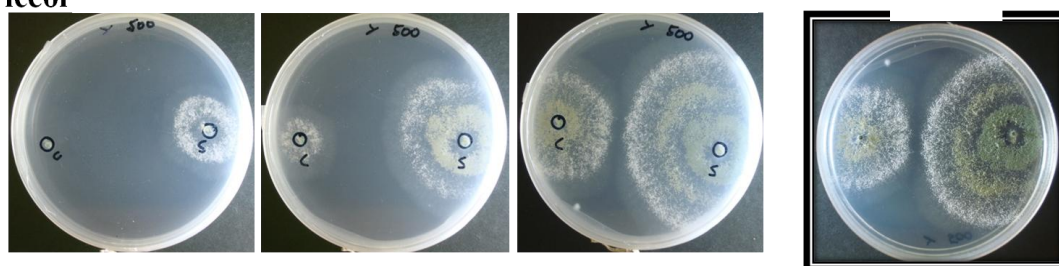


Fig. 10 Mycelia growth and sporulation promotion of *Trichoderma* by the 4-hydroxybenzaldehyde (HBA) and 4-hydroxyacetophenone (Piceol) in $500 \mu\text{g mL}^{-1}$.

4. Discussion

The main purpose of this research was to isolate and purify the molecules that possessed efficiently antifungal capability from *Trichoderma* metabolites. And it will be hoped to understand how these antifungal molecules influence the growth of pathogenic.

1-hydroxy-3-methyl-9,10-anthraquinone had inhibited of *R. solani* growth rate (Liu *et al.*, 2009). Methyl 4-hydroxybenzoate had high antibacterial and low toxicity (Pelz *et al.*, 2008; Zhou *et al.*, 2010), and effective preservatives for cosmetics, skin care products, drugs, beverages and food (Mahuzier *et al.*, 2001; Mahuziera *et al.*, 2001; Borremans *et al.*, 2004). Methyl 4-hydroxycinnamate had antifungal activity such as *pythium* spp. (Tawata *et al.*, 1996; Daayf *et al.*, 1997), inhibition of tyrosinase (Kubo *et al.*, 2004), antioxidative (Piattelli *et al.*, 1996), anti-lipid peroxidation (Kwon and Kim, 2003) and antibacterial activity (Gopalakrishnan *et al.*, 2007). 4-hydroxybenzaldehyde had antibacterial activity such as *E. coli*, *P. aeruginosa*, *S. aureus*, *S. epidermidis*, *S. aureus*, *K. pneumoniae*, and *V. parahemolyticus* (Chang *et al.*, 2001), antifungal activities such as *C. versicolor* and *L. Sulphureus* (Chang *et al.*, 2001) and inhibition of GABA shunt enzymes (Tao *et al.*, 2006). 4-hydroxyacetophenone had antifungal activities (Nascimento *et al.*, 2004) and inhibition of GABA shunt enzymes

(Tao *et al.*, 2006).

The result of antifungal confrontation assay against phytopathogenic by antagonistic *Trichoderma* spp. revealed that the *T. koningii* RIS 3-8 showed the best antifungal potency to against phytopathogenic. We isolated the major secondary metabolites produced by *T. koningii* RIS 3-8. Six known compounds obtained from *Trichoderma* cultivated medium were extracted and characterized (Fig. 9). 1-hydroxy-3-methylanthracene-9,10-dione, methyl 4-hydroxybenzoate, methyl 4-hydroxycinnamate, 4-hydroxybenzaldehyde, 4-hydroxyacetophenone that all but 1-hydroxy-3-methylanthracene-9,10-dione were firstly isolated from *T. koningii*. The antibiosis assays (Table. 3) showed that the secondary metabolites produced by *T. koningii* have different activities towards the pathogens tested, suggesting that individual compounds could have specific modes of action.

The activity against *F. solani*, *F. oxysporum*, *R. solani* and *B. cinerea* were strong for 4-hydroxyacetophenone, methyl 4-hydroxybenzoate and methyl 4-hydroxycinnamate. In the future it will be hoped to understand how these antifungal molecules influence the growth of pathogenic, and then had correlation between antifungal molecules and antifungal capability.

5. Conclusion

Biocontrol agents generally do not perform well enough under field conditions to compete with chemical fungicides. In this research, we investigated bioactivity in metabolites of *T. koningii* RIS 3-8. Five compounds were isolated, four 4-hydroxybenzaldehyde derivatives and one anthraquinone. Further studies on the secondary metabolites isolated from *T. koningii* supported by a ‘metabolomic approach’ (Weckwerth and Fiehn, 2002) are required to better our understanding of both the mechanisms of action of these bioactive compounds during the antagonism and their role in the interaction between biocontrol fungi, plant and microbial pathogens. In addition, the study of *Trichoderma* spp. as a source of biologically active metabolites is especially significant and ensures interest on this subject for years to come.

6. References

- Bartnicki-Garcia S. 1968. Cell Wall Chemistry, Morphogenesis, and Taxonomy of Fungi. *Annual Review of Microbiology* 22:87-108.
- Compant S, Duffy B, Nowak J, Clement C, Barka EA. 2005. Use of Plant Growth-Promoting Bacteria for Biocontrol of Plant Diseases: Principles, mechanisms of action, and future prospects. *Applied and Environmental Microbiology* 71:4951-4959.
- Chena LW, Cheng MJ, Peng CF, Chen Is. 2010. Secondary Metabolites and Antimycobacterial Activities from the Roots of *Ficus nervosa*. *Chemistry and Biodiversity* 7.
- Daayf F, Bel-Rhlid R, Bélanger RR. 1997. Methyl Ester of p-coumaric Acid: A Phytoalexin-like Compound from Long English Cucumber Leaves. *Journal of Chemical Ecology* 23:1517-1526.
- Fajardo A, Martinez JL. 2008. Antibiotics as Signals that Trigger Specific Bacterial Responses. *Curr Opin Microbiol* 11:161-167.
- Halawany AM, Ma CM, Hattori M. 2008. Anti-HIV-1 Protease Activity of Lanostane Triterpenes from the Vietnamese Mushroom *Ganoderma Colossum*. *Journal of Natural Products* 71 (6):1022-1026.
- Harman GE, Howell CR, Viterbo ACI, Lorito M. 2004. *Trichoderma* Species: Opportunistic, Avirulent Plant Symbionts. *Nature Reviews Microbiology* 2:43-56.
- Hetland G, Johnson E, Lyberg T, Bernardshaw S, Tryggestad AMA, Grinde B. 2008. Effects of the Medicinal Mushroom *Agaricus Blazei* Murill on Immunity, Infection and Cancer. *Journal compilation* 68:363 - 370.
- Hermosa MR, Grondona I, Iturriaga EA, Diaz-Minguez JM, Castro C, Montee, Garcia-Acha I. 2000. Molecular Characterization and Identification of Biocontrol Isolates of *Trichoderma* spp. *Applied and Environmental Microbiology*:1890-1898.
- Liu SY, Lo CT, Shibu MA, Leu YL, Jen BY, Peng KC. 2009. Structure-Activity Relationship Study of Biologically Active Anthraquinone Derivatives from *Trichoderma harzianum* strain Th-R16. *Journal of Agricultural and Food Chemistry* 57:7288-7292.
- Meselhy M. 1998. Hopane-Type Saponins from *Polycarpon Succulentum* - II. *Phytochemistry* 48:1415-1421.
- Mueller GM SJ. 2007. Fungal Biodiversity: What do we know? What can we predict?. *Biodiversity and Conservation* 16:1-5.
- Pavel AJr, Karolina Jk, Vincent ML, Philip AG, Jonathan LS. 1999. Calix[4]pyrroles Containing Deep Cavities and Fixed Walls. Synthesis, Structural Studies, and Anion Binding Properties of the Isomeric Products Derived from the Condensation of p-Hydroxyacetophenone and Pyrrole. *J Am Chem Soc* 121:11020-11021.
- Reino AP SM, de la Riva ABM, Henriquez JM. 2008. Severe hypotension during spinal anesthesia induced by angiotensin-converting enzyme inhibitors Reply. *Medicina Clinica* 131:677-678.
- Reino JQ, Guerrero RF, Hernández-Galán R, Collado IG. 2008. Secondary Metabolites from Species of the Biocontrol Agent *Trichoderma*. *Phytochemistry Reviews* 7:89-123.

- Sivasithamparam K. 1998. Root cortex-The final Frontier for theBbiocontrol of Root-rot with Fungal Antagonists: A Case Study on a Sterile red Fungus. *Annual Review of Phytopathology* 36:439-452.
- Sweetingham MW CW, Buirchell BJ, Brown AGP, Shivas RG. 1995. Anthracnose of lupins in Western Australia. *Australasian Plant Pathology* 24:271-271.
- Vey A HR, Butt TM. 2001. Toxic Metabolites of Fungal Biocontrol Agents. Fungi as Biocontrol Agents: Progress, Problems and Potential. CAB International, *Bristol*: 311–346.
- Vinale F FG, Sivasithamparam K, Lorito M, Marra R, Skelton BW, Ghisalberti EL. 2009. Harzianic Acid, an Antifungal and Plant Growth Promoting Metabolite from *Trichoderma harzianum*. *Journal of Natural Products* 72:2032-2035.
- Vinale F GE, Sivasithamparam K, Marra R, Ritieni A, Ferracane R, Woo S, Lorito M. 2008a. Factors Affecting the Production of *Trichoderma harzianum* Secondary Metabolites During the Interaction with Different Plant Pathogens. *Letters in Applied Microbiology*.
- Vinale F SK, Ghisalberti EL, Marra R, Woo SL, Lorito M. 2008b. *Trichoderma*-Plant-Pathogen Interactions. *Soil Biology & Biochemistry* 40:1-10.
- Vijayan N, Ramesh Babu R, Gunasekaran M, Gopalakrishnan RP. 2003. Growth, Optical, Thermal and Mechanical Studies of Methyl 4-hydroxybenzoate Single Crystals. *Journal of Crystal Growth* 256:174–182.
- Verma M, Brar SK, Tyagi RD, Surampalli RY, Val ´ero JR. 2007. Antagonistic Fungi, *Trichoderma* spp.: Panoply of Biological Control. *Biochemical Engineering Journal* 37:1–20.

Part II
Imidazolium salts 合成的化合物之殺真菌功能
Ionic Liquids and Antibiotic Properties of the Ethoxy ether
Functionalized Imidazolium Salts

1. Introduction

Ionic liquids (ILs), have earned intensive attention in the past two decades due to their distinguished physico-chemical properties, i.e. low vapor pressure, high polarity, high thermal stability, high ionic conductivity, tuneability and non-flammability, etc. (Deetlefs and Seddon, 2006; Welton, 1999; Wasserscheid and Keim, 2000; Sheldon, 2001; Fei *et al.*, 2006). With these unique properties, ILs have been widely employed as a new generation of solvents for electrochemical reactions and chemical transformations. These ILs also show great potentials in the fabrication of solar cells (Zakeeruddin and Grätzel, 2009), fuel cells (Nakamoto *et al.*, 2007), and nano-materials (Li *et al.*, 2009). Potential application in the biocatalysis (Dreyer and Kragl, 2008; Wehofsky *et al.*, 2008) and medicine (Hough *et al.*, 2007) (enhancement active pharmaceutical ingredients) are the recent advancement for the ILs. Simultaneously, research of ILs intriguing characters extend their applications onto antibioactivity toward microorganisms, which evolve troublesomes multidrug-resistance character both in the hospitals in the crop fields, also have been appeared (Ranke *et al.*, 2004; Pernak and Chwal, 2003; Grabińska-Sota and Kalka, 2006; Ganske and Bornscheuer, 2006; Lee *et al.*, 2005; Pernak and Chwal, 2003; Pernak *et al.*, 2004b; Pernak *et al.*, 2003; Docherty *et al.*, 2005;

Demberelnyamba *et al.*, 2004). To meet the designated purposes, antibiotics have to cross the bioenvelop, which consists of cell walls and biomembrane, surrounding the outer-sphere of bacteria and fungi. The composition of fungi cell wall are mainly chitin, 1,3- and 1,6-glycan. Biomembrane, a selective permeable membrane, consists of a bilayer lipid with hydrophilic character facing out- and in-ward at both sides while with hydrophobicity in-betweens. Organelles such as mitochondria and nucleus presented inside the eukaryotic cells are also surrounded by bilayer membrane. So, successfully deliver agents through any of these barriers is a key factor to be an effective antibiotics.

Imidazolium based ILs have been the most widely studied in their antimicrobial activity against *Escherichia coli*, *Salmonella typhimurium*, *Staphylococcus aureus*, *Bacillus subtilis*, *Vibrio fischeri* (Pernak *et al.*, 2004a), *Chlorella regularis* and *Candida albicans* (Carson *et al.*, 2009). Their antimicrobial potency has been attributed partly to the lipophilicity of the imidazolium salts, which correlate to the alkyl chain length and functionality of the cationic moiety. However, reports on the lipophilicity of imidazolium salts are very limited. In general speaking, lipophilicity can be known by measuring partition coefficients (P_{ow}), which provides an information of relative solubility in two phases (common 1-octanol / water).

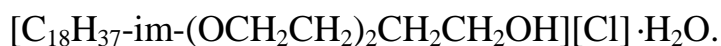
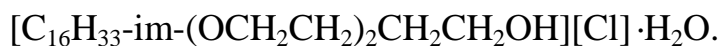
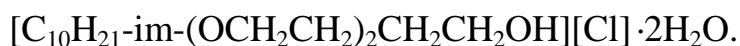
The first experimental report of P_{ow} was four ILs of 1-alkyl-3-methyl imidazolium chlorides (Urszula *et al.*, 2003) following various methods to determine the P_{ow} (Ropel *et al.*, 2005; Lee, 2009). The value of $\log P_{ow}$ supplies quantitative information to easily understanding of solubility, the positive value indicate more lipophilic and negative value indicate more hydrophilic.

In this work, $[C_n\text{-im-3OEG}][Cl]$, amphiphilic ionic liquids and ionic liquid crystals were tested their fungicidal potency. We investigated along with their antibiotic properties against fungal phytopathogen. Rupture of the bioenvelop appears to be operative in the process of antifungal activity. The significant antibiotic properties and the environmental benign characters suggest that the ILs / ILCs may have potential applications in the modern biotechnology.

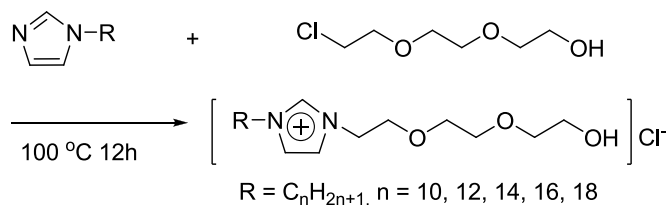
2. Experimental Materials and Methods

2.1 Preparation of ethoxy ether functionalized imidazolium salts

1-octadecyl-3-(2-(2-(2-hydroxyethoxy)ethoxy)ethyl)-imidazolium chloride $\cdot \text{H}_2\text{O}$. (Scheme. 1).



The five compounds from the National Dong Hwa University Department of Chemistry, Ivan J.B. Lin professor laboratory.



Scheme. 1 Synthetic pathway for the $[\text{C}_n\text{-im-3OEG}][\text{Cl}]$ (Roy T. W. Huang.)

2.2 *Rhizoctonia* cultivation

R. solani was incubated on 39 g L⁻¹ of potato dextrose agar (PDA) (Difco, Becton, Dickinson and Company, Franklin Lakes, NJ, USA) medium. The PDA medium was autoclaved at 121 °C, 1.2 kg cm⁻² for 15 min, and then stored at 4 °C until use. *R. solani* was inoculated on the center of PDA plate and cultivated at 28 °C for 5 days.

2.3 Antifungal assays

Tested concentration of each [C_n-im-3OEG][Cl] was 15 µg. A *R. solani* mycelial plug of 0.5 cm diameter was placed at the center of 8 mL PDA. The hyphae growth in diameter were recorded at 8, 16, 24, 32, 40, 48, 56 hour post inoculation (hpi). Each treatment consisted of three replicates.

2.4 IC₅₀ determination

Each tested [C_n-im-3OEG][Cl] of 0, 0.0001, 0.001, 0.01, 0.1, 0.5, 1, 2, 5, 8 and 10 mM were mixed with PDA. A 5 mm plug of *R. solani* was placed in the center of the PDA. The hyphae growth was recorded at 8, 16, 24, 32, 40 hpi. Each treatment consisted of three replicates.

2.5 Morphological observation by fluorescent stereomicroscope

R. solani was cultivated in potato dextrose broth (PDB) (Difco, Becton, Dickinson and Company, Franklin Lakes, NJ, USA) containing 130 μ M [C₁₄-im-3OEG][Cl] in a 250 mL Erlenmeyer flask, 180 rpm, 28 °C. An aliquot of *R. solani* hyphae on 24, 48, 72, 96, 120, and 144 hpi was removed and lactophenol blue solution (Sigma-Aldrich, St Louis, MO, USA) applied to stain the fungal cell wall. The hyphae were observed under the fluorescent stereomicroscope (Olympus IX70, Olympus, Tokyo, Japan) to count the number of septa, measure the distance between two septa. Besides, nuclei stained with the Hoechst stain (Invitrogen, Carlsbad, CA, USA) for 30 min at 144 hpi were observed under fluorescent stereomicroscope.

3. Results

3.1 Antifungal activity

Among the compounds of various alkyl chain lengths, [C₁₄-im-3OEG][Cl] shows the best inhibition capacity, a 91 % inhibition against *R. solani* after treating with of 15 µg of the compounds for 40 hpi while with n = 10, 12, 16 and 18 show 0 %, 67 %, 67 % and 63 % inhibition, respectively (Fig. 1). IC₅₀ of n = 12, 14, 16, and 18 of [C_n-im-3OEG][Cl] are 0.600, 0.130, 0.590, and 0.720 mM, respectively.

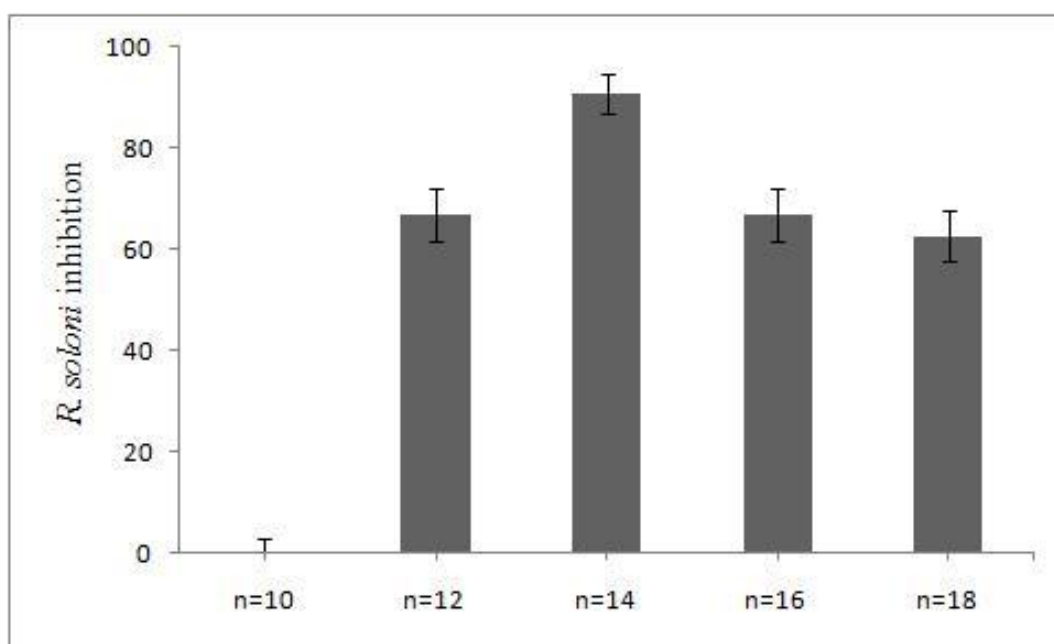


Fig. 1 The inhibition capacity of various alkyl length of the [C_n-im-3OEG][Cl] compounds to *R. solani*.

3.2 Morphological observation

The morphology change of the *R. solani* upon treatment with [C₁₄-im-3OEG][Cl] was further investigated under fluorescence microscope for a duration of 144 hpi, and a control group was employed for comparison (Fig. 2). Dramatic changes in the number of septa and the hyphae length of the *R. solani* were observed. At the first 24 hpi, there is an increase in the number of septa together with a shortening of the hyphae length from 0.92 ± 0.02 to 0.21 ± 0.01 mm (Fig. 2 A and B). At 72 hpi, there is a further increase in the septa number and shortening of the hyphae from 0.68 ± 0.03 to 0.13 ± 0.04 mm (Fig. 2 C and D). After 144 hpi the hyphae length further reduces to 0.09 ± 0.01 mm as compared to the 0.70 ± 0.04 mm for the control (Fig. 2 E and F). In the other hand, the number of the septa per 1mm are also increasing when control vs. [C₁₄-im-3OEG][Cl] treatment. The number of the septa per 1mm of 24, 72 and 144 hpi, shows control were 1.09 ± 0.03 , 1.47 ± 0.07 and 1.44 ± 0.08 , respectively, and treatment were 4.66 ± 0.2 , 8.48 ± 2.96 and 11.13 ± 0.77 , respectively (Fig. 2). We also notice that there is a progressive swelling of hyphae during at 144 hpi, the hyphae cell wall incomplete and debris (Fig. 2 F). Especially, treatment with [C₁₄-im-3OEG][Cl] was 2000 μ M more significant observation (Fig. 2 G). Furthermore, the nuclei morphology changes

significantly in the number of nuclear stained spots under 600 x fluorescent stereomicroscope (Fig. 3), showed the treated hyphae 72 hpi obvious nuclear was incomplete showed brightness and size of the nucleus were unusual (Fig. 3 C and D), this is compared to the control (Fig. 3 A and B), implying possible apoptosis but further evidences required.

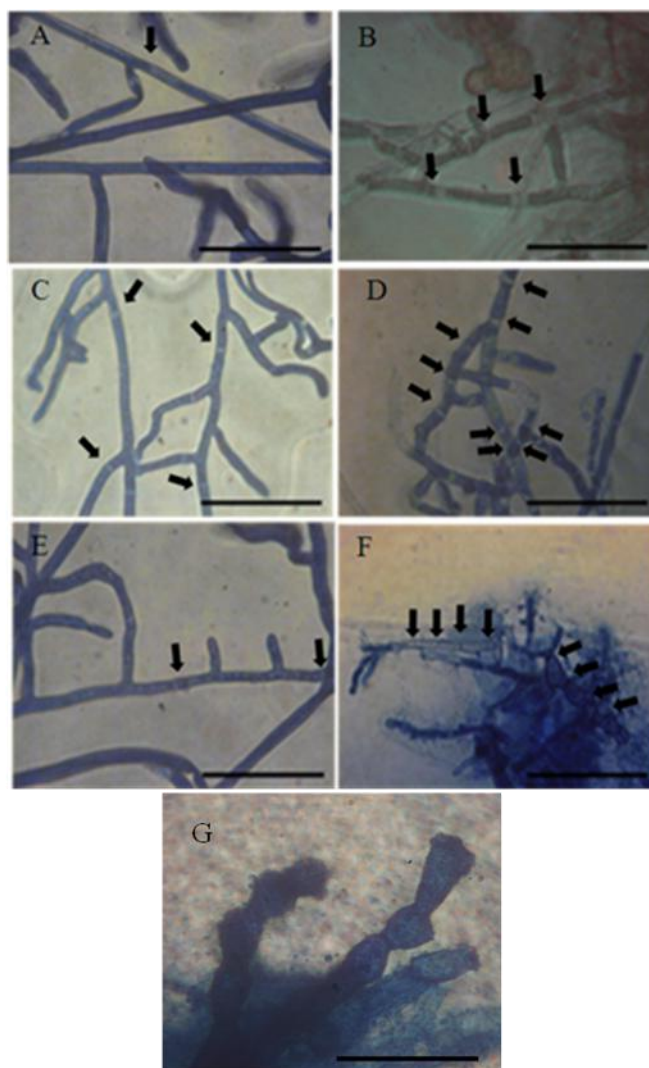


Fig. 2 The *R. soloni* morphology observation in the present of 130 μ M [C₁₄-im-3OEG][Cl] under the 600 x Fluorescent stereomicroscope. Scale bars = 0.5 mm. The more septa and hyphae swelled along with longer period of treatment. Many tiny blue dots and blue smear area were debris of lysed hyphae. Arrow indicated the position of the septum. Control groups (A), (C), (E); [C₁₄-im-3OEG][Cl] treatment groups (B), (D), (F). 24hpi (A), (B); 72hpi (C), (D); and 144hpi (E), (F). Treatment the present of 2000 μ M, 144hpi (G).

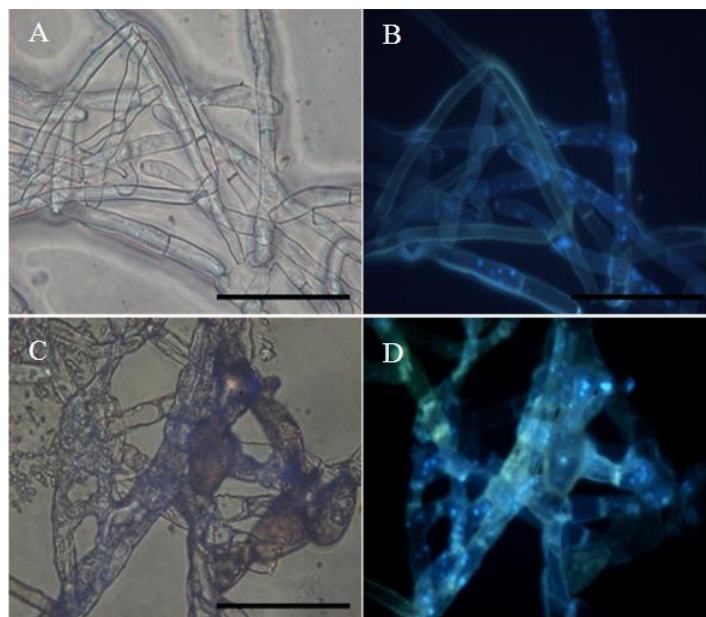


Fig. 3 The *R. soloni* nuclei morphology observation in the present of 130 μ M [C₁₄-im-3OEG][Cl] 72 hpi under the 600 x Fluorescent stereomicroscope. Scale bars = 0.5 mm. More bright spots, represented nuclei, showed in the [C₁₄-im-3OEG][Cl] treated hyphae 72 hpi (D) then control group (B). Also, the septa shorter and hyphae swelled can be observed.

4. Discussion

The amphiphilic nature of an imidazolium salt depends on (1) the imidazolium ring heads, (2) the N-substituents, and (3) the counter anions. In this work, most commercial fungicides might function via disrupting the cell membrane permeability of polyenes, the inhibiting the transcription or translation of pyrimidines, or inhibiting the free radical activity of azoles. The fungicidal activity of the $[C_n\text{-im-3OEG}][Cl]$ on *R. solani*, a very notorious phytopathogens that cost huge damages to many crops and vegetables every year, are investigated in this research. The results shown (Fig. 1) indicate that the antifungal activity of the $[C_n\text{-im-3OEG}][Cl]$ compounds increases with increasing chain length from $n = 10$ to 14, it then gradually decreases. Under microscope the hyphae morphology of the $[C_n\text{-im-3OEG}][Cl]$ treated *R. solani* changes along with time; first there is an increase in the number of septa number vacuole, then hyphae swells, and cell wall collapses (Fig. 2), finally the nuclei fragmentation occurs (Fig. 3). We propose that these imidazolium salts might damage the cell membrane, which would cause the leakage of cytoplasm. This process possibly leads to an increasing septa number and the shortening of the knob in the hyphae to prevent further leakages of interior fluid. Exterior materials, such as water, flooding in and cells contain it in the increasing

number of vacuoles. This osmosis stress further works on the hyphae by creating outward force against hyphae cell wall to expand causing the hyphae swelling and, finally, collapse the cell wall. The [C_n-im-3OEG][Cl] might also dissipate the chemical potential of the mitochondria, so the ATP synthesis, via punching holes in the outer and inner membranes. This damage might accelerate the death process of the *R. solani*. Most other reports concerning antifungal activity of the imidazolium are tested on the singular cell yeast-like fungi, such as *Candida spp.* and *Rhodotorula spp.* (Pernak *et al.*, 2003; Pernak *et al.*, 2004). In this research, the multicellular fungus *R. solani* is the first reported antifungal activity. The proposed working mechanism of [C_n-im-3OEG][Cl] against the *R. solani* is also reported.

5. Conclusion

Many fungal phytopathogens may cause crops disease result in tremendous harvest damages. *Rhizoctonia* has earned notorious fame for their parasitism onto many economically important crops, such as soybean, papaya, eggplant, potato and wheat, causing the damping off or blight syndromes. Fungicides are the major agents to reduce the population of the *Rhizoctonia* spp. but are designed to eliminate or adversely affect living organisms causing adverse effects to humans, animals, and the environment. In this work, a series of amphiphilic ILs comprising a cationic imidazolium head group, a hydrophobic N-alkyl chain, and an N-2-(2-(2-ethoxy)ethoxy)ethanol functional group are reported. While these ILs of $n = 16$ and 18 possesses thermotropic liquid crystalline properties, compounds of $n = 14, 16$, and 18 also exhibit lyotropic liquid crystal properties. These ILs show effective antibiotic activity against infectious pathogens in fungi. Experimental results show lipophilicity correlates with alkyl chain number and may play an important role in antibiotic activities. The antibiotic processes were examined under the fluorescent stereomicroscope. A comparison of morphological change between the $[C_n\text{-im-3OEG}][Cl]$ and cell wall synthesis-related inhibitors. No conclusive mechanism is found. The proposed working mechanism of

[C_n-im-3OEG][Cl] against the *R. solani* might contribute to the

[C_n-im-3OEG][Cl] created osmosis stress.

References

- Carson L, Chau PKW, Earle MJ, Gilea MA, Gilmore BF, Gorman SP, McCann MT, Seddon KR. 2009. Antibiofilm Activities of 1-alkyl-3-methylimidazolium chloride Ionic Liquids. *Green Chemistry* 11:492–497.
- Deetlefs M, Seddon KR. 2006. Ionic Liquids: Fact and Fiction. *Chim Oggi* 24:16–23.
- Demberelnyamba D, Kim KS, Choi S, Park SY, Lee H, Kimb CJ, Yoo ID. 2004. Synthesis and Antimicrobial Properties of Imidazolium and Pyrrolidinium Salts. *Bioorg Med Chem* 12:853–857.
- Docherty KM, Kulpa CF, Jr. 2005. Toxicity and Antimicrobial Activity of Imidazolium and Pyridinium Ionic Liquids. *Green Chemistry* 7:185–189.
- Dreyer S, Kragl U. 2008. Ionic Liquids for Aqueous Two Phase Extraction and Stabilisation of Enzymes. *Biotechnology and Bioengineering* 99:1416–1424.
- Fei Z, Geldbach TJ, Zhao D, Dyson PJ. 2006. From Dysfunction to Bis-function: On the Design and Applications of Functionalised Ionic Liquids. 12:2122 – 2130.
- Ganske F, Bornscheuer UT. 2006. Growth of *Escherichia coli*, *Pichia Pastoris* and *Bacillus cereus* in the Presence of the Ionic Liquids [BMIM][BF₄] and [BMIM][PF₆] and Organic Solvents. *Biotechnol Lett* 28:465–469.
- Grabińska-Sota E, Kalka J. 2006. Toxicity of Imidazolium Chlorides to Aquatic Organisms. *Pol J Environ Stud* 15:405–409.
- Hough WL, Smiglak M, Rodriguez H, Swatloski RP, Spear SK, Daly DT, Pernak J, Grisel JE, Carliss RD, Soutuollo MD, Davis JH, Jr., Rogers RD. 2007. The Third Evolution of Ionic Liquids: Active Pharmaceutical Ingredients. *New J Chem* 31:1429–1436.
- Lee SH, Lee SB. 2009. Octanol/Water Partition Coefficients of Ionic Liquids. *J Chem Technol Biotechnol* 84:202–207.
- Lee SM, Chang WJ, Choi AR, Koo YM. 2005. Influence of Ionic Liquids on the Growth of *Escherichia coli*. *Korean J Chem Eng* 22:687–690.
- Li C, Hua B, Shi G. 2009. Conducting Polymer Nanomaterials: Electrosynthesis and Applications. *Chem Soc Rev* 38:2397–2409.
- Nakamoto H, Noda A, Hayamizu K, Hayashi S, Hamaguchi H, Watanabe M. 2007. Proton-Conducting Properties of a Bronsted Acid-Base Ionic Liquid and Ionic Melts Consisting of Bis(Trifluoromethanesulfonyl)Imide and Benzimidazole for Fuel Cell Electrolytes. *J Phys Chem* 111:1541–1548.
- Pernak J, Chwal P. 2003. Synthesis and Anti-Microbial Activities of Choline-like Quaternary Ammonium Chlorides. *European Journal of Medicinal Chemistry* 38:1035–1042.
- Pernak J, Sobaszkiewicz K, Mirska I. 2003. Antimicrobial Activity of Dicationic Ionic Liquids. *Green Chemistry* 5:52–56.
- Pernak J, Goc I, Mirska I. 2004. Anti-Microbial Activities of Protic Ionic Liquids with Lactate Anion. *Green Chemistry* 6:323–329.
- Pernak J, Goc I, Mirska I. 2004a. Anti-Microbial Activities of Protic Ionic Liquids with Lactate Anion. *Green Chemistry* 6:323–329.
- Pernak J, Sobaszkiewicz K, Foksoicz-Flaczyk J. 2004b. Ionic Liquids with Symmetrical Dialkoxymethyl-Substituted Imidazolium Cations. *Chem Eur J* 10:3479–3485.
- Pernak J, Sobaszkiewicz K, Mirsk I. 2003. Anti-Microbial Activities of Ionic Liquids. *Green Chemistry* 5:52–56.

- Ranke J, ter KM, Stock F, Bottin-Weber U, Poczobutt J, Hoffmann J, Ondruschka B, Filser J, Jastorff B. 2004. Biological Effects of Imidazolium Ionic Liquids with Varying Chain Lengths in Acute *Vibrio Fischeri* and WST-1 Cell Viability Assays. *Ecotoxicology and Environmental Safety* 58:396–404.
- Ropel L, Belve`ze LS, Aki SNVK, Stadtherr MA, Brennecke JF. 2005. Octanol–Water Partition Coefficients of Imidazolium-Based Ionic Liquids. *Green Chem* 7:83–90.
- Sheldon R. 2001. Catalytic Reactions in Ionic Liquids. *Chem Commun*:2399-2407.
- Urszula D, Ewa BĚ, Rafa BE. 2003. 1-Octanol/Water Partition Coefficients of 1-Alkyl-3-methylimidazolium Chloride. *Chem Eur J* 9:3033 -3041.
- Wasserscheid P, Keim W. 2000. Ionic Liquids - NEW "Solutions" for Transition Metal Catalysis. *Angew Chem Int Ed* 39:3772-3789.
- Wehofsky N, Wespe C, Cerovsky V, Pech A, Hoess E, Rudolph R, Bordusa F. 2008. Ionic Liquids and Proteases: A Clean Alliance for Semisynthesis. *ChemBioChem* 9:1493–1499.
- Welton T. 1999. Room-Temperature Ionic Liquids. Solvents for Synthesis and Catalysis. *Chemrev* 99:2071-2083.
- Zakeeruddin SM, Grätzel M. 2009. Solvent-Free Ionic Liquid Electrolytes for Mesoscopic Dye-Sensitized Solar Cells. *Adv Funct Mater* 19:2187–2202.

7. Appendix

7.1 Fungicides screening from the *Trichoderma* secondary metabolites

Appendix 7.1.1 Characteristics of Common Organic Solvents

Solvent	formula	MW	boiling point (°C)	melting point (°C)	density (g/mL)	solubility in water (g/100g)	Dielectric Constant ^{3,4}	flash point (°C)
acetic acid	C ₂ H ₄ O ₂	60.05	118	16.6	1.049	Miscible	6.15	39
acetone	C ₃ H ₆ O	58.08	56.2	-94.3	0.786	Miscible	20.7(25)	-18
acetonitrile	C ₂ H ₃ N	41.05	81.6	-46	0.786	Miscible	37.5	6
benzene	C ₆ H ₆	78.11	80.1	5.5	0.879	0.18	2.28	-11
1-butanol	C ₄ H ₁₀ O	74.12	117.6	-89.5	0.81	6.3	17.8	35
2-butanol	C ₄ H ₁₀ O	74.12	98	-115	0.808	15	15.8(25)	26
2-butanone	C ₄ H ₈ O	72.11	79.6	-86.3	0.805	25.6	18.5	-7
<i>t</i> -butyl alcohol	C ₄ H ₁₀ O	74.12	82.2	25.5	0.786	Miscible	12.5	11
carbon tetrachloride	CCl ₄	153.82	76.7	-22.4	1.594	0.08	2.24	--
chlorobenzene	C ₆ H ₅ Cl	112.56	131.7	-45.6	1.1066	0.05	2.71	29
chloroform	CHCl ₃	119.38	61.7	-63.7	1.498	0.795	4.81	--
cyclohexane	C ₆ H ₁₂	84.16	80.7	6.6	0.779	<0.1	2.02	-20
1,2-dichloroethane	C ₂ H ₄ Cl ₂	98.96	83.5	-35.3	1.245	0.861	10.42	13
diethyl ether	C ₄ H ₁₀ O	74.12	34.6	-116.3	0.713	7.5	4.34	-45
diethylene glycol	C ₄ H ₁₀ O ₃	106.12	245	-10	1.118	10	31.7	143
diglyme (diethylene glycol dimethyl ether)	C ₆ H ₁₄ O ₃	134.17	162	-68	0.943	Miscible	7.23	67
1,2-dimethoxy-ethane (glyme, DME)	C ₄ H ₁₀ O ₂	90.12	85	-58	0.868	Miscible	7.2	-6
dimethylether	C ₂ H ₆ O	46.07	-22	-138.5	NA	NA	NA	-41
dimethyl-formamide (DMF)	C ₃ H ₇ NO	73.09	153	-61	0.944	Miscible	36.7	58
dimethyl sulfoxide (DMSO)	C ₂ H ₆ OS	78.13	189	18.4	1.092	25.3	47	95
dioxane	C ₄ H ₈ O ₂	88.11	101.1	11.8	1.033	Miscible	2.21(25)	12
ethanol	C ₂ H ₆ O	46.07	78.5	-114.1	0.789	Miscible	24.6	13
ethyl acetate	C ₄ H ₈ O ₂	88.11	77	-83.6	0.895	8.7	6(25)	-4
ethylene glycol	C ₂ H ₆ O ₂	62.07	195	-13	1.115	Miscible	37.7	111
glycerin	C ₃ H ₈ O ₃	92.09	290	17.8	1.261	Miscible	42.5	160
heptane	C ₇ H ₁₆	100.20	98	-90.6	0.684	0.01	1.92	-4
Hexamethylphosphoramide (HMPA)	C ₆ H ₁₈ N ₃ OP	179.20	232.5	7.2	1.03	Miscible	31.3	105

Solvent	formula	MW	boiling point (°C)	melting point (°C)	density (g/mL)	solubility in water (g/100g)	Dielectric Constant ^{3,4}	flash point (°C)
Hexamethylphosphorous triamide (HMPT)	C ₆ H ₁₈ N ₃ P	163.20	150	-44	0.898	Miscible	??	26
hexane	C ₆ H ₁₄	86.18	69	-95	0.659	0.014	1.89	-22
methanol	CH ₄ O	32.04	64.6	-98	0.791	Miscible	32.6(25)	12
methyl <i>t</i> -butyl ether (MTBE)	C ₅ H ₁₂ O	88.15	55.2	-109	0.741	5.1	??	-28
methylene chloride	CH ₂ Cl ₂	84.93	39.8	-96.7	1.326	1.32	9.08	1.6
<i>N</i> -methyl-2-pyrrolidinone (NMP)	CH ₅ H ₉ NO	99.13	202	-24	1.033	10	32	91
nitromethane	CH ₃ NO ₂	61.04	101.2	-29	1.382	9.50	35.9	35
pentane	C ₅ H ₁₂	72.15	36.1	-129.7	0.626	0.04	1.84	-49
Petroleum ether (ligroine)	--	--	30-60	-40	0.656	--	--	-30
1-propanol	C ₃ H ₈ O	88.15	97	-126	0.803	Miscible	20.1(25)	15
2-propanol	C ₃ H ₈ O	88.15	82.4	-88.5	0.785	Miscible	18.3(25)	12
pyridine	C ₅ H ₅ N	79.10	115.2	-41.6	0.982	Miscible	12.3(25)	17
tetrahydrofuran (THF)	C ₄ H ₈ O	72.11	66	-108.4	0.886	30	7.6	-21
toluene	C ₇ H ₈	92.14	110.6	-93	0.867	0.05	2.38(25)	4
triethyl amine	C ₆ H ₁₅ N	101.19	88.9	-114.7	0.728	0.02	2.4	-11
water	H ₂ O	18.02	100.00	0.00	0.998	--	78.54	--
water, heavy	D ₂ O	20.03	101.3	4	1.107	Miscible	??	--
<i>o</i> -xylene	C ₈ H ₁₀	106.17	144	-25.2	0.897	Insoluble	2.57	32
<i>m</i> -xylene	C ₈ H ₁₀	106.17	139.1	-47.8	0.868	Insoluble	2.37	27
<i>p</i> -xylene	C ₈ H ₁₀	106.17	138.4	13.3	0.861	Insoluble	2.27	27

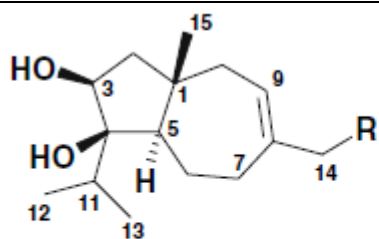
Notes:

1. This table was originally from: [Prof. Murov's Orgsoltab](#), which was edited and reposted by [Erowid](#)
2. You can find more detailed information (Health & Safety, Physical, Regulatory, Environmental) on various organic solvents from [NCMS](#)
3. The values in the table above were obtained from [ChemFinder Web Server](#), the CRC, or Vogel's *Practical Organic Chemistry* (5th ed.).
4. T = 20 °C unless specified otherwise.

Appendix 7.1.2 The secondary metabolites of the most important fungal *Trichoderma*, include classes and structures. (Reino *et al.*, 2008)

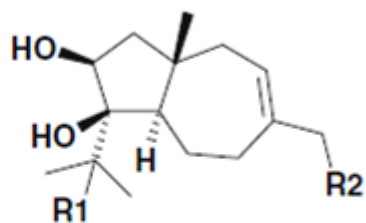
Classes Structure	Anthraquinones and xanthone derivatives	
	$R_1 = R_2 = H$	$R_1 = OH, R_2 = H$
	$R_1 = R_2 = OH$	
	$R = H$	$R = COCH_3$

Daucanes



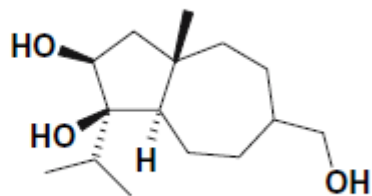
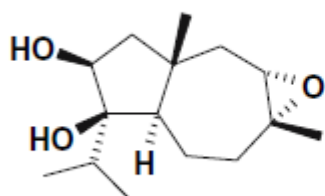
R = H

R = $\text{OCO}(\text{CH}_2)_7\text{CH}=\text{CH}(\text{CH}_2)_7\text{CH}_3$

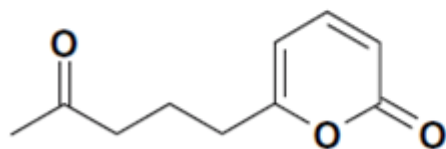
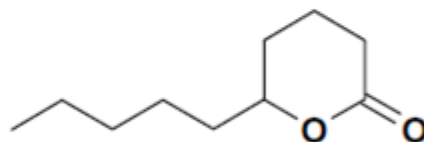
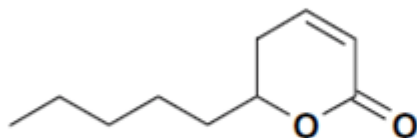
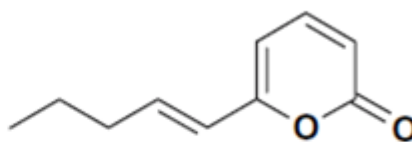
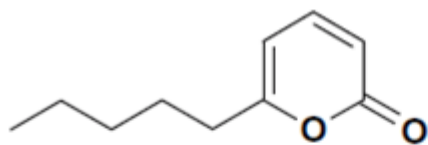


R1 = H, R2 = OH

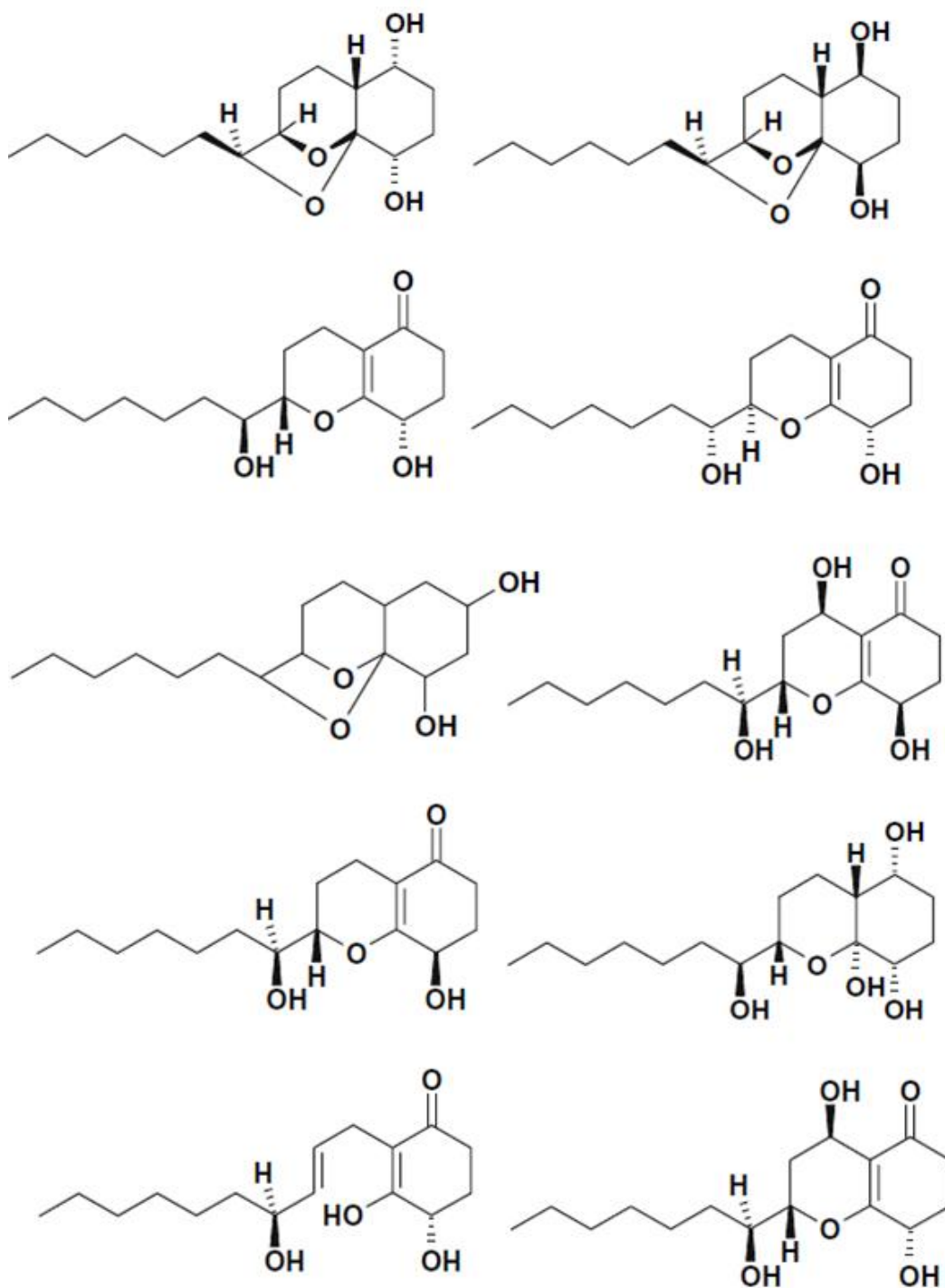
R1 = R2 = OH



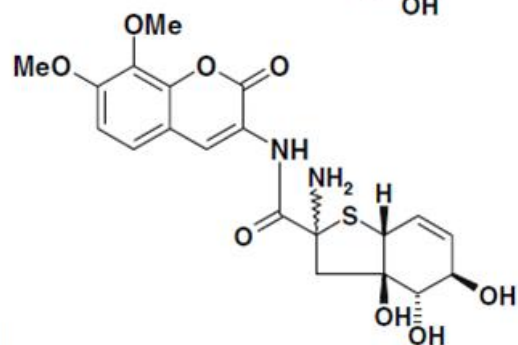
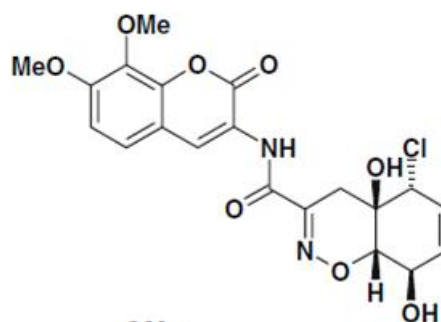
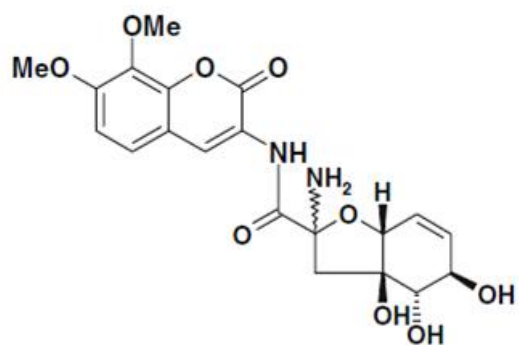
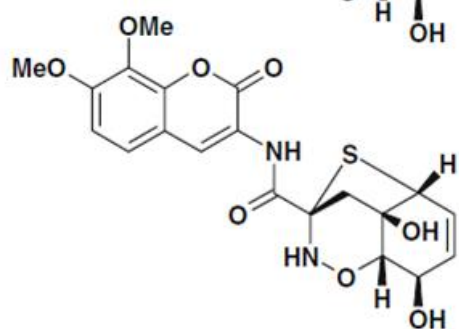
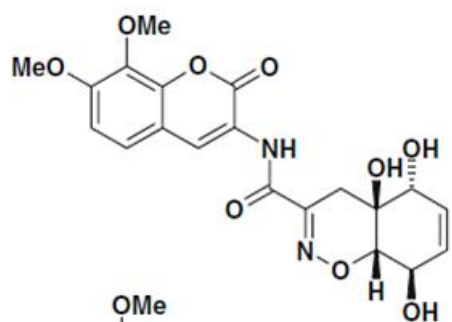
Pyrones metabolites



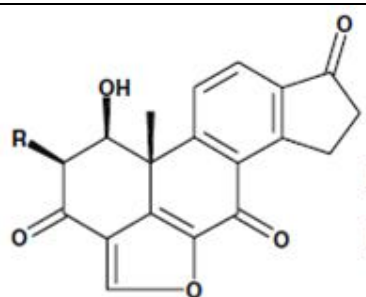
Koninginins and derivatives



Trichodermamides

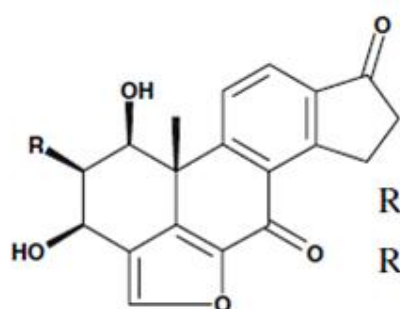
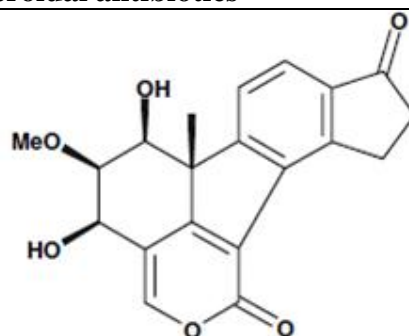


Viridins family of steroidal antibiotics



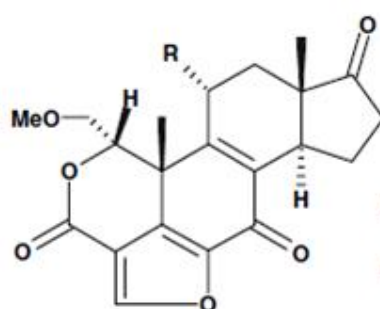
R= OCH₃

R= H



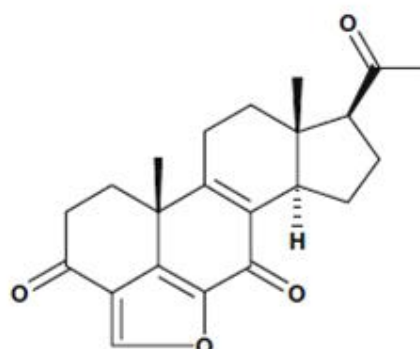
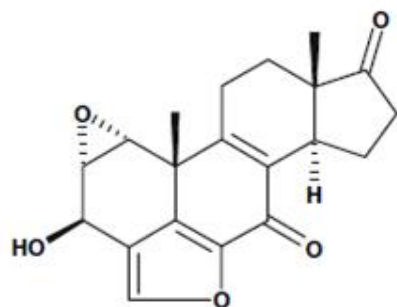
R= OCH₃

R= H

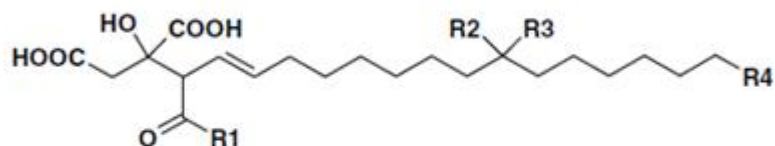
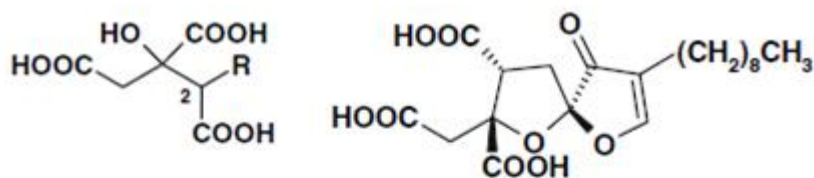


R= OAc

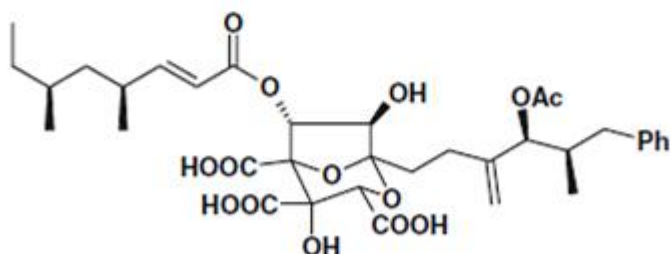
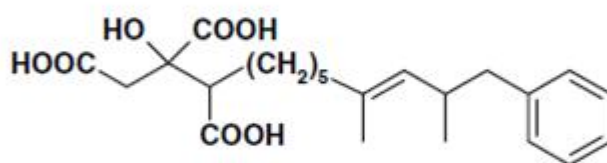
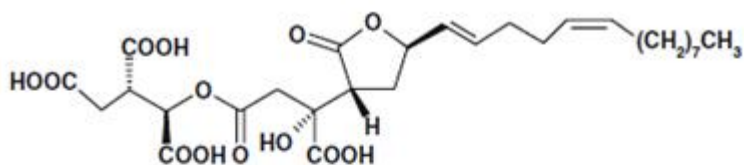
R= H



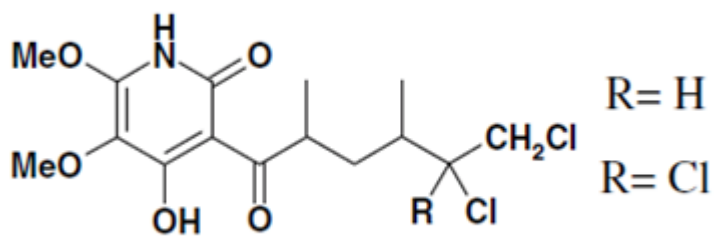
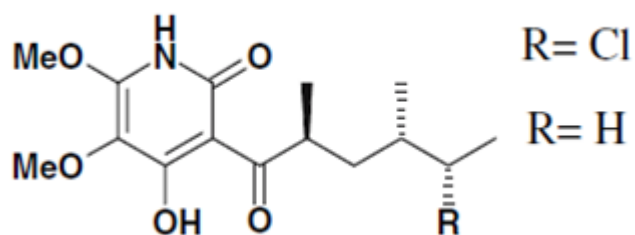
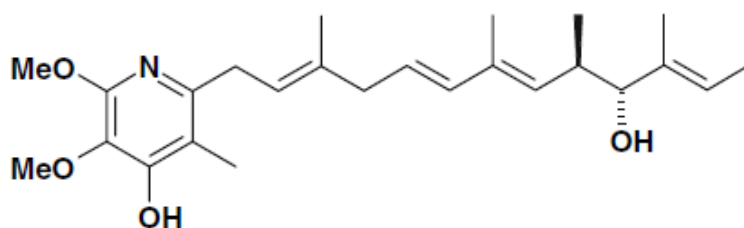
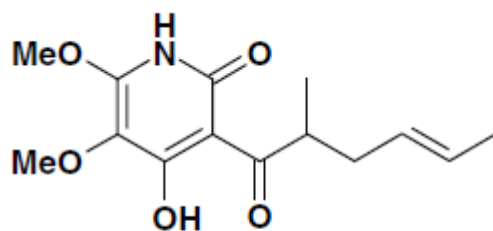
Viridifungins and alkyl citrate derivatives



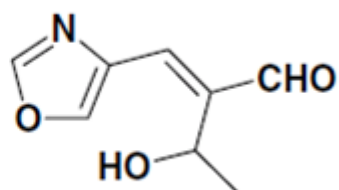
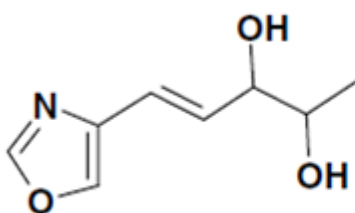
R1= Tyrosine; R2, R3 = O; R4= Me
 R1= Phenylalanine; R2, R3= O; R4= Me
 R1= Tryptophan; R2, R3= O; R4= Me
 R1= Tyrosine; R2= OH; R3= H; R4= Me
 R1= Tyrosine; R2= R3= H; R4= Me
 R1= Tyrosine; R2, R3= O; R4= H
 R1= Tyrosine; R2, R3= O; R4= n-Pr
 R1= Phenylalanine; R2=R3= H; R4= Me
 R1= OH; R2=R3= H; R4= Me



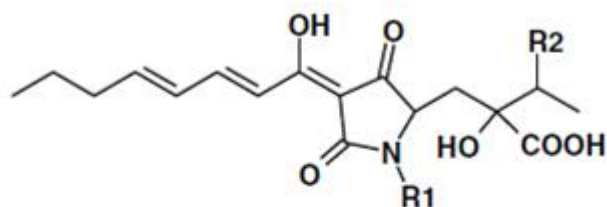
Pyridine ringcontaining fungal metabolites



Oxazol derivatives



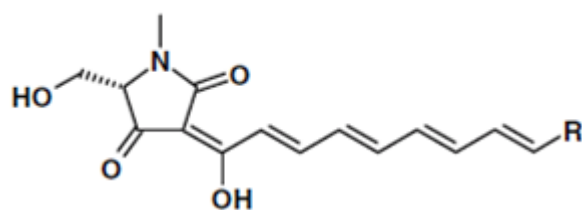
Pirrolidinediones



R1= Me, R2= Me

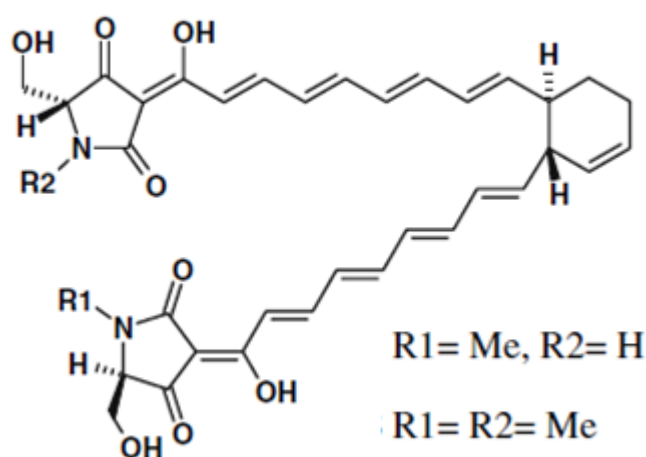
R1= H, R2= Me

R1= Me, R2= Et



R= -CH=CH-COOH

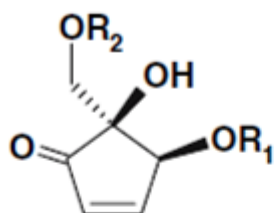
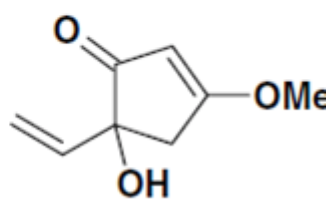
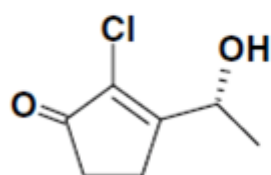
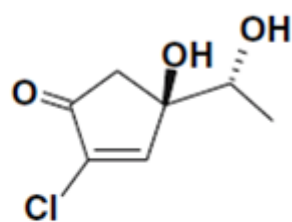
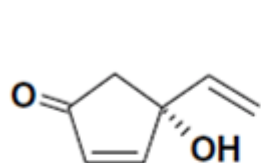
R= -COOH



R1= Me, R2= H

R1= R2= Me

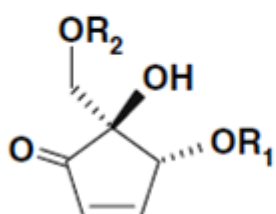
Trichodenones and other cyclopentenones



R1= R2= H

R1= Ac, R2= H

R1= H, R2= Ac

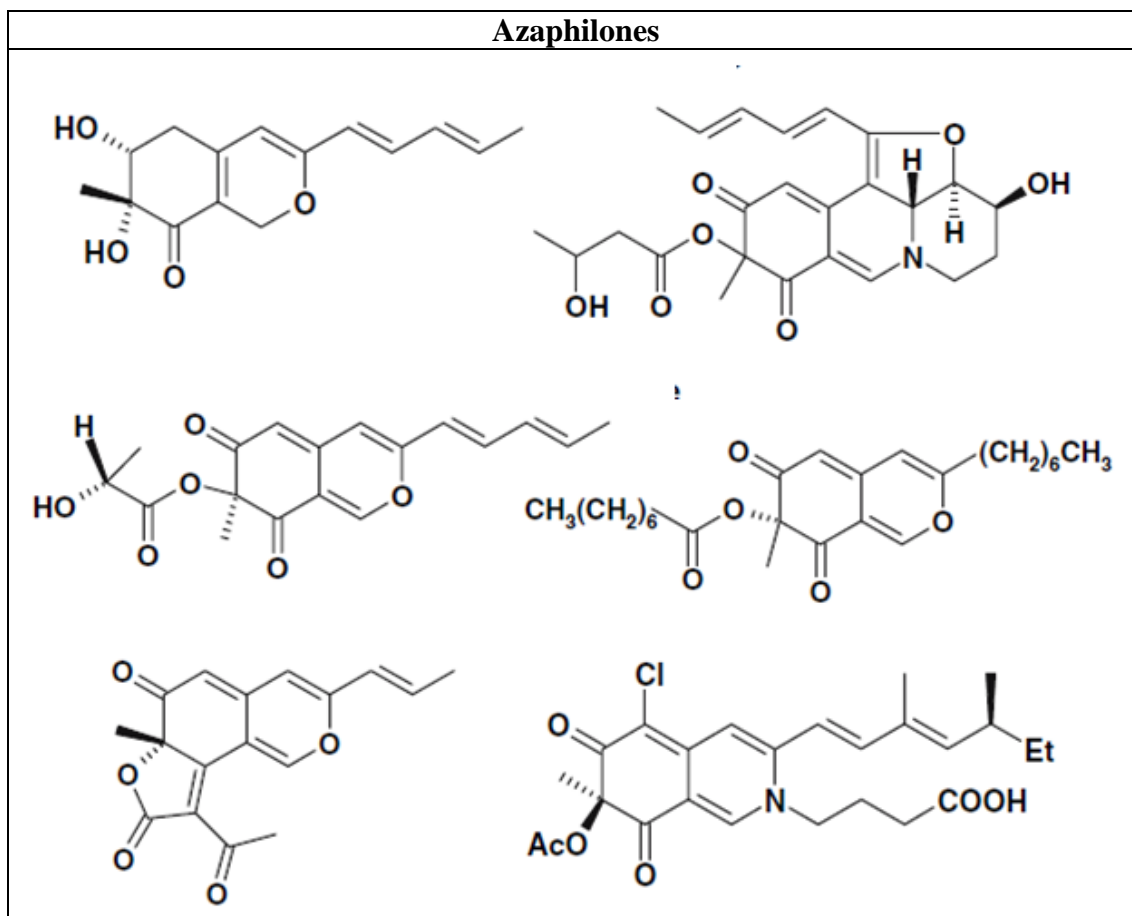


R1= R2= H

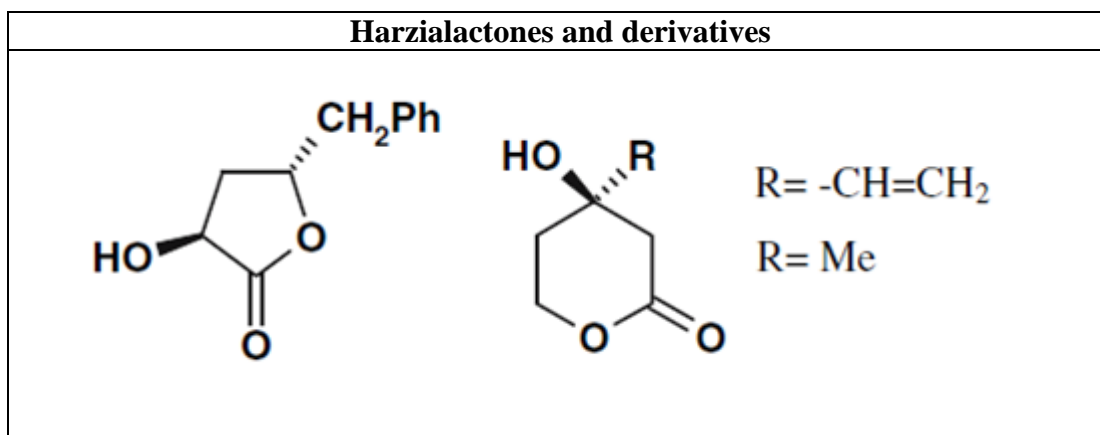
R1= Ac, R2= H

R1= H, R2= Ac

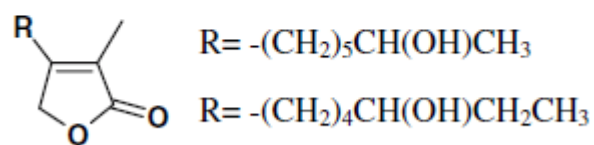
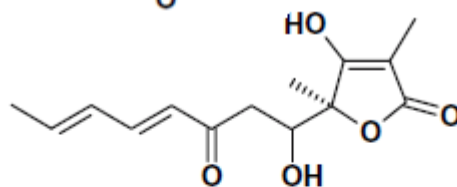
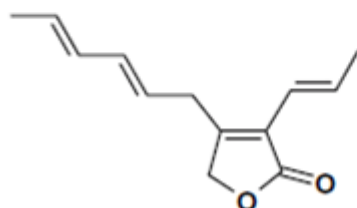
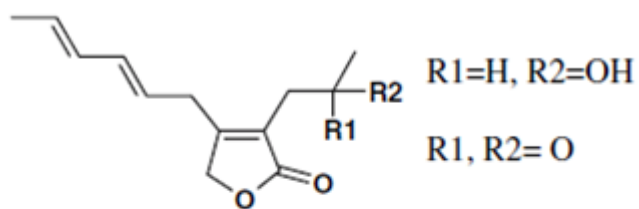
Azaphilones



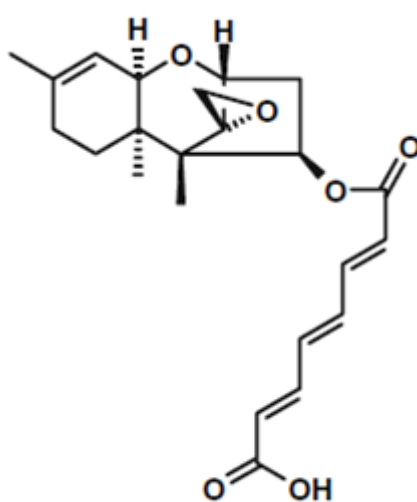
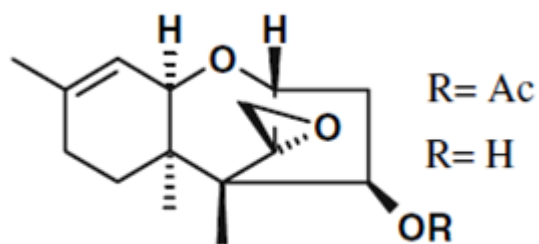
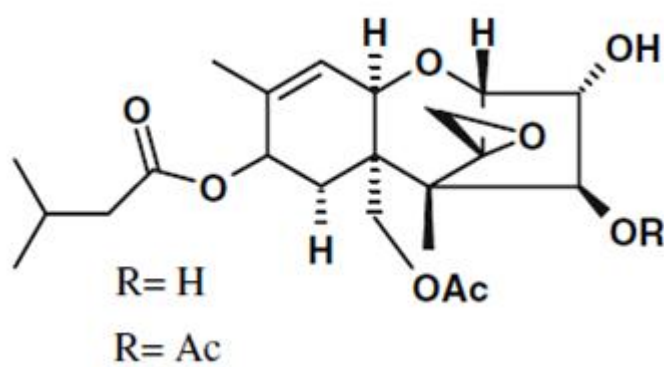
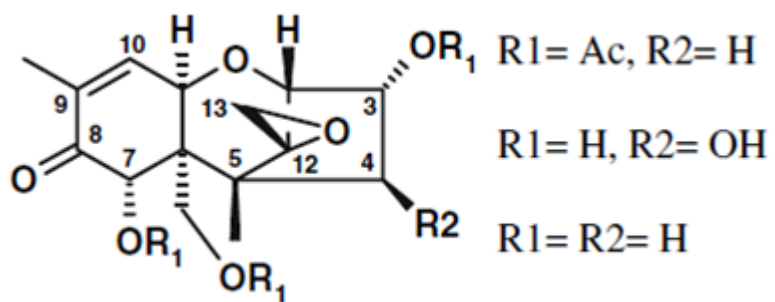
Harzialactones and derivatives



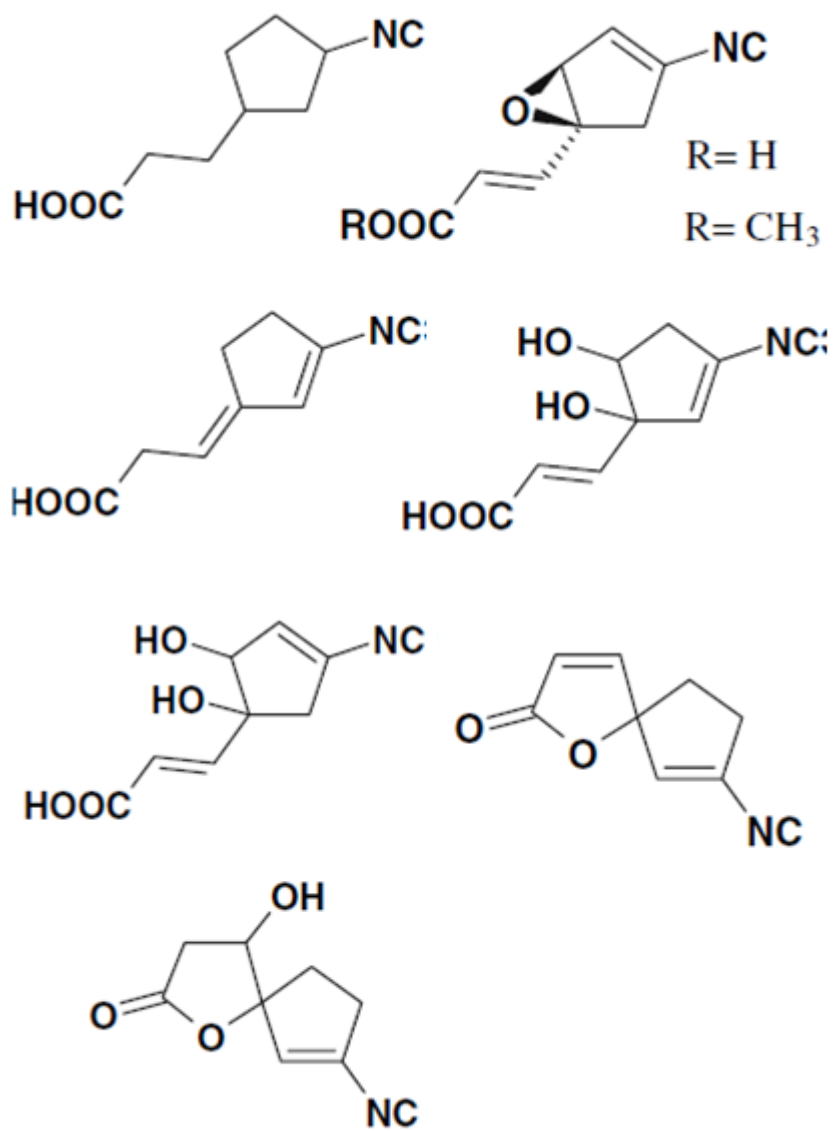
Butenolides



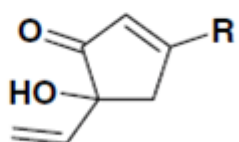
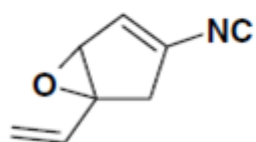
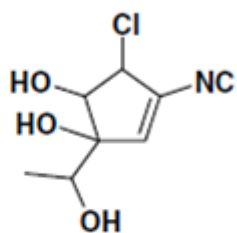
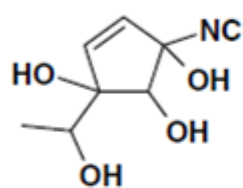
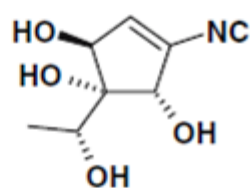
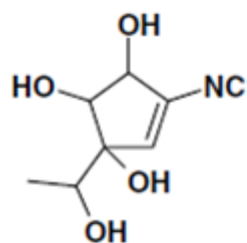
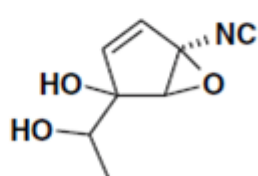
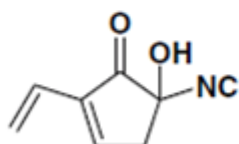
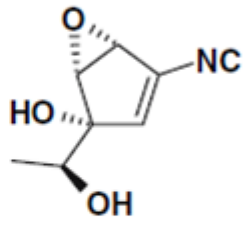
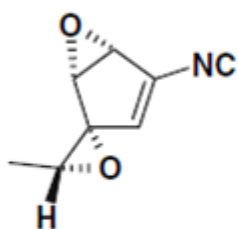
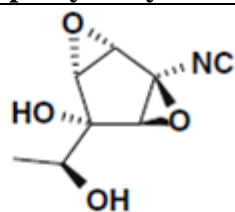
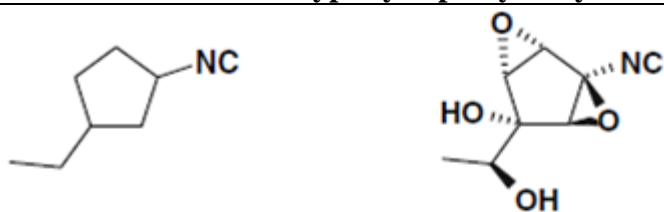
Trichothecenes



Dermadin-type cyclopentylisocyanides



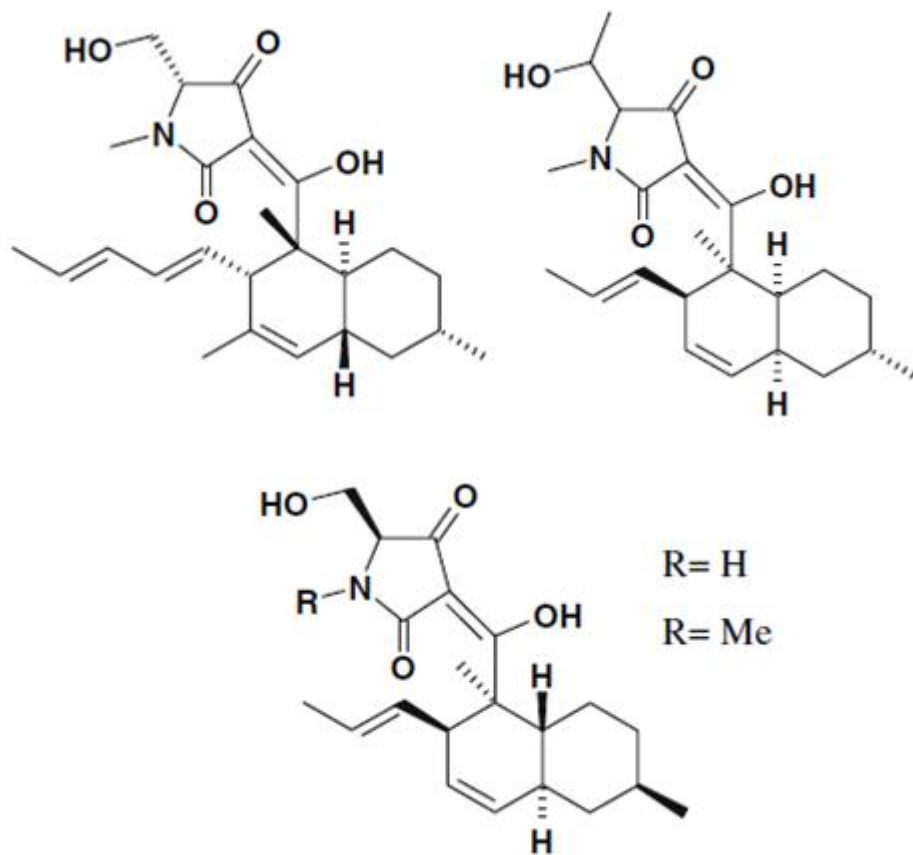
Trichoviridin-type cyclopentylisocyanides



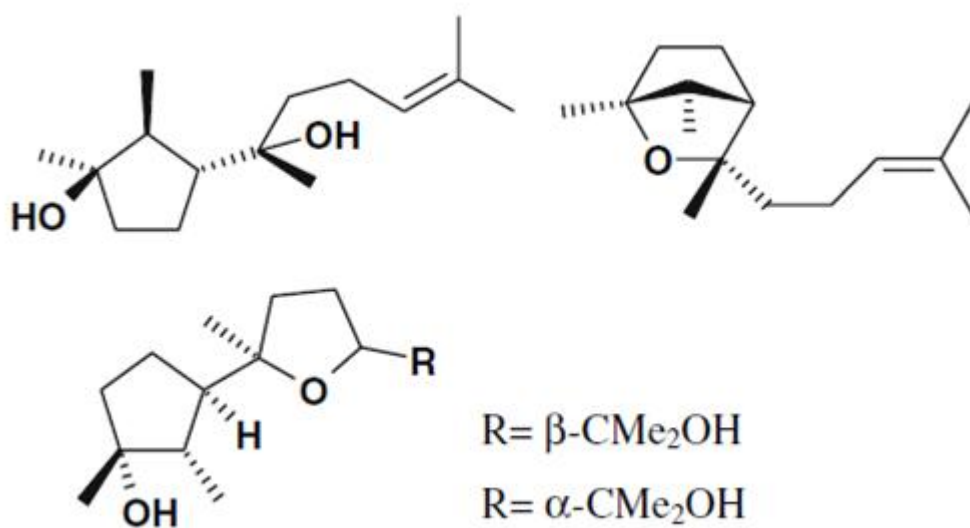
R= NC R= NHCHO

R= NH₂ R= N(CH₃)₂

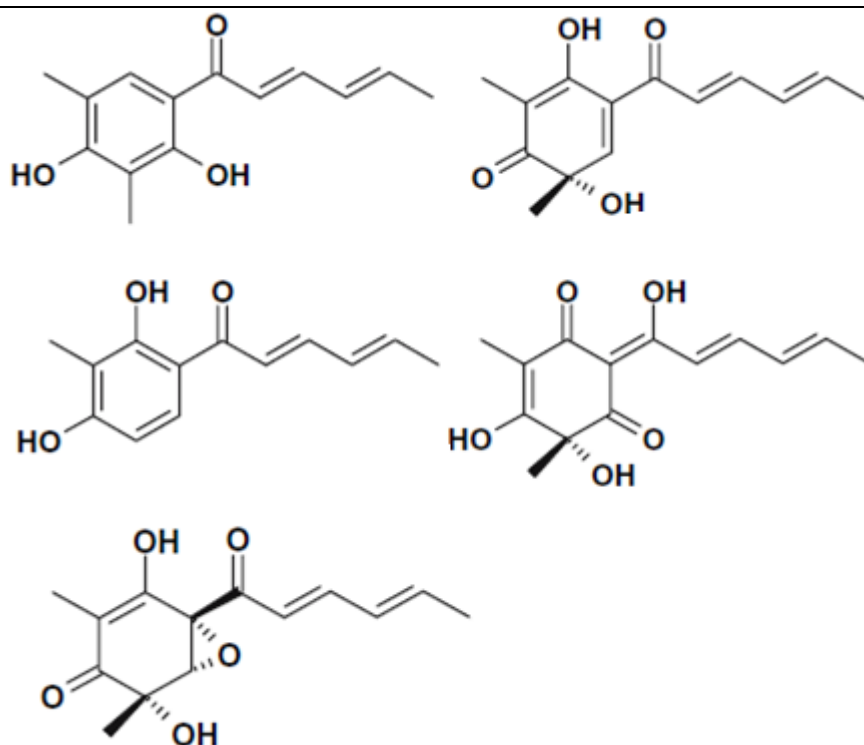
Setin-like antibiotics



Cyclonerodiol derivatives

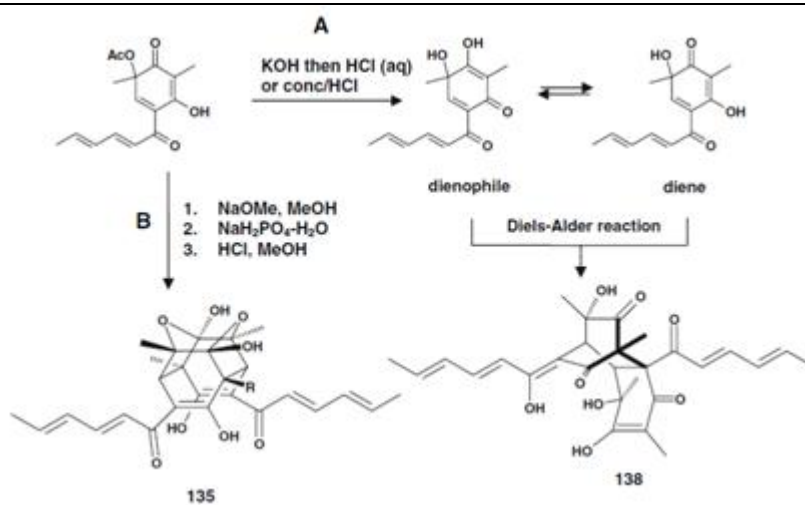


Sorbicillin derivatives

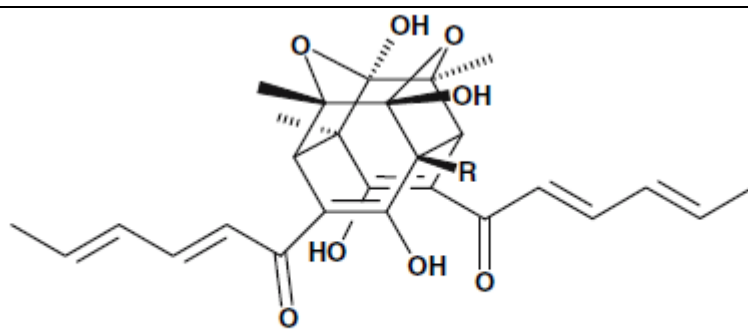


Biomimetic total syntheses of 138 by Nicolaou et al. (Path A) and of 135 by

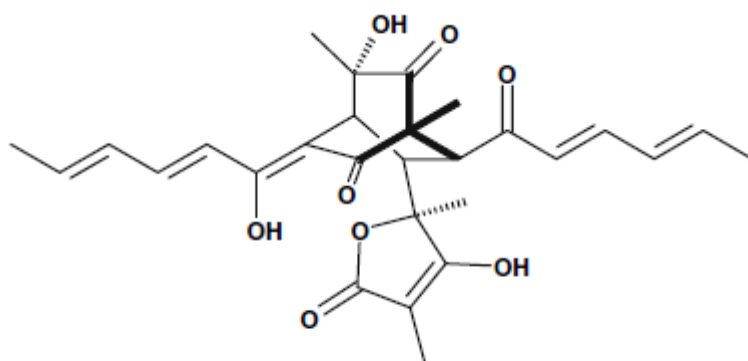
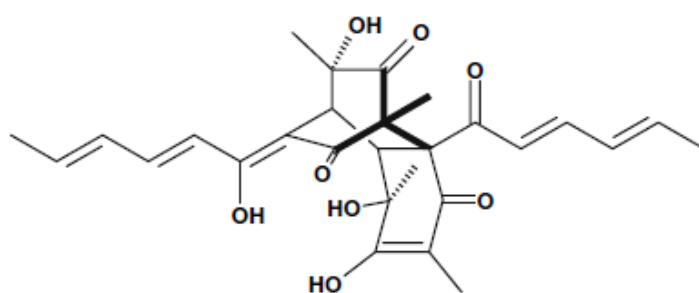
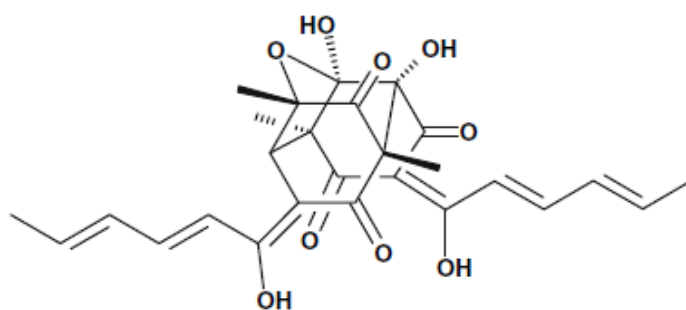
Barnes–Seeman and Corey (Path B)

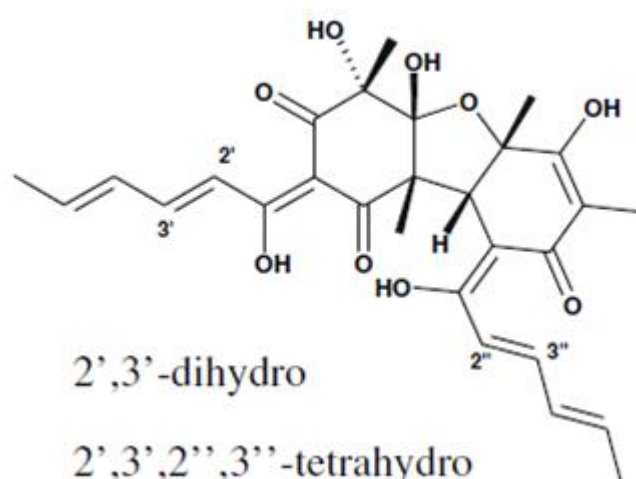
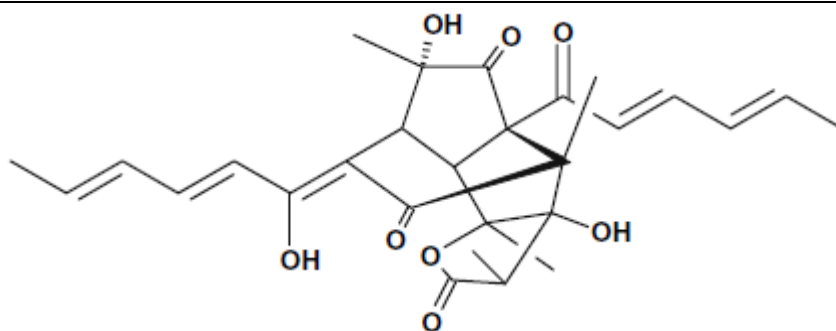


Bisorbicillinoids

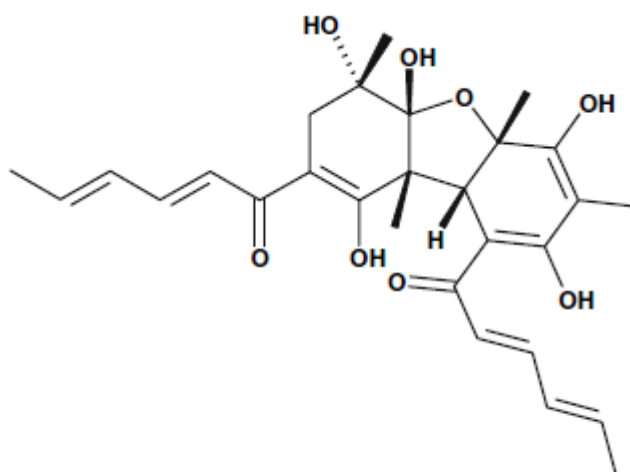


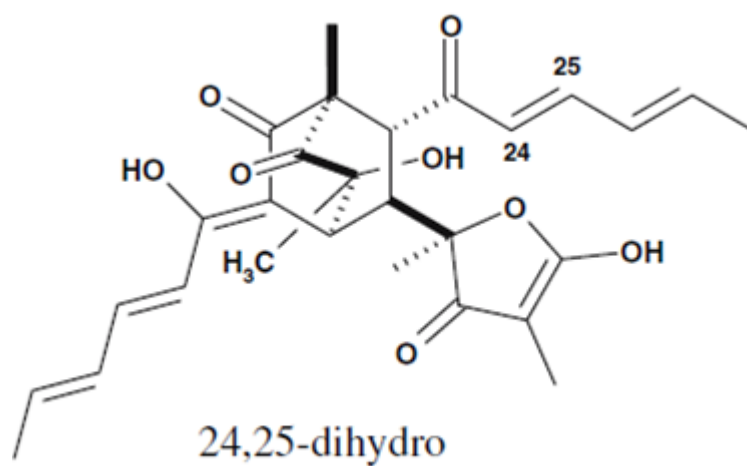
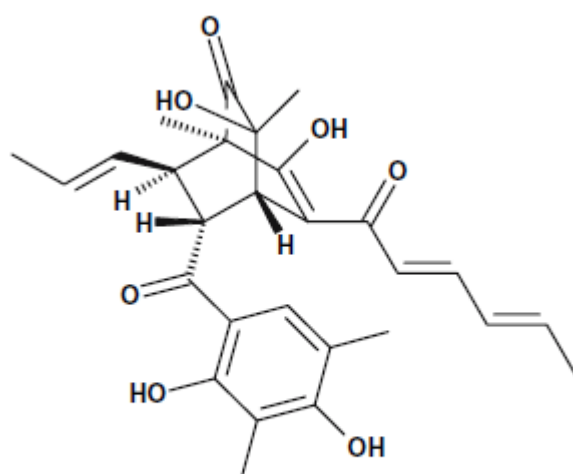
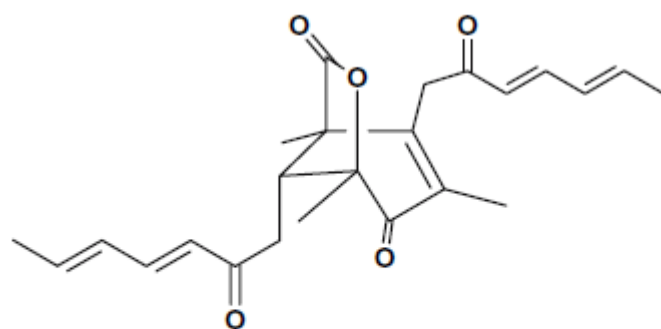
R= Me R= H



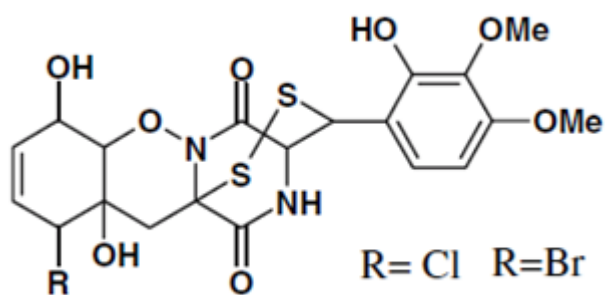
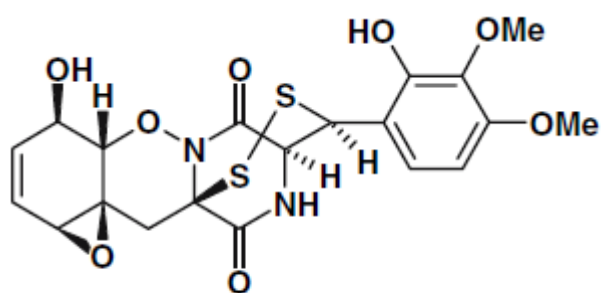
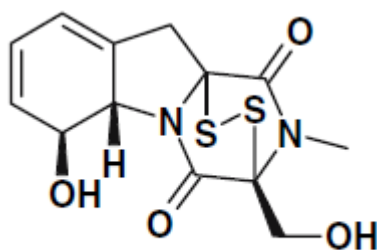


2',3',2'',3''-tetrahydro

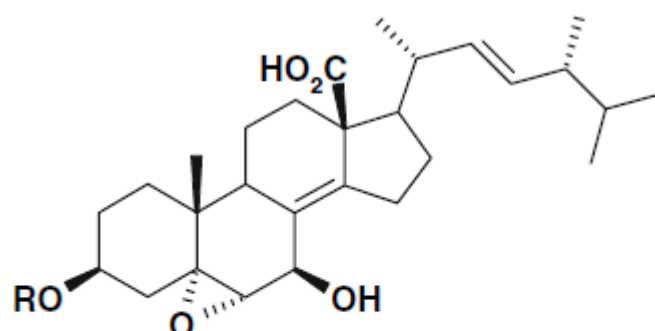
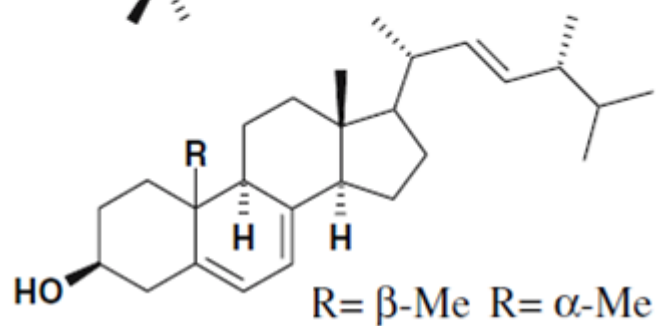
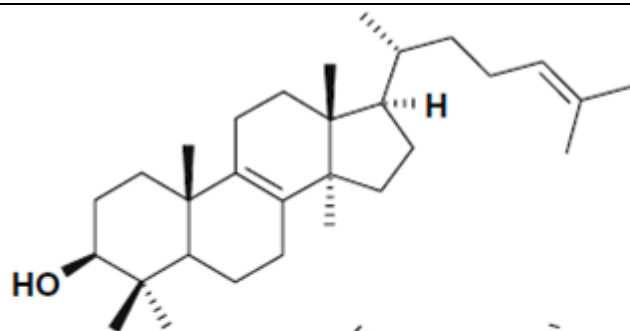




Diketopiperazines



Sterols



$R = \text{COCH}(\text{NH}_2)\text{CH}(\text{OSO}_3\text{H})\text{CHMe}_2$

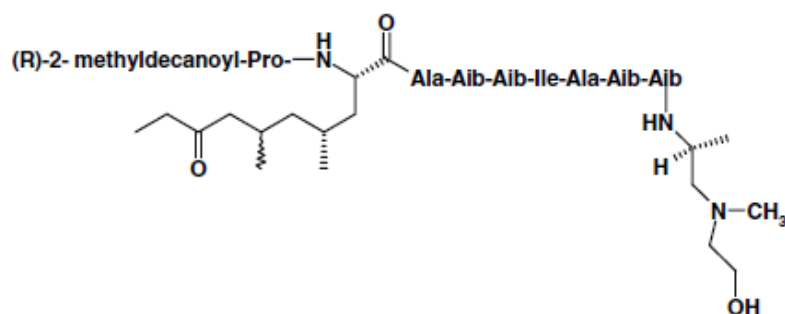
$R = \text{H}$

$R = \text{COC}(\text{NH}_2)\text{Me}_2$

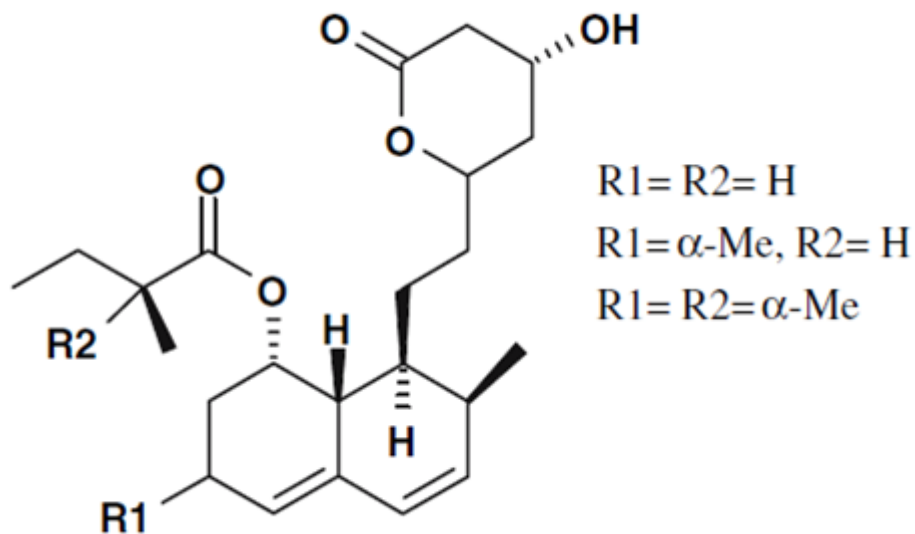
Peptaibols structures

Ac-Aib-Pro-Aib-Ala-Aib-Ala-Gln-Aib-Val-Aib-Gly-Leu-Aib-Pro-Val-Aib-Aib-Glu-Gln-Phe-OH

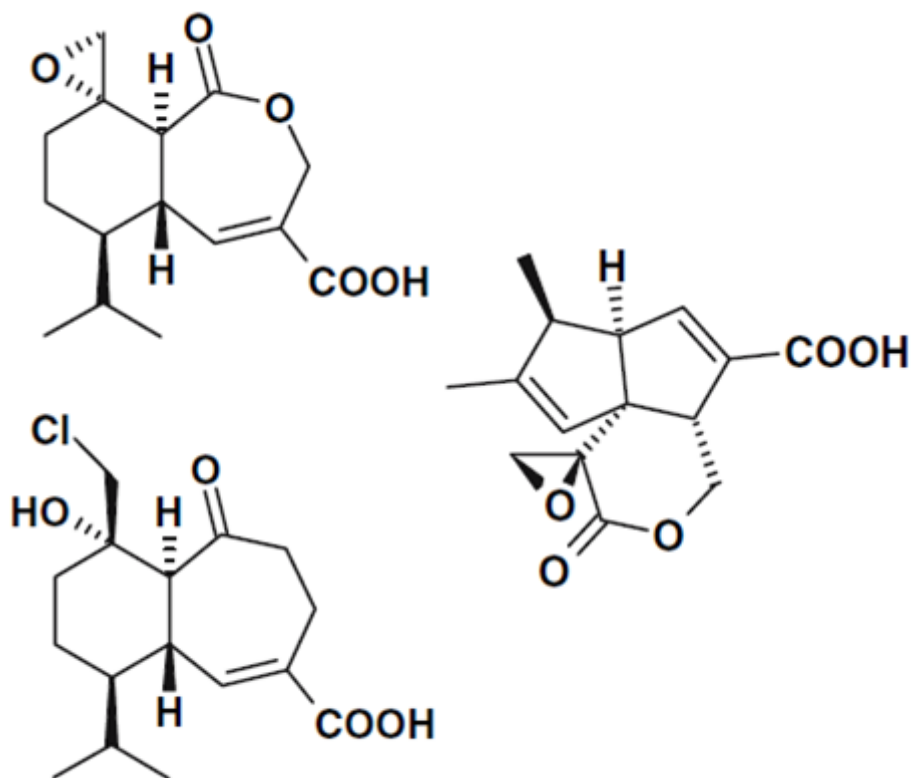
$\text{Me}(\text{CH}_2)_4\text{CH}=\text{CH}(\text{CH}_2)_3\text{CO-Gly-Gly-Leu-Aib-Gly-Ile-Leucinol}$



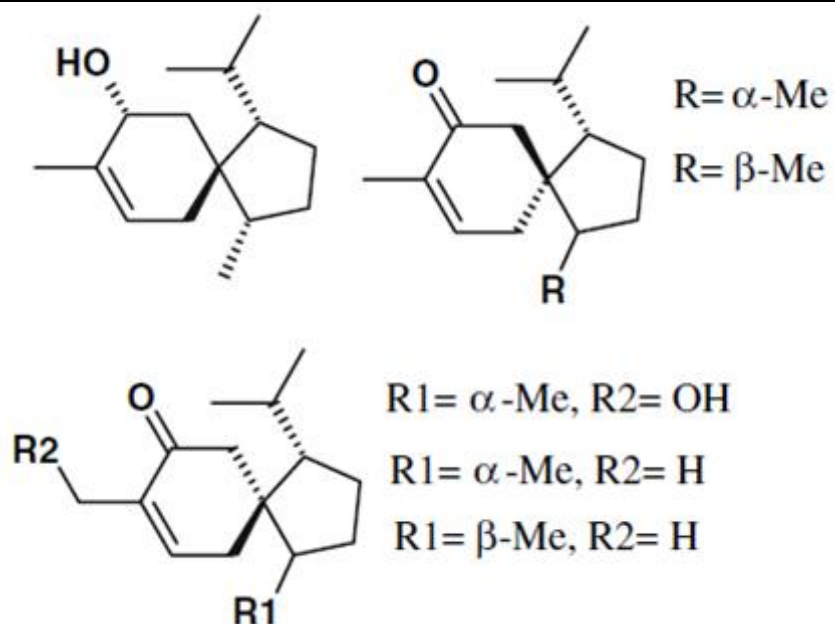
Statins



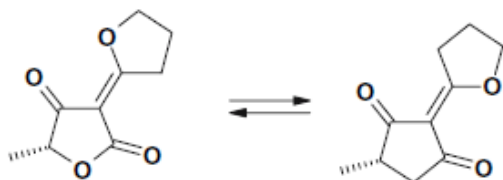
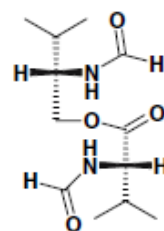
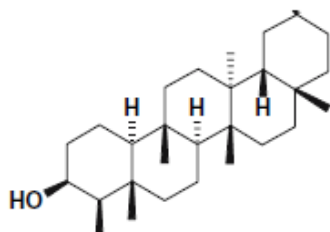
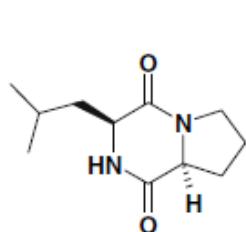
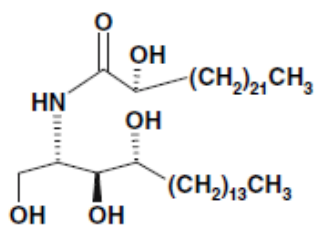
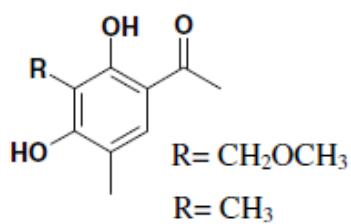
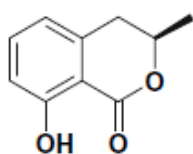
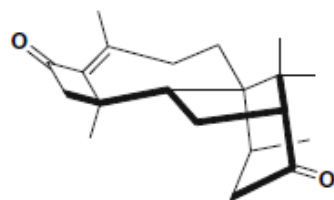
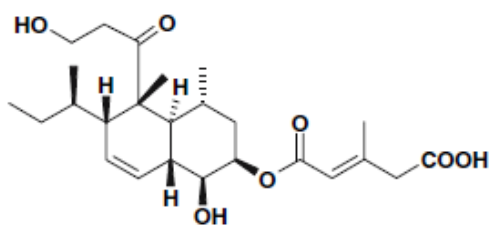
Heptelidic acid and closely related compounds



Acoranes



Miscelanea



Appendix 7.1.3 Purification the antifungal molecules by TLC and HPLC



Fig. 11 The fractions A1-1-1, and observed by 254 nm (a). The wavelengths of UV light were 254 nm (green background).

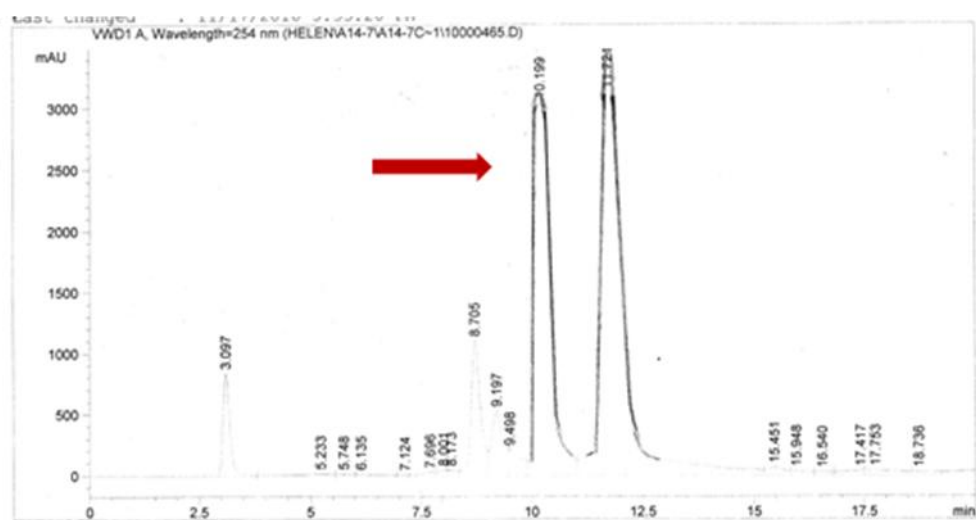
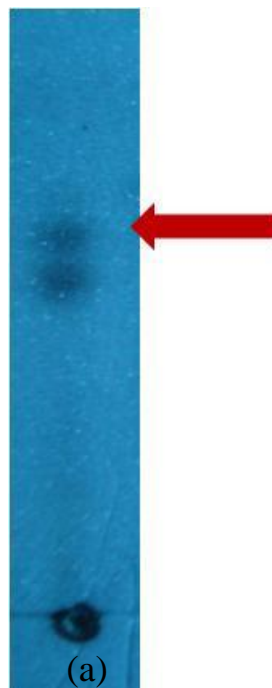


Fig. 12 The pure compound A14-7-2 was separated from A14-7. The fractions A14-7, and observed by 254 nm (a); The HPLC chromatogram (b).

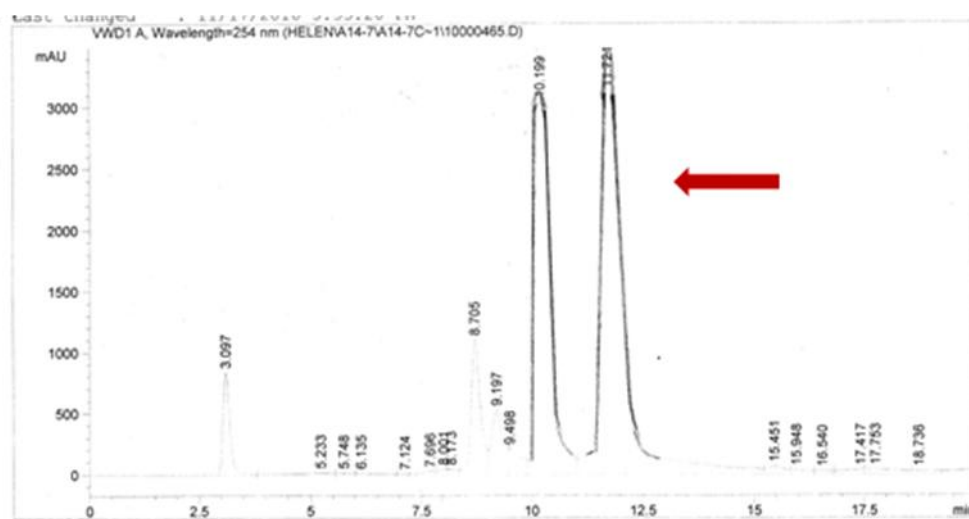
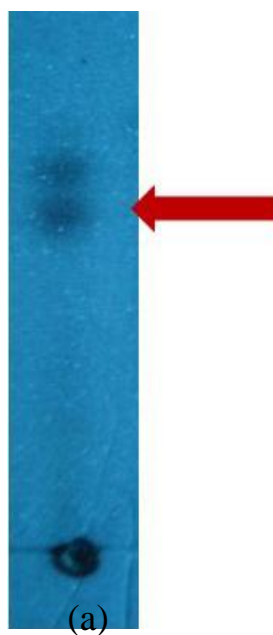


Fig. 13 The pure compound A14-7-3 was separated from A14-7. The fractions A14-7, and observed by 254 nm (a); The HPLC chromatogram (b).

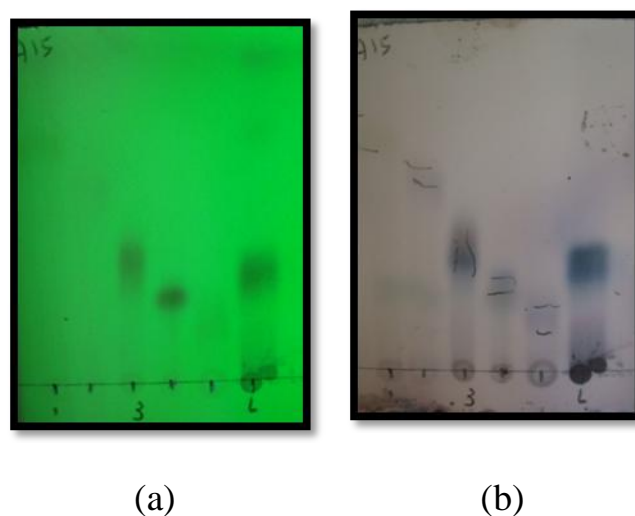


Fig. 14 The distribution of components from fractions A15-1 to A15-6.

Lane 1: A15-1, lane 2: A15-2, lane 3: A15-3, lane 4: A15-4, lane 5: A15-5, lane 6: A15-6, and observed by 254 nm (a) and burning TLC (b). The wavelengths of UV light were 254 nm (green background) and burning TLC (gray background).

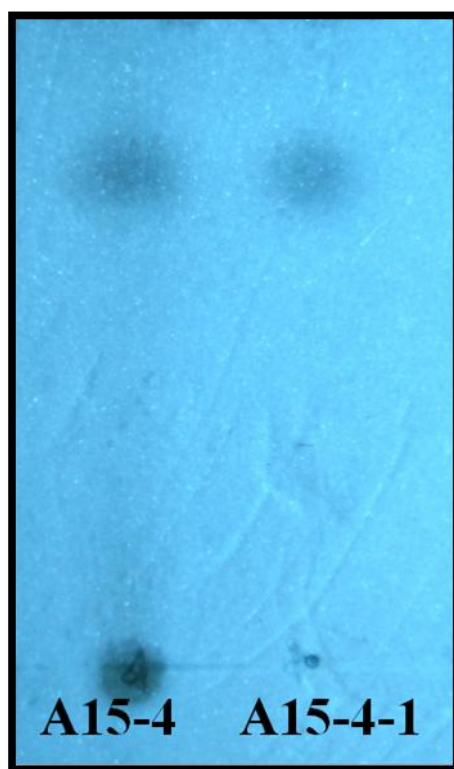
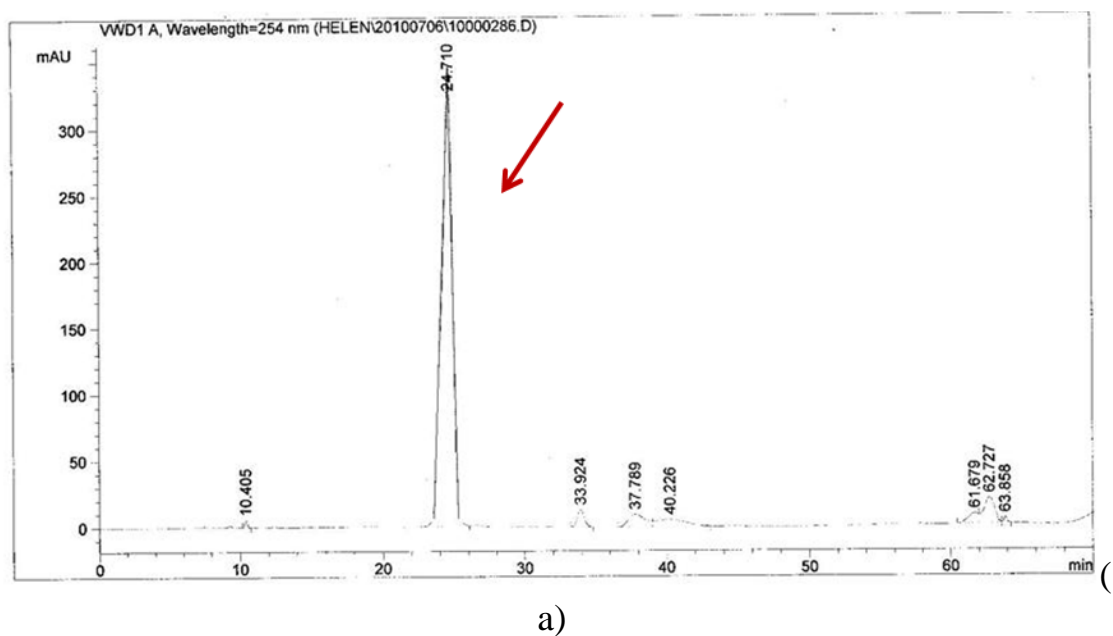


Fig. 15 The pure compound A15-4-1 was separated from A15-4. The HPLC chromatogram (a); The wavelengths of UV light were 254 nm (b).

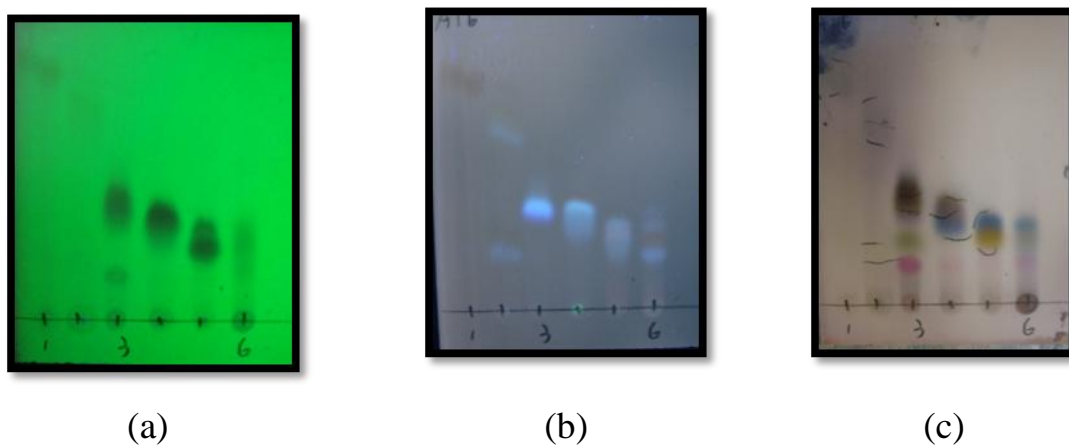
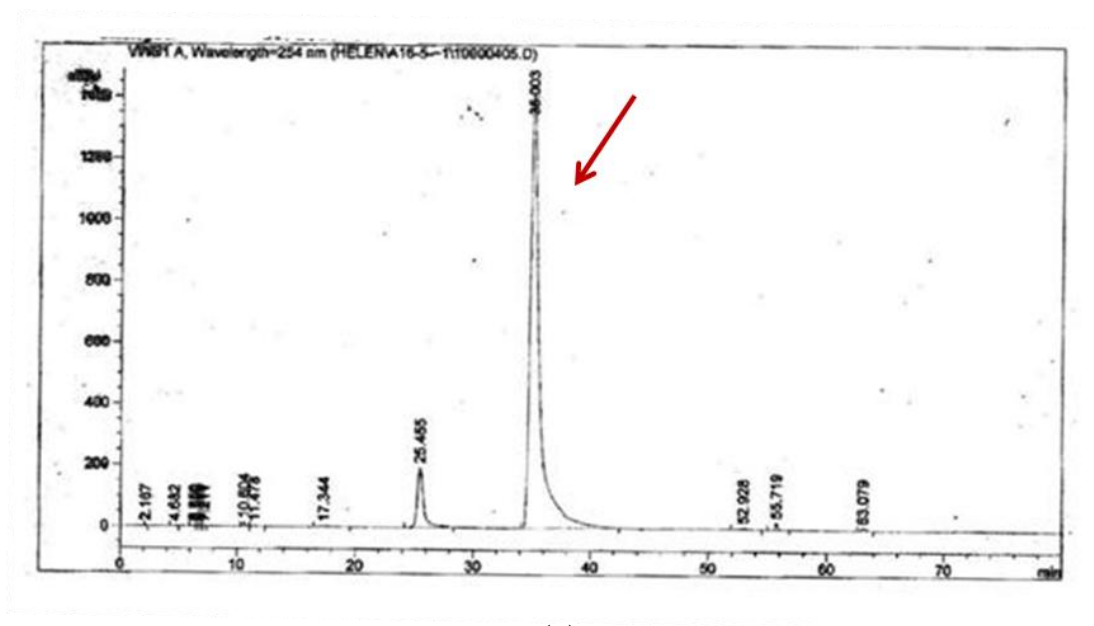


Fig. 16 The distribution of components from fractions A16-1 to A16-6.

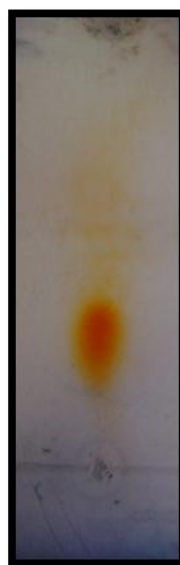
Lane 1: A16-1, lane 2: A16-2, lane 3: A16-3, lane 4: A16-4, lane 5: A16-5, lane 6: A16-6, and observed by 254 nm (a), 365 nm (b) and burning TLC (c). The wavelengths of UV light were 254 nm (green background), 365 nm (blue background) and burning TLC (gray background).



(a)



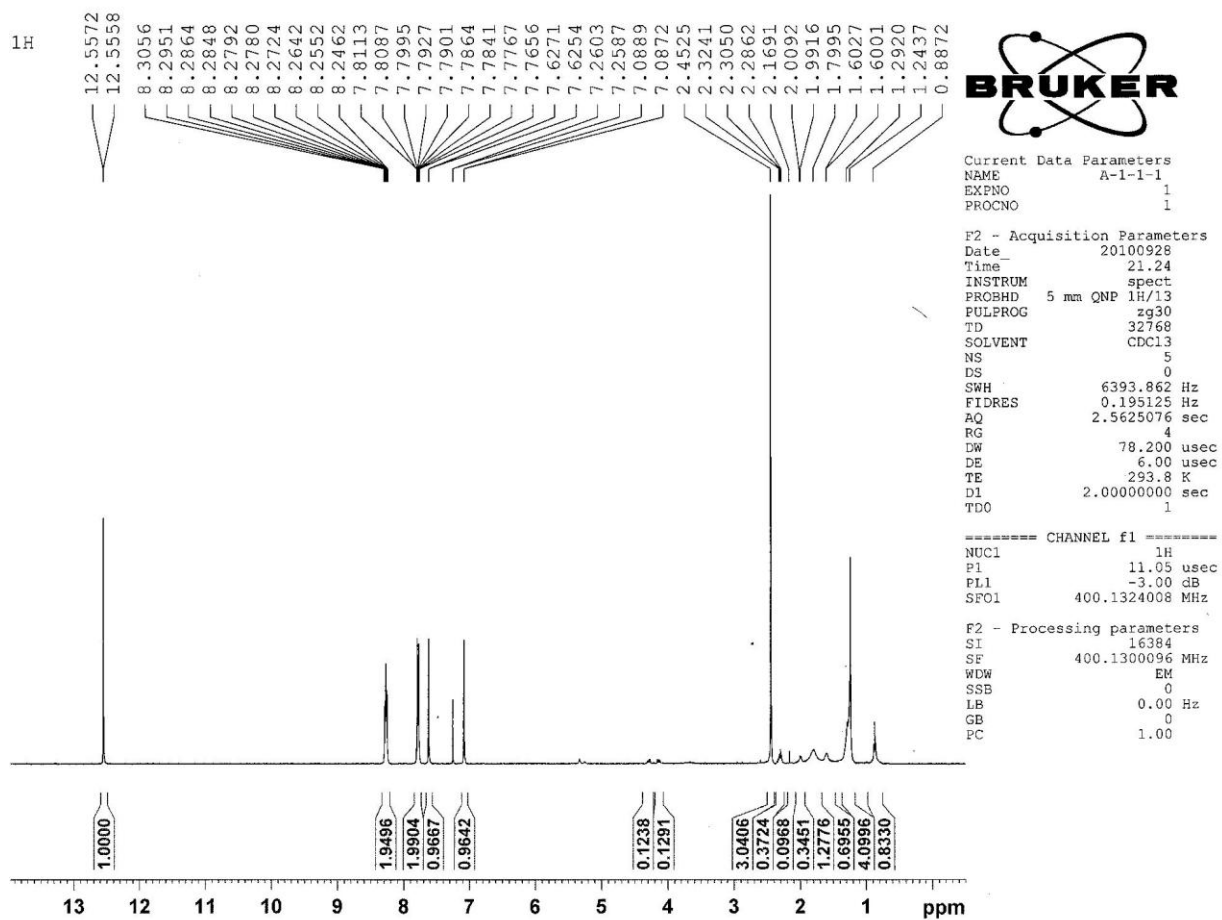
(b)



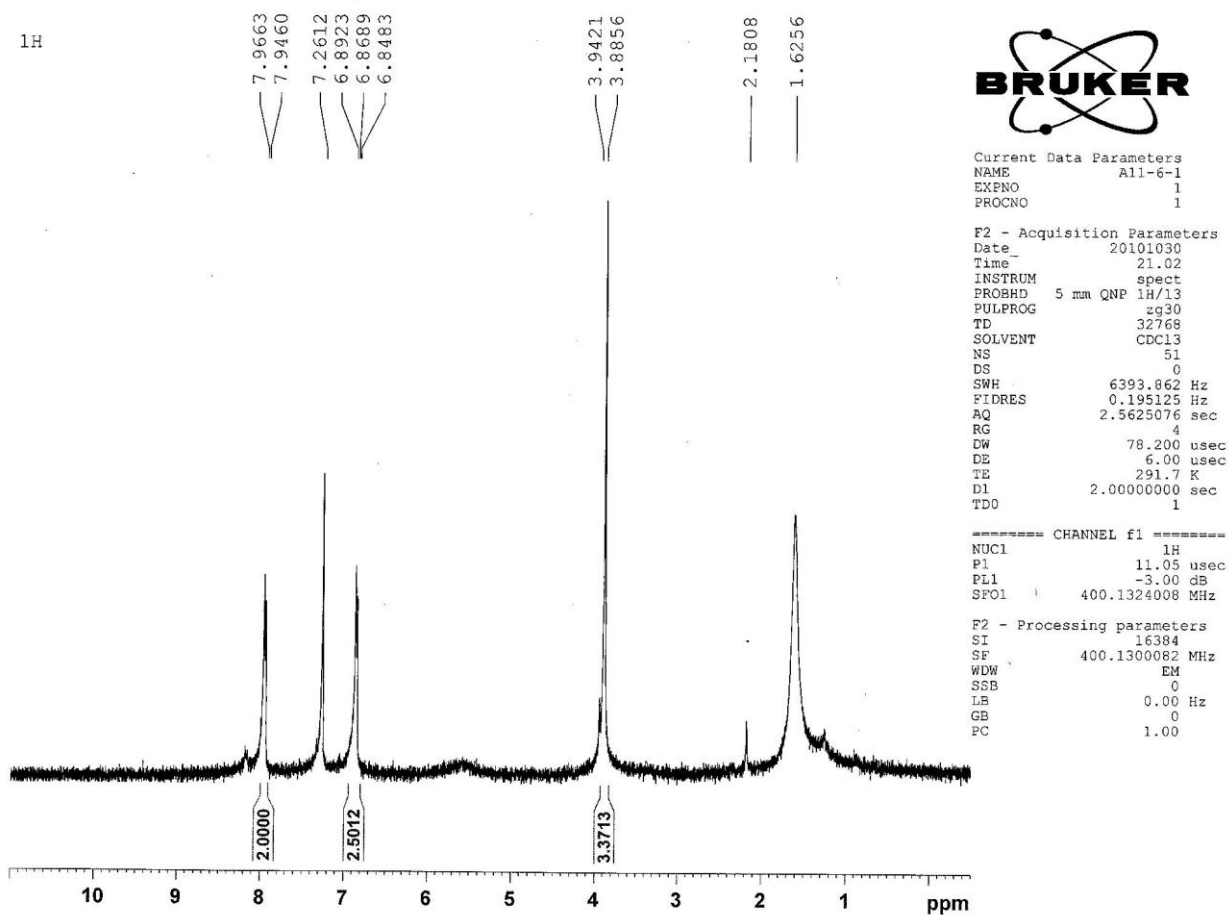
(c)

Fig. 17 The pure compound A16-5-1 was separated from A16-5. The HPLC chromatogram (a); The wavelengths of UV light were 254 nm (b); burning TLC (c).

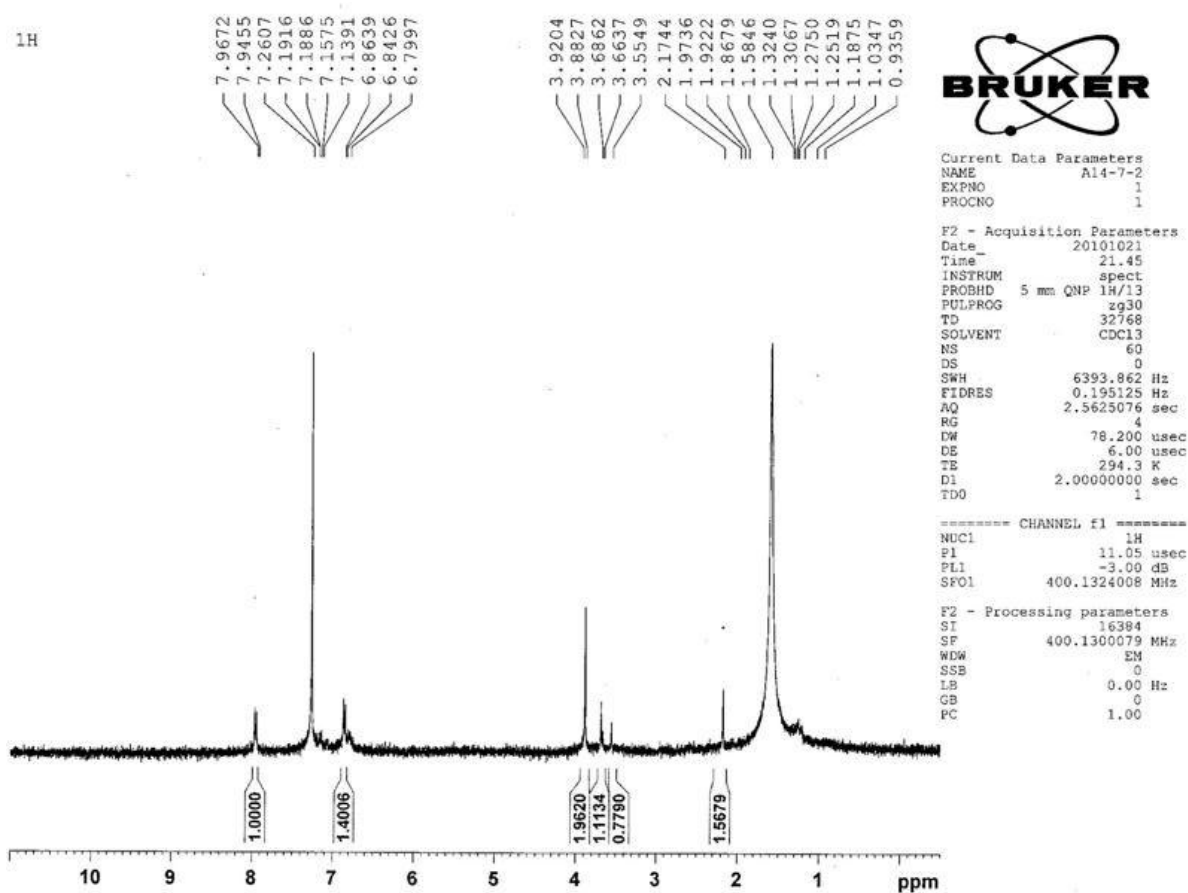
Appendix 7.1.4 ^1H -NMR spectra of Compound A



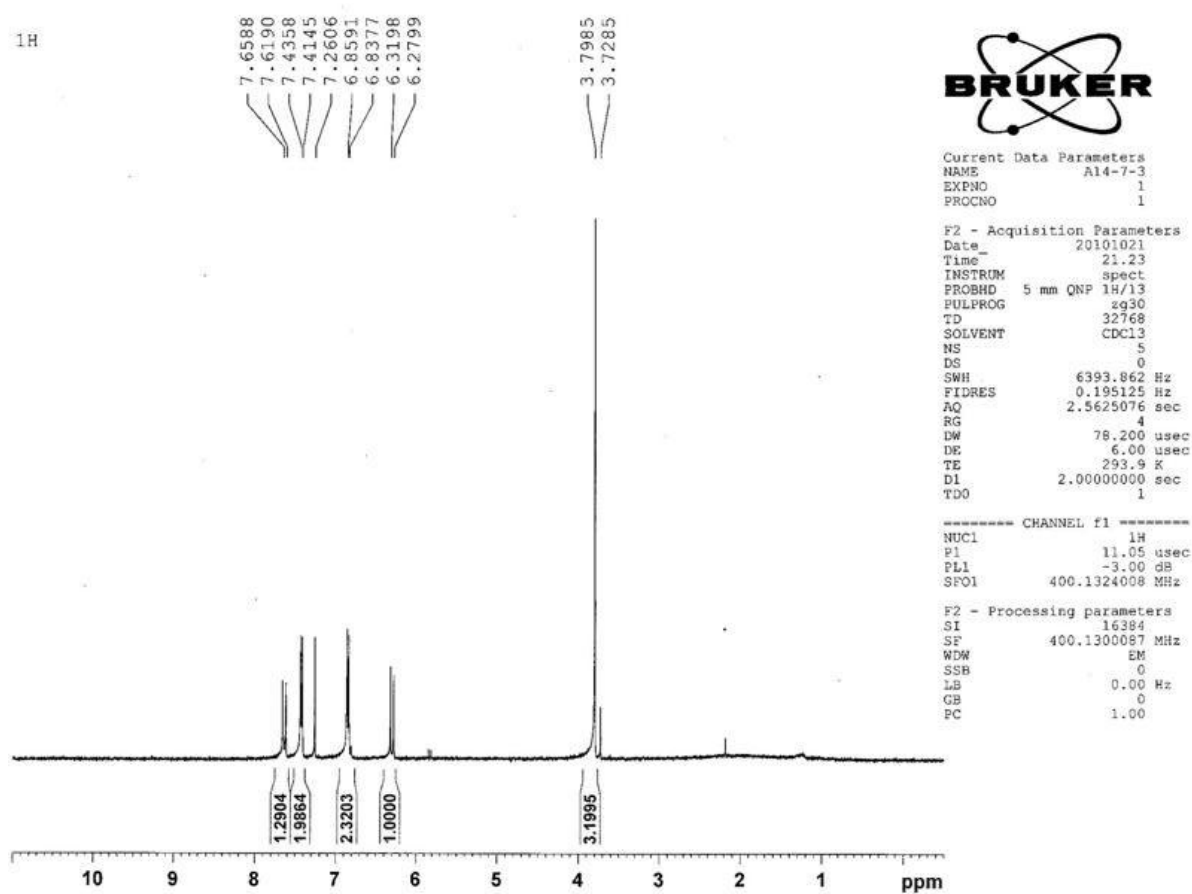
Appendix 7.1.5 ^1H -NMR spectra of Compound B



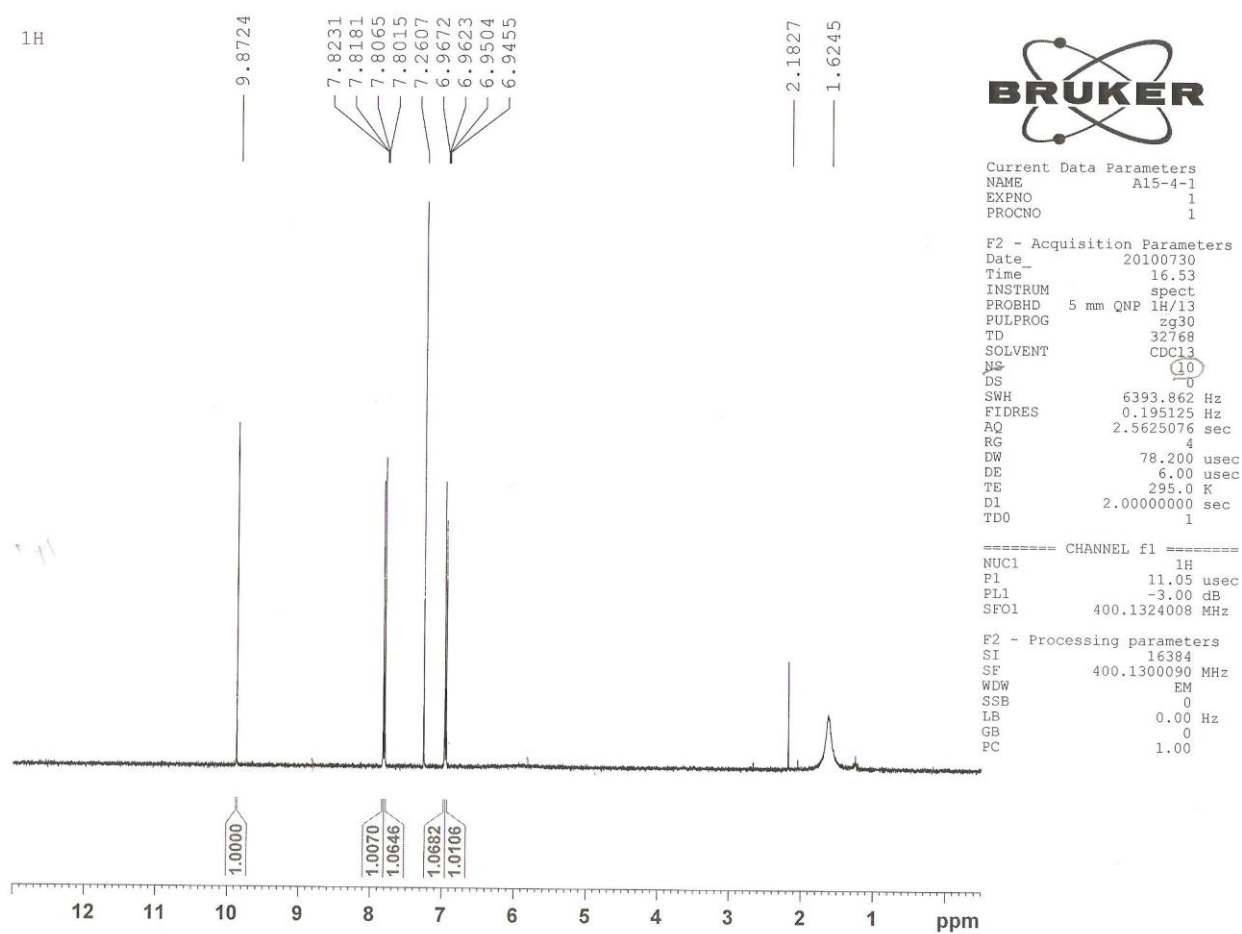
Appendix 7.1.6 ¹H-NMR spectra of Compound C



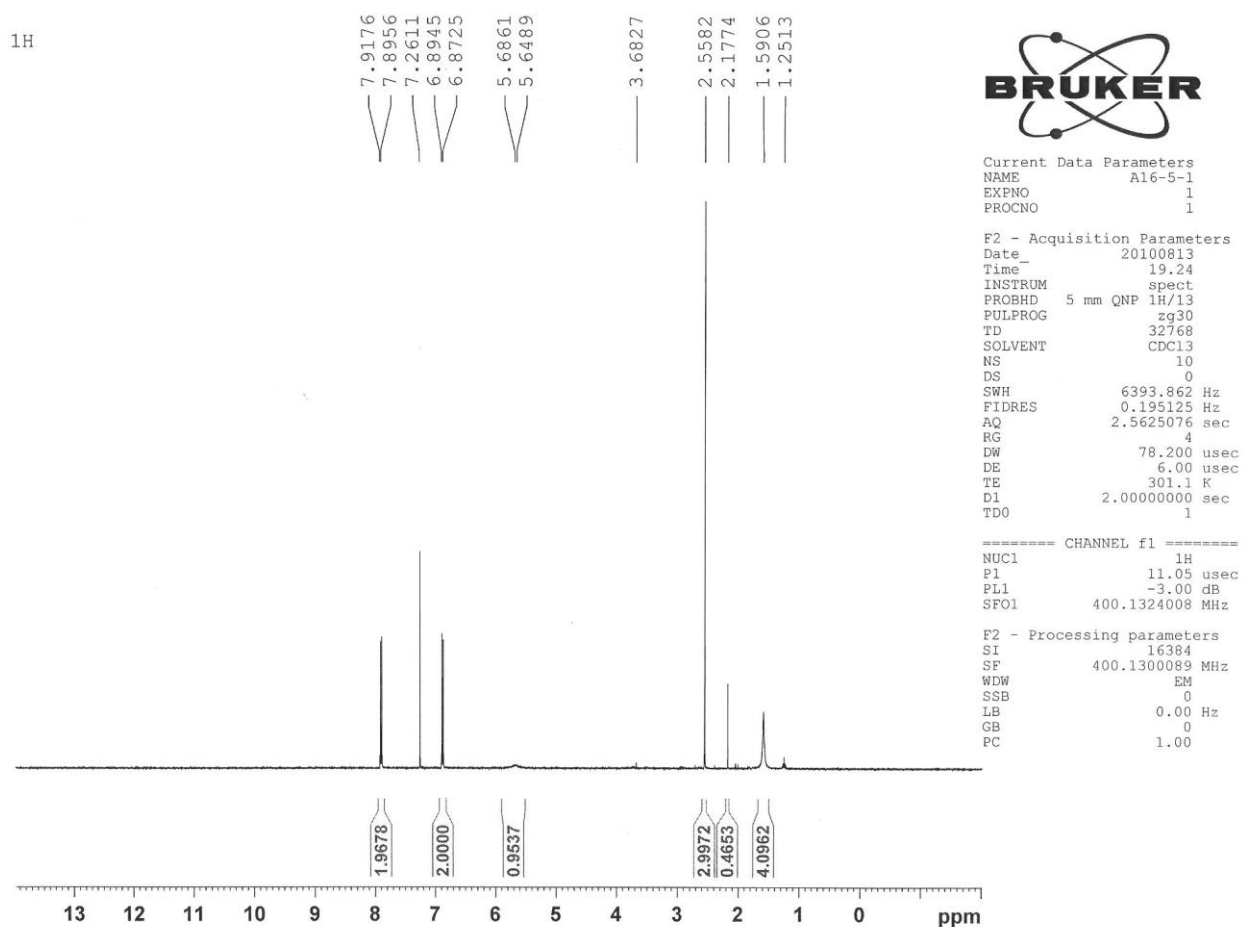
Appendix 7.1.7 ^1H -NMR spectra of Compound D



Appendix 7.1.8 ^1H -NMR spectra of Compound E

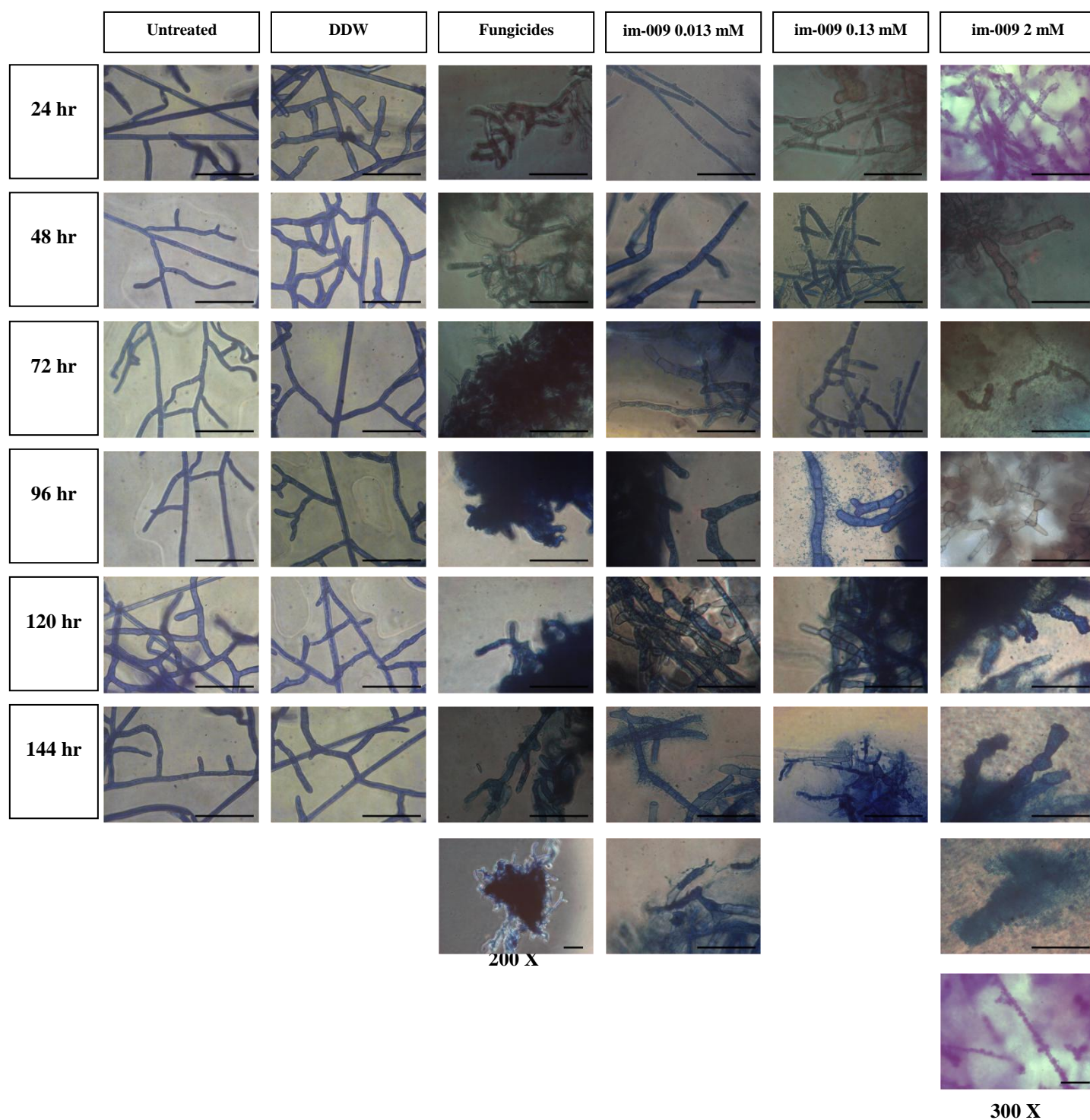


Appendix 7.1.9 ^1H -NMR spectra of Compound F

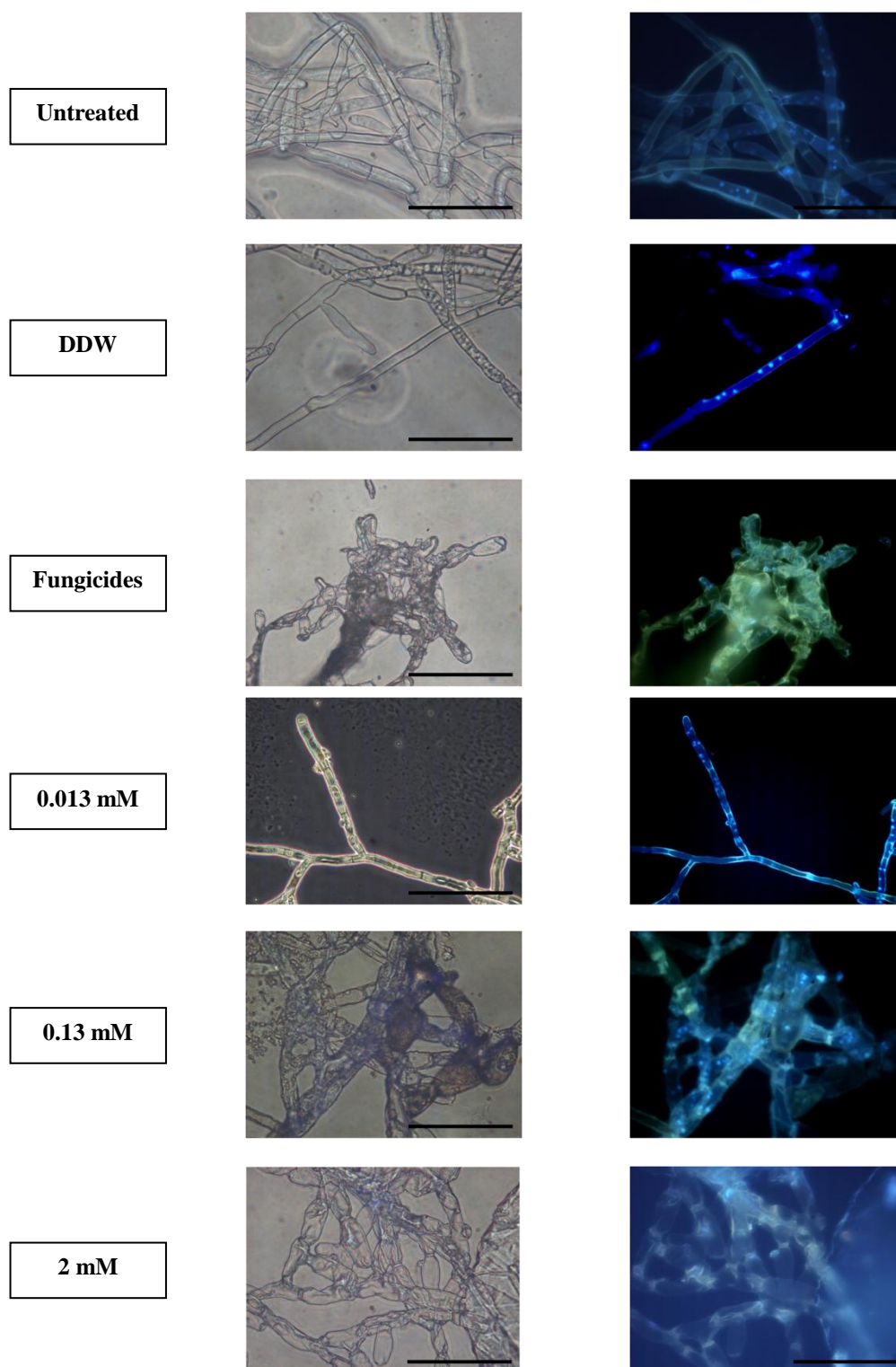


7.2 Antifungal potency of the organic ethoxy ether functionalized imidazolium salts

Appendix 7.2.1 The *R. soloni* morphology cell wall observation in the present of 13 μ M, 130 μ M, 2mM [C₁₄-im-3OEG][Cl] under the 600 x Fluorescent stereomicroscope.



Appendix 7.2.2 Photomicrographs of pathogens *R. solani* after treated by [C₁₄-im-3OEG][Cl] and observed nucleus by Fluorescent stereomicroscope.



Appendix 7.2.3 Calculate the hyphal length and the hyphae amount

Sample	24 hr		48 hr		72 hr		96 hr		120 hr		144 hr	
	Hyphal length (mm)	Hyphae amount (1/mm)	Hyphal length (mm)	Hyphae amount (1/mm)	Hyphal length (mm)	Hyphae amount (1/mm)	Hyphal length (mm)	Hyphae amount (1/mm)	Hyphal length (mm)	Hyphae amount (1/mm)	Hyphal length (mm)	Hyphae amount (1/mm)
untreated	0.94 ± 0.01	1 ± 0.01	0.87 ± 0.02	1 ± 0.02	0.74 ± 0.03	1 ± 0.05	0.59 ± 0.03	2 ± 0.09	0.73 ± 0.01	1 ± 0.02	0.74 ± 0.02	1 ± 0.04
DDV	0.92 ± 0.02	1 ± 0.03	0.86 ± 0.03	1 ± 0.04	0.68 ± 0.03	1 ± 0.07	0.59 ± 0.02	2 ± 0.06	0.69 ± 0.03	1 ± 0.07	0.7 ± 0.04	1 ± 0.08
fungicide	Spherical	not calculated	Spherical	not calculated	Spherical	not calculated	Spherical	not calculated	Spherical	not calculated	Spherical	not calculated
0.013 mM	0.34 ± 0.03	3 ± 0.24	0.36 ± 0.02	3 ± 0.12	0.23 ± 0.03	4 ± 0.48	0.26 ± 0.04	4 ± 0.49	0.15 ± 0.00	6 ± 0.21	0.17 ± 0.03	6 ± 1.00
0.13 mM	0.21 ± 0.01	5 ± 0.2	0.23 ± 0.02	4 ± 0.31	0.13 ± 0.04	8 ± 2.96	0.11 ± 0.01	9 ± 0.90	0.1 ± 0.01	10 ± 1.43	0.09 ± 0.01	11 ± 0.77
2 mM	0.12 ± 0.02	9 ± 1.32	0.14 ± 0.02	7 ± 1.04	0.10 ± 0.03	11 ± 2.74	0.09 ± 0.01	11 ± 1.08	0.09 ± 0.01	11 ± 1.08	0.08 ± 0.00	12 ± 0.24

※ Not calculated: Hyphae wound together.

Hyphal length: Round off to the 2nd decimal place.

Hyphae amount: Round off to integral number